Universitat Autònoma de Barcelona

Escola d'Enginyeria
Departament d'Enginyeria Química

Removal of cadmium (II), lead (II) and chromium (VI) in water with nanomaterials

PhD Thesis

Ada Rebeca Contreras Rodríguez

September, 2015

GICOM
Departament d' Enginyeria Química
Escola d' Enginyeria
Universitat Autònoma de Barcelona

ANTONI SÁNCHEZ FERRER i XAVIER FONT SEGURA professor titular i professor agregat del Departament d'Enginyeria Química de la Universitat Autònoma de Barcelona,

CERTIFIQUEN:

Que la enginyera química, ADA REBECA CONTRERAS RODRÍGUEZ ha realitzat sota la nostra direcció el treball amb títol *"Removal of cadmium (II), lead (II) and chromium (VI) in water with nanomaterials"* que es presenta en aquesta memòria i que constitueix la seva Tesi per optar al Grau de Doctor per la Universitat Autònoma de Barcelona.

I per a què se'n prengui coneixement i consti als afectes oportuns, presentem a l'Escola de Postgrau de la Universitat Autònoma de Barcelona l'esmentada Tesi, signant el present certificat a

Bellaterra, 29 de setembre de 2015

Dr. Antoni Sánchez Ferrer Dr. Xavier Font Segura

A Laura Rodríguez y Javier Contreras.
Por todo.

A Josefina Rodríguez.
Dónde sea que estés hoy.

Acknowledgements

Ada Rebeca Contreras Rodríguez, member of the GICOM group in the Universitat Autònoma de Barcelona, is grateful for the Beca en el extranjero (2011-2015) from CONACYT (Consejo Nacional de ciencia y tecnología de México), that allow her to conduct her research.

Thank you to the Department of Chemical Engineering in the Universitat Autònoma de Barcelona.

Thank you to Dr. Antoni Sánchez Ferrer and Dr. Xavier Font Segura and, to all the members of the GICOM group.

Table of contents

Abbreviations

AC	Activated carbon
AM	Acrylamide
ARC	Agència de Residus de Catalunya
BSA	Bovine Serum Albumin
CeO_2	Cerium oxide
DMF	N,N-Dimethylformamide
DOPA	3,4-dihydroxyphenylalanine
EPA	US Environmental Protection Agency
Fe_3O_4	Iron oxide
GO	Graphene oxide
ICN2	Institut Catala de Nanociència i Nanotecnologia
ICP-MS	Inductively Coupled Plasma Mass Spectrometry
ICP-OES	Inductively Coupled Plasma Optical Emission Spectrometry
LMWWTP	Local municipal wastewater treatment plant
MEM	Modified Eagle's Medium
N/A	Not available
Nm	Nanometers
NMOs	Metal oxide nanoparticles
NP/NPs	Nanoparticle/Nanoparticles
PBS	Phosphate saline buffer
PDA	Polydopamine
PMC	Polymer metal complex
PVP	Poly(vinylpyrrolidone)
q_t	Adsorption capacity
RGO	Reduced graphene oxide
ROS	Reactive oxygen species
SEM	Scanning electron microscopy
TEM	Transition electron microscopy
TiO_2	Titanium oxide
Trp	Tryptophan
UAB	Universitat Autònoma de Barcelona

WHO	World Health Organization
XTT	2,3-bis-(2-methoxy-4-nitro-5-sulfophenyl)-2H-tetrazolium-5 carboxanilide
UE	Council of European Union

Abstract/Resumen/Resum

Abstract

A great challenge for this century lies in cleaning-up the waste generated during industrial, domestic and agricultural activities. Water, as vital part of the life cycle is heavily affected by these activities and eventually, turns it unusable. Among the numerous contaminants found in water, heavy metals require special attention, as they are non-biodegradable, and often accumulate in the environment causing both short and long term adverse effects, even at low concentrations. The adsorption process proved to be economically feasible and efficient over other technologies, especially for removing pollutants from dilute solutions. In this sense new adsorbents based on nanomaterials are being extensively studied. With this in mind, the development of new, efficient and low cost nanomaterials for their application in water/wastewater has been of great interest in the last years, due to the special properties such as high reactivity and strong sorption.

In this framework, the feasibility of using different nanomaterials for the removal of cadmium (II), lead (II) and chromium (VI) dissolved in water has been studied. The nanomaterials used could be grouped into three main groups: i) metal oxides nanoparticles (NMOs), cerium oxide (CeO_2) titanium oxide (TiO_2) and iron oxide (Fe_3O_4), ii) polymer, catechol-based nanoparticles (NPs) and iii) graphene oxide (GO)-based nanomaterials, CeO_2 NPs attach to reduced graphene oxide (RGO). The viability of using NMOs for the adsorption of dissolved Cd (II) was tested obtaining the adsorption and kinetics parameters. CeO_2 NPs also were tested with different operational parameters, two different pH and in single and multicomponent system. The results show that the NPs could remove the metal ions in both systems, favored at high pH. The catechol-based NPs adsorption experiments were performed at par with activated carbon, obtaining the higher adsorption capacity with the NPs. Bioluminescent test and cytotoxic assays also were performed in order to assess the toxicity of the nanomaterial. Finally, GO and CeO_2/RGO nanomaterials were characterized and tested in adsorption process. The attachment of CeO_2 to GO follow two different strategies, in situ-growth and self-assembly approach.

The nanomaterials presented high affinity for Pb(II) ions; high adsorption capacities were obtained with lower initial metal concentrations. In conclusion, nanomaterials showed

promising results in the removal of heavy metals, and in this way is reaffirmed once again that nanomaterials can be used as effective adsorbents for water/wastewater treatment.

Resumen

Un gran desafío para este siglo es el saneamiento de los residuos generados durante las actividades industriales, domésticas y agrícolas. El agua, como parte vital del ciclo de vida, está fuertemente afectada por estas actividades y finalmente se puede volver inutilizable. Entre los numerosos contaminantes que se encuentran en el agua, los metales pesados requieren atención especial ya que no son biodegradables y con frecuencia se acumulan en el medio ambiente causando efectos negativos, tanto a corto plazo como a largo plazo, incluso en bajas concentraciones. Los procesos de adsorción han demostrado ser economicament viables y eficientes en comparación con otras tecnologías, especialmente para la eliminación de contaminantes a partir de soluciones diluidas. Por consiguiente, el desarrollo de nuevos nanomateriales eficientes y de bajo coste para su aplicación en el tratamiento del agua y de las aguas residuales ha sido de gran interés en los últimos años, debido a las propiedades especiales, tales como alta reactividad y fuerte sorción.

En este contexto, se ha estudiado la viabilidad de utilizar diferentes nanomateriales para la eliminación de cadmio (II), plomo (II) y cromo (VI) disueltos en agua. Los nanomateriales utilizados podrían agruparse en tres principales grupos: i) las nanopartículas (NPs) de óxidos metálicos (NMOs), óxido de cerio (CeO_2), óxido de titanio (TiO_2) y óxido de hierro (Fe_3O_4), ii) polímero, nanopartículas a base de catecol y iii) los nanomateriales con óxido de grafeno (GO) y NPs de CeO_2 unidas a óxido de grafeno reducido (RGO). La viabilidad del uso de MNOs para la adsorción de Cd (II) disuelto se puso a prueba y se obtuvieron los parámetros cinéticos y de adsorción. Las NPs de CeO_2 también se probaron con diferentes parámetros de funcionamiento, dos pH diferentes y en sistemas uni/multi componentes. Los resultados muestran que las NPs son capaces de eliminar iones metálicos en ambos sistemas, favoreciéndose a pH alto. Los experimentos de adsorción con las NPs de catecol se realizaron a la par con carbón activado, obteniéndose una mayor capacidad de adsorción con las NPs. También se realizaron ensayos con microorganismos bioluminiscentes y ensayos citotóxicos para evaluar la toxicidad del nanomaterial. Por último, se caracterizaron y utilizaron en procesos de adsorción GO y los nanomateriales CeO_2/RGO . El ensamblaje de CeO_2 en la superficie del GO siguió dos estrategias diferentes, el crecimiento *in situ* y el enfoque de auto-ensamblaje. Los nanomateriales presentan una gran

afinidad por los iones Pb (II); las altas capacidades de adsorción se obtienen a bajas concentraciones iniciales de metal.

En conclusión, los nanomateriales mostraron resultados prometedores en la eliminación de metales pesados, de esta manera se reafirma una vez más que los nanomateriales pueden ser utilizados como adsorbentes eficaces para el tratamiento de agua y de aguas residuales.

Resum

Un dels grans desafiaments per aquest segle és el sanejament dels residus generats durant les activitats industrials, domèstiques i agrícoles. L'aigua, com a part vital del cicle de vida, està fortament afectada per aquestes activitats i es pot tornar, finalment, inutilitzable. Entre els nombrosos contaminants que es troben a l'aigua, els metalls pesants requereixen una atenció especial ja que no són biodegradables i sovint s'acumulen en el medi ambient causant efectes negatius, tant a curt termini com a llarg termini, fins i tot en baixes concentracions. Els processos d'adsorció han demostrat ser econòmicament viables i eficients en comparació amb altres tecnologies, especialment per a l'eliminació de contaminants a partir de solucions diluïdes. Per aquest motiu, en els darrers anys, ha estat de gran interès el desenvolupament de nous nanomateriales, eficients, de baix cost i amb alta reactivitat i forta capacitat de sorció, per a la seva aplicació al tractament d'aigua i aigües residuals.

En aquest context, s'ha estudiat la viabilitat d'utilitzar diferents nanomaterials per a l'eliminació de cadmi (II), plom (II) i crom (VI) dissolts en aigua. Els nanomaterials utilitzats podrien agrupar-se en tres principals grups: i) nanopartícules (NPs) d'òxids metàl·lics (NMOS), òxid de ceri (CeO_2), òxid de titani (TiO_2) i òxid de ferro (Fe_3O_4), ii) polímers basats en catecol que formen nanopartícules i iii) nanomaterials d'òxid de grafè (GO) i NPs de CeO_2 unides a òxid de grafè reduït (RGO). Es va determinar la viabilitat de l'ús de MNOs per l'adsorció de Cd (II) dissolt i es van obtenir els paràmetres cinètics i d'adsorció. En el cas de les NPs de CeO_2 es van assajar diferents paràmetres de funcionament, concretament, dos pH diferents i en sistemes uni / multi components. Els resultats mostren que les NPs són capaces d'eliminar ions metàl·lics en els dos sistemes, afavorint-se el procés a pH alt. Els experiments d'adsorció amb les NPs de catecol es van realitzar utilitzant carbó activat com a adsorbent de referència, obtenint-se una major capacitat d'adsorció amb les NPs. També es van realitzar assajos amb microorganismes bioluminescents i assajos de citotoxicitat per avaluar la toxicitat del nanomaterial. Finalment, es van caracteritzar i utilitzar en processos d'adsorció el GO i els nanomaterials CeO_2/RGO. Per l'acoblament del CeO_2 en la superfície del GO es van seguir dues estratègies diferents, el creixement in situ i l'enfocament d'auto-acoblament. Els resultats

van mostrar que aquests nanomaterials presenten una gran afinitat pels ions Pb (II); obtenint-se altes capacitats d'adsorció a baixes concentracions inicials de metall.

En conclusió, els nanomateriales utilitzats en aquest estudi van mostrar resultats prometedors en l'eliminació de metalls pesants, d'aquesta manera es reafirma, un cop més, que els nanomaterials poden ser utilitzats com a adsorbents eficaços per al tractament d'aigua i d'aigües residuals.

1. General introduction, objectives and thesis outline

1.1. General Introduction

It is very appropriate to say that water is vital, both as universal solvent as well as being an important component of metabolic process within the human body. Clean and fresh water is essential for the existence of life [1]. However, the world's supply of fresh water is running out and the contaminant levels allowed are getting stringent, which generate challenges to meet these standards.

Heavy metal contamination of wastewater is of significant concern worldwide because the release of these metals into aquatic and soil environments potentially impacts human health and ecosystems. Heavy metals are considered to be the most important pollutant in source and treated water due to their non-biodegradable nature and hence, their tendency to accumulate for long time. Some of these toxic elements are cadmium, lead and chromium. Heavy metal toxicity could result, for instance, from drinking-water contamination (e.g. lead pipes), increased ambient air concentrations near sources of emission, or ingestion via the food chain. The increased use of heavy metals in industry has resulted in increased availability of metallic substances in natural water sources [2–4]. Therefore, the development of new technologies to improve the quality in the area of water treatment is fundamental.

One of the promising technologies is based on nanotechnology devices and products. Nanotechnology is the engineering of functional systems at the molecular scale (1-100nm), which offer new products and process alternatives for water purification. The main advantage of using nanoparticles compared to conventional materials is the high surface area, which means a large space for the development of chemical reactions, physic interchanges, etc. In addition to that, nanomaterials effectively remove contaminant even at low concentrations, generate less waste post-treatment and novel reactions take place at nonmetric scale due to the increase of the number of surface atoms [1].

1.2. Objectives

With the previous framework in mind, the main purpose of the present work is to explore the possibilities of using a series of nanomaterials (cerium, iron and titanium oxides

nanoparticles, catechol-based nanoparticles and cerium oxide nanoparticles attached to reduced graphene oxide) for the adsorption of dissolved cadmium (II), lead (II) and chromium (VI) in single and in multicomponent systems. To achieve this general objective, the work described in this thesis has been organized to fit the following specific objectives:

a) Specific objectives regarding the adsorption process using cerium, titanium and iron oxide nanoparticles.
    - To obtain the adsorption isotherms for each metal oxide nanoparticle, as well as, the kinetics isotherms for the removal of cadmium (II).
    - To use the cerium oxide nanoparticles in a multicomponent system (cadmium, lead and chromium) using a factorial experimental design at two different pH.
b) Specific objectives regarding the adsorption process using catechol-based nanoparticles.
    - To test the adsorption capacity for the removal of cadmium (II), lead (II) and chromium (VI) of the novel nanoparticles using a factorial experiment design.
    - To use activated carbon as a comparative adsorbent.
    - To test the toxicity of the nanoparticles using a bioluminescent test and a cytotoxicity assay.
c) Specific objectives regarding the adsorption process using cerium oxide nanoparticles attached to reduced graphene oxide.
    - To synthetized graphene oxide.
    - To anchor cerium oxide nanoparticles to reduced graphene oxide by two different approaches, the self-assembly and the in-situ growth.
    - To characterize the nanomaterials using TEM and Raman instrumental techniques.
    - To evaluate the final nanomaterials for the removal of cadmium (II), lead (II) and chromium (VI) obtaining the adsorption isotherms.

1.3. Thesis outline

This document is divided into six chapters.

Chapter 1 gives a general introduction follow by the objectives and the thesis outline.

Chapter 2 comprises the literature review, with the aim to give a framework in which the nanotechnology for the water/wastewater presents itself as an emerging and competitive method for the removal of heavy metal and the importance of its elimination.

Chapter 3 contains a description of the colorimetric methodology used to test the heavy metals.

The main results obtained in this work are presented in Chapter 4, which itself is divided into four sections:

Section 4.1 includes the adsorption and kinetics experiments for the removal of cadmium using metal oxide nanoparticles.

Section 4.2 describes the adsorption of multicomponent systems at two different pH using CeO_2 NPs. The empirical modeling for the adsorption of each metal is also obtained.

Section 4.3 discusses the adsorption capacity of the catechol-based nanoparticles at low concentrations as well as the assessment of the novel nanoparticles by two different toxicity test, bioluminescent and cytotoxicity.

Section 4.4 details three different pathways to synthesize a nanomaterial based on cerium oxide nanoparticles and graphene oxide, as well as the characterization and the application in the removal of the three heavy metals, in collaboration with the Trinity College (Dublin). Is worthwhile to observe that, the methodology used in Section 4.1 and 4.2 to synthesized cerium oxide nanoparticles has been modified to obtain these nanoparticles anchored to the graphene oxide.

In section 4.5 a summary of the adsorption capacities obtained in this work are shown.

Chapter 5 presents a preliminary study for the removal of heavy metals in real wastewaters with cerium oxide nanoparticles. Also in this chapter some results of the use metallurgical slag as adsorbent for the removal of heavy metals are shown. These results were obtained as a result of collaboration with the Universidad Nacional Autónoma de México.

Finally, Chapter 6 contains the general conclusions and future work, follow by the references.

2. *Literature review*

2.1. Water pollution and water pollutants

The water crisis is the number one global risk based on impact to society (as a measure of devastation), and the number eight global risk based on likelihood (likelihood of occurring within 10 years) as announced by the World Economic Forum [5].

The challenge of providing and ensure clean and fresh water is rapidly growing as the world's population increases, there are currently more than 0.78 billion people around the world who do not have access to safe water resources [6], causing major health problems. Furthermore the estimation of 9 billion of habitants by 2050, increase the concern that water supply will become even more important in the near future [7]. Global climate change also threatens to take away a large fraction of already scarce fresh water resource due to seawater intrusion, municipal and industrial wastes that continue to pollute water supplies and larger quantities of water are used to produce increasing amounts of energy from traditional sources [8]. Clean water is also a critical feedstock in a variety of key industries including electronics, pharmaceuticals and food [9].

Although the nature of pollutants may vary, they are typically due to inadequate sanitation, algal blooms fertilized by the phosphorous and nitrogen contained in human and animal wastes, detergents and fertilizers, pesticides, chemicals, heavy metals, salinity caused by widespread and inefficient irrigation and high sediment loads resulting from upstream soil erosion [10]. Among the aquatic pollutants, heavy metals have gained relatively more significance in view of their persistence, bio-magnification and toxicity [11]. Heavy metals can easily enter the food chain through a number of pathways and cause progressive toxic effects with gradual accumulation in living organisms over their life span. Therefore, reliable methods are needed to remove heavy metals from water and to detect it in environmental and biological samples [12].

A great deal of effort has been devoted to the effective removal of heavy metal ions. The most widely used methods for removing heavy metals from wastewaters include ion exchange, chemical precipitation, reverse osmosis, evaporation, membrane filtration and adsorption. However, research interest in the production of effective and cheaper

adsorbents (used in adsorption process) to replace costly wastewater treatment methods, are attracting attention of scientists [13,14].

2.2. Characteristics of heavy metals and its environmental impacts

Heavy metals are significant environmental pollutants, and their toxicity is a problem of increasing significance for ecological, evolutionary, nutritional and environmental reasons. The term ‘‘heavy metals’’ refers to any metallic element that has a relatively high density and is toxic (non-biodegradable) or poisonous even at low concentration [15]. This is because many inorganic metals are non-biodegradable and may have a carcinogenic effect even at low concentrations. Heavy metals such as Cr(VI), Pb(II) and Cd(II), commonly found in the effluents of mining industries, batteries industries,… have been identified by USEPA as priority and toxic pollutants and should be treated before discharging into municipal sewers [16].

2.3. Occurrence of heavy metals

Lead

Lead occurs in 0 and +2 oxidation states. Pb(II) is the more common and reactive form of lead. Low solubility compounds are formed by complexation with inorganic (Cl^-, CO_3^{2-}, SO_4^{2-}, PO_4^{3-}) and organic ligands (humic and fulvic acids, EDTA, amino acids) [17].

Lead was widely used for more than 5000 years because this metal is corrosion resistant, dense, ductile and malleable. Therefore, was used for building materials, pigments to glaze ceramics, water pipes, ammunition, ceramics glazers, glass and crystals, paints, protective coatings, acid storage batteries, gasoline additives, cosmetics (face powders, lipstick, mascara, etc.), spermicidal (e.g. for birth control), and as a wine preservative (stops fermentation). Due to its wide application, humans are exposed to lead derivatives and have a daily lead intake by food, drinking water and by inhalation [18]. However, this exposure to environmental lead was relatively low before the industrial revolution but has increased with industrialization and large-scale mining. Globally, the extensive processing of lead ores is estimated to have released about 300 million tons of lead into the environment over the past five millennia, mostly within the past 500 years [19].

Cadmium

Cadmium is regularly found in ores together with zinc, copper and lead. Cadmium show only valence "+2" in their compounds; they are also generally similar in reactivity, zinc being the more reactive, and cadmium showing a slightly greater tendency to form covalent bonds, especially with sulfur [20]. Cadmium is widely used in industrial processes, e.g.: as an anticorrosive agent, as a stabilizer in PVC products, as a color pigment, a neutron absorber in nuclear power plants or in the fabrication of nickel-cadmium batteries [21]. Phosphate fertilizers also show a big cadmium load. Although some cadmium-containing products can be recycled, a large share of the general cadmium pollution is caused by dumping and incinerating cadmium-polluted waste. Total global emission of cadmium amounts to 7000 t/year [22].

Chromium

Chromium can exist in several chemical forms displaying oxidation numbers from 0 to VI [23]. Only two of them, trivalent and hexavalent chromium, are, however, stable enough to occur in the environment. Cr(IV) and Cr(V) form only unstable intermediates in reactions of trivalent and hexavalent oxidation states with oxidizing and reducing agents, respectively [24]. The distribution of chromium species in an aqueous solution is shown in Figure 2.1, from pH 0 to 14.

Trivalent chromium (chromium III) exists in natural waters in hydrolyzed $Cr(H_2O)_4OH_2^+$ form and complexes and even adsorbed on colloidal matter. It is an essential micronutrient in the body and combines with various enzymes to transform sugar, protein and fat. Chromium (III) is also used in a number of commercial products, including dyes, paint pigments and salts for leather tanning [25].

Hexavalent chromium (chromium VI), which is found as CrO_4^{2-}, $HCrO_4^-$ or $Cr_2O_7^{2-}$, depending on the pH of the medium. It is known to be carcinogenic and mutagenic and it induces dermatitis [26]. It occurs in a range of compounds used in industrial processes, such as chrome plating. Cr(VI) and Cr(III) enter the environment as a result of effluent discharged from industries and cooling-water towers. Chromium can also enter drinking

water supply systems via corrosion inhibitors used in water pipes and containers or via contamination of underground water leaching from sanitary landfill [25].

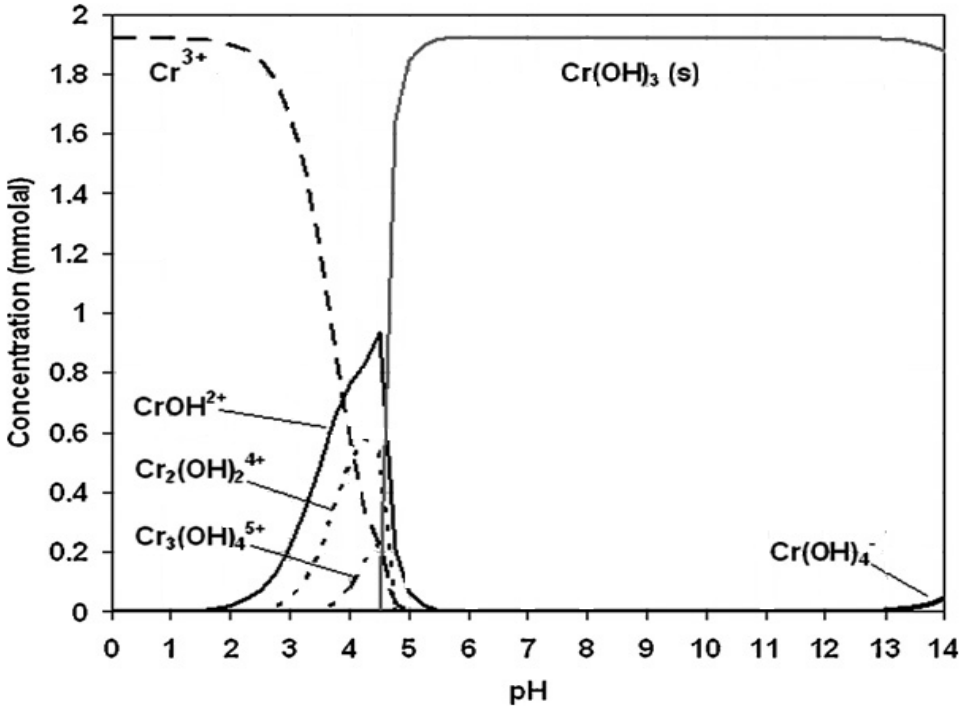

Figure 2.1 Distribution of Cr(VI) species at Different pH. Adapted from García-Reyes et al. [27].

The local increase in chromium concentration in waters (mainly in rivers) is caused by discharge of wastewater from the metallurgical industry, electroplating and tanning industries, from dying, from sanitary landfill leaching, water cooling towers and other chemical industries. The number and type of chromium species present in effluents depend on the character of the industrial processes using chromium [24].

2.4. Contamination of: Cadmium Chromium, lead

Heavy metal pollution can originate from both, natural and anthropogenic sources. There are different sources of heavy metals in the environment such as, natural sources (geologic parent material or rock outcroppings), agricultural sources (inorganic and organic fertilizers), atmospheric deposition (vehicle exhaust, tires, asphalt wear, gasoline/oil leakage, etc.) and industrial sources (smelting and metal finishing and recycling of metals,

mining, etc.) [15,28]. Table 2.1 shows some of the metals contained into the waste effluents of different industries.

Other sources for the metal wastes include; the wood processing industry where a chromated copper-arsenate wood treatment produces arsenic containing wastes; inorganic pigment manufacturing producing pigments that contain chromium compounds and cadmium sulfide. All of these generators produce a large quantity of wastewaters, residues, and sludges that can be categorized as hazardous wastes requiring extensive waste treatment [29].

Table 2.1. Occurrence of metals or their compounds in effluence from various industries [15].

	Metals																														
Industry	Al	Ag	As	Au	Ba	Be	Bi	Cd	Co	Cr	Cu	Fe	Ga	Hg	In	Mn	Mo	Os	Pb	Pd	Ni	Sb	Sn	Ta	Ti	Tl	U	V	W	Zn
Mining operations and ore processing	X		X					X						X		X	X		X								X	X		
Metallurgy and electroplating		X	X			X	X	X		X	X			X	X				X		X								X	X
Chemical industries	X		X		X			X		X	X	X	X	X				X	X			X	X	X	X		X			X
Dyes and pigments	X		X					X			X	X							X			X			X	X				
Ink manufacturing									X		X	X		X							X									
Pottery an porcelain			X							X												X					X			
Alloys					X	X							X		X			X		X				X						
Print										X								X	X						X					X
Photography		X		X				X		X							X			X							X			
Glass			X		X				X												X			X	X			X		
Paper mills	X									X	X			X						X		X		X	X			X		
Leather training	X		X		X					X	X	X		X																X
Pharmaceuticals	X										X	X	X	X				X												
Textiles	X		X		X			X			X	X		X				X			X	X								
Nuclear technology					X			X							X												X			X
Fertilizer	X		X					X		X	X	X		X		X				X	X									X
Chlor-alkali production	X		X					X		X		X		X		X				X			X							X
Petroleum refining	X		X							X		X	X	X					X		X									X

Cadmium, lead and chromium are significant environmental pollutants, and their toxicity is a problem of increasing significance for ecological, evolutionary, nutritional and environmental reasons [15]. Due to that, safe limits or maximum contaminant levels have been defined for drinking water by different organizations. Table 2.2 show the standards and guidelines in drinking water recommended by the World Health Organization (WHO) and Environmental Protection Agency (EPA) and the Council of European Union (EU) for chromium, lead, cadmium [30,31].

Table 2.2. Standards and guidelines for heavy metals in drinking water recommended by the WHO and EPA.

Metal	WHO (mg/L)	EPA (mg/L)	EU (mg/L)
Pb	0.01	0.015	0.01
Cr	0.05	0.10	0.05
Cd	0.003	0.005	0.005

2.5. Heavy metal removal technologies

Heavy metals contaminated wastewaters have been treated with different techniques with the aim of decreasing the generation of these wastewaters and also to improve the quality of the treated effluent. Although various treatments such as ion exchange, chemical precipitation and adsorption can be employed to remove heavy metals from contaminated wastewater, each one has their inherent advantages and limitations [32].

2.5.1. Chemical precipitation

Chemical precipitation is widely used for heavy metal removal from effluents [33]. After pH adjustment to the basic conditions, the dissolved metal ions are converted to the insoluble solid phase via a chemical reaction with a precipitant agent (Figure 2.2) [32]. Lime and calcium carbonate are used as precipitant agent however, sulfide precipitation result as a more effective process for the treatment of industrial waste containing highly toxic heavy metals. The attractive features of this process are the effective precipitation of

certain metals even at very low pH levels as well as attainment of a high degree of metal removal over a broad pH range and fast reaction [34].

Nevertheless, some disadvantages of the chemical precipitation are the large amount of chemicals to reduce metals to an acceptable level for discharge, as well as the substantial production of sludge, containing also precipitant agents, that requires further treatment due the long-terms environmental impacts of sludge disposal. Moreover, the precipitating agents not only increase the cost of the process but, also precipitated with the metals therefore; the presence of these chemicals has to be taken into account when performing the post-treatment of sludge [32].

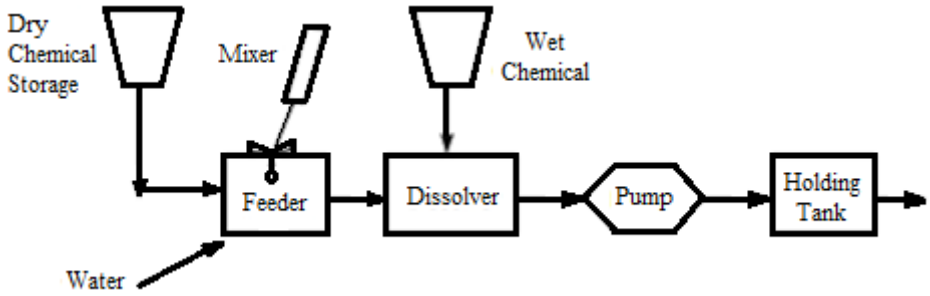

Figure 2.2. Chemical precipitation treatment process [33].

2.5.2. Ion exchange

Ion exchange process seems to be very effective to remove several heavy metals from wastewater, one of the advantages of this process is that the resin can be easily recovered and reused by regeneration operation. The process is based in the exchange of ions from the solution to a solid matrix which, in turn release ions of a different type but of the same charge (Figure 2.3). Ion exchange is a physical separation process in which the ions exchanged are not chemically altered [35].

The most common cation exchangers are strongly acidic resins with sulfonic acid groups (-SO_3H) and weakly acid resins with carboxylic acid groups (-COOH). Hydrogen ions in the sulfonic group or carboxylic group of the resin can serve as exchangeable ions with metal

cations. As the solution containing heavy metal passes through the cations column, metal ions are exchanged for the hydrogen ions on the resin [36].

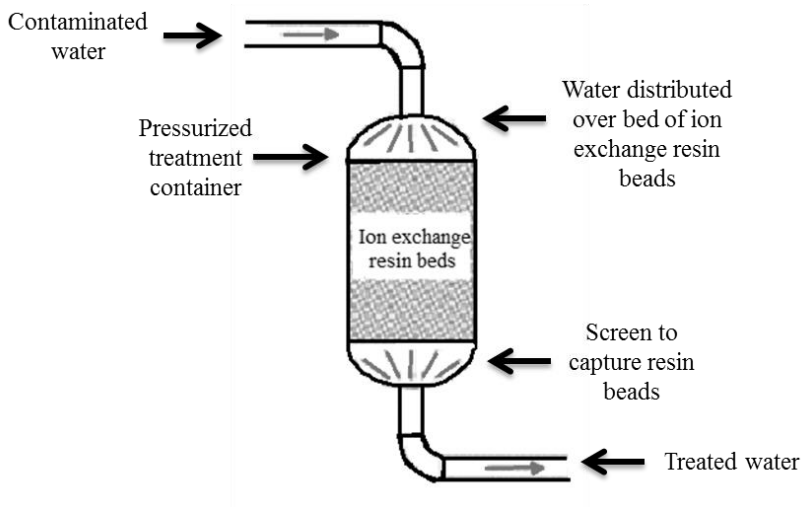

Figure 2.3. Ion exchange treatment process

Selectivity is achieved by new types of ion exchangers with specific affinity to definite metal ions or groups of metals. For the elimination of lead, cation exchanger chelating with functional aminophosporic and phosponic groups are applied. In the case of cadmium, chelating ion exchangers containing also phosphonic groups as well as chelating resin based on sulphonic groups twinned with diphosphonic groups are widely used [37].

In the removal of chromium (VI), the initial solution is purified by passing through the strongly acidic polystyrenesulphonic cation exchanger and subsequently through strongly basic anion exchanger metal ions and other cationic impurities are removed on the cation exchanger whereas chromates on the anion exchanger [38].

Regardless of these advantages, ion exchange also has some limitations in treating wastewater with heavy metals. Appropriate pretreatment systems for the effluent, such as the removal of suspended solids from wastewater previous to ion exchange is required, moreover suitable ion exchange resins are not available for all heavy metals [32].

2.5.3. Adsorption process

Sorption is the transfer of ions from water to the soil, i.e from solution phase to the solid phase (Figure 2.4). Sorption actually describes a group of processes, which includes adsorption and precipitation reactions [29,32,39]. Adsorption is now recognized as an effective and economic method for heavy metal wastewater treatment. The adsorption process offers flexibility in design and operation and in many cases will produce high-quality treated effluent. In addition, because adsorption is sometimes reversible, adsorbents can be regenerated by suitable desorption process [36].

Sorbents are widely used as separation media in water purification to remove inorganic and organic pollutants from contaminated water [9]. An adsorbent material must have some important properties, such as, high internal volume accessible to the different target components, a high surface area, particularly the internal surface area, pore size distribution and the nature of the pores that markedly influence the type of adsorption processes. [40].

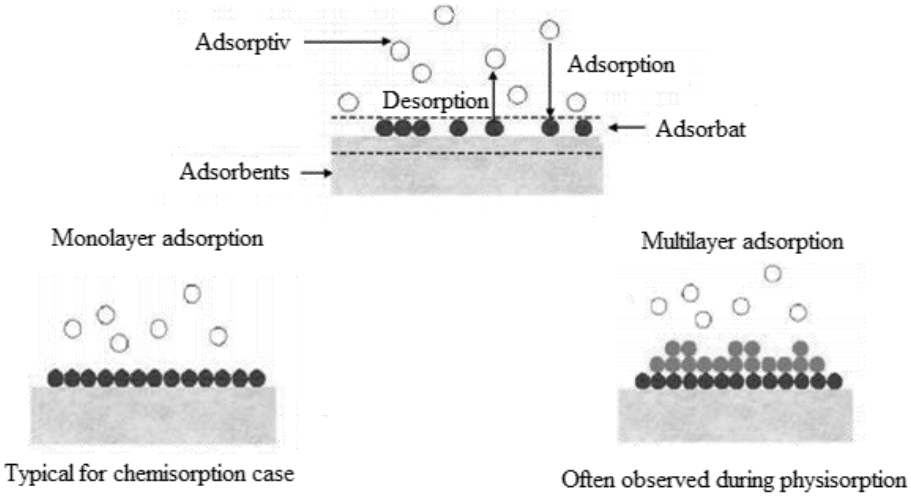

Figure 2.4. Adsorption process and adsorption types [41].

It is also important that the adsorbent has good mechanical properties such as strength and resistance to destruction and particles of appropriate size and form. The chemical properties of the adsorbent, namely, degree of ionization at the surface, types of functional groups present, and the degree to which these properties change in contact with the solution are

important considerations in determining the adsorption capacity of a solid. The presence of active functional groups on the adsorbent surface allows chemical interactions that usually produce effects different from and less reversible than physical adsorption

Researches have been experimenting with all kinds of material to obtain an optimal adsorbent of heavy metal, from activated carbon that is also the most common to clay minerals [39], chitosan [42], agricultural waste, bioadsorbents, fly ash [43], carbon nanotubes and metal oxide nanoparticles, with the last ones very promising results in the removal of heavy metals were obtained, which could lead to a deep removal of toxic metals to meet increasingly strict regulations. However we have to keep in mind that the technical applicability and cost-effectiveness are the key factors that play major roles in the selection of the most suitable adsorbent to treat inorganic effluent [29].

2.5.3.1 Adsorption isotherm

When the retention of a solute on solid particles is investigated, the remaining solute concentration of the compound C (mg/L) can be compared with the concentration of this compound retained on solid particles q (mg/g). The relationship q = f(C) is named the ‘‘sorption isotherm’’. The uniqueness of this relation requires several conditions to be met: (i) the various reaction equilibria of retention/release must have been reached, and (ii) all other physico-chemical parameters must remain constant. The word ‘‘isotherm’’ was specifically chosen because of the influence of the temperature on sorption reactions; temperature must be kept constant and specified [44,45]. Giles et al. [46] classified sorption isotherms based on their initial slopes and curvatures. They distinguished between high affinity (H), Langmuir (L), constant partition (C), and sigmoidal-shaped (S) isotherm classes (Figure 2.5).

The ‘‘C’’ isotherm: the curve is a line of zero-origin (Figure. 2.5a). It means that the ratio between the concentration of the compound remaining in solution and adsorbed on the solid (K_d) remain the same at any concentration [47]. This isotherm is often used as an easy-to-use approximation (for a narrow range of concentration or very low concentrations such as observed for trace pollutants) rather than an accurate description. For example, if the solid

has a limited quantity of adsorption sites, the isotherm could be nonlinear because of a possible saturation plateau [48].

The ‘‘L’’ isotherm: correspond to a decrease of site availability as the solution concentration increases, providing a concave curve (Figure 2.5b), suggesting a progressive saturation of the solid [49]. One usually makes two sub-groups: (i) the solid has a limited sorption capacity, and (ii) the solid does not show clearly a limited sorption capacity [48].

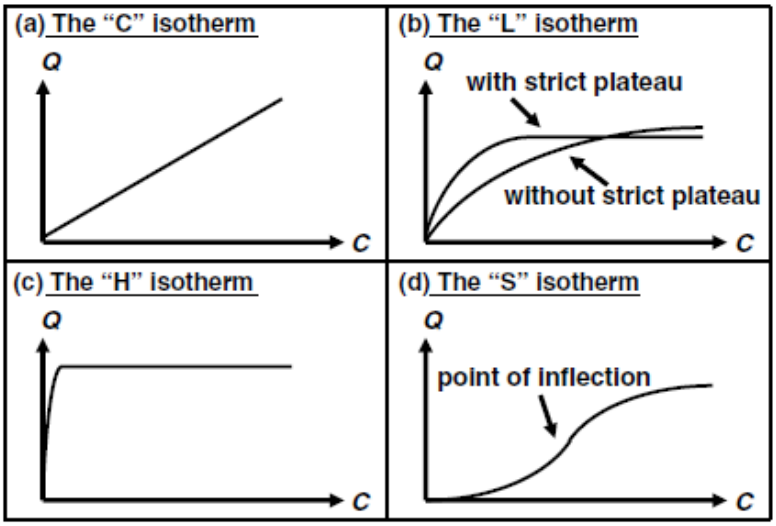

Figure 2.5. The four main types of isotherms [48].

The ‘‘H’’ isotherm: this is only a particular case of the ‘‘L’’ isotherm, where the initial slope is very high (Figure 2.5c). This case was distinguished from the others because the compound exhibits sometimes such a high affinity for the solid that the initial slope cannot be distinguished from infinity, even if it does not make sense from a thermodynamic point of view [50].

The ‘‘S’’ isotherm: the curve is sigmoidal and thus has got a point of inflection (Figure 2.5d). This type of isotherm implies that adsorption becomes easier as the concentration in the liquid phase increases. As far as adsorption is concerned, means that the solute molecule has a fairly large hydrophobic part and a marked localization of the force of attraction for the substrate. For a given molecule, this character may depend on both the nature of the adsorbent surface and the nature of the solvent [49]. The point of inflection illustrates the concentration for which the adsorption overcomes the complexation [48].

2.5.3.2 Adsorption isotherms models

The Langmuir isotherm assumes monolayer adsorption on a uniform surface with a finite number of adsorption sites. Once a site is filled, no further sorption can take place at that site. As such the surface will eventually reach a saturation point where the maximum adsorption of the surface will be achieved. The linear form of the Langmuir isotherm model is described as:

$$C_e/q_e = 1/K_L q_m + C_e/q_m \quad (1)$$

where K_L is the Langmuir constant related to the energy of adsorption and q_m is the maximum adsorption capacity (mg/g) [51,52].

The Temkin isotherm model assumes that the adsorption energy decreases linearly with the surface coverage due to adsorbent–adsorbate interactions. The linear form of Temkin isotherm model is given by the equation:

$$q_e = Rt/b \ ln \ K_T + RTblnC_e \quad (2)$$

where b is the Temkin constant related to the heat of sorption (J/mol) and K_T is the Temkin isotherm constant (L/g) [52,53]

The Freundlich isotherm is applicable to both monolayer (chemisorption) and multilayer adsorption (physisorption) and is based on the assumption that the adsorbate adsorbs onto the heterogeneous surface of an adsorbent. The linear form of Freundlich equation is expressed as:

$$log \ q_e = log \ K_F + 1/n \ log \ C_e \quad (3)$$

where K_F and n are Freundlich isotherm constants related to adsorption capacity and adsorption intensity, respectively and C_e is the equilibrium concentration (mg /L) [51,52]. A value of n ~1 reduces Equation 3 to the linear isotherm typically observed for the adsorption of dyes onto solid adsorbents [54].

2.5.3.3 Kinetic isotherms models

Two models were proposed to fit the experimental kinetic data: pseudo first-order and pseudo second-order. Pseudo first-order kinetics simply an adsorption site in the NP surface for each cadmium atom and may be expressed as Equation 4:

$$log(q_e - q_t) = log\ q_e - (k_1/2.303)t \quad (4)$$

where q_e and q_t (mg/g) are the adsorption capacities at equilibrium (steady state, infinite time) and at any time t, respectively, and k_1 (h^{-1}) is the first order kinetic constant.

The pseudo second-order kinetic model is widely used [54] and it is normally applied to describe chemical adsorption in liquid media. The model is expressed as Equation 5:

$$t/q_t = 1/k_2 q^2_e + (1/ q_e)t \quad (5)$$

where k_2 (g/mg h) is the second order kinetic constant and the rest of parameters are the same as those presented in Equation 4.

2.6. Nanotechnology and water/wastewater treatment: a general vision

Nanotechnology is the understanding and control of matter at dimensions of roughly 1–100 nm, where unique phenomena enable novel applications. Figure 2.6 shows the comparison of nanomaterials with large-sized materials. Nanotechnologies are the design, characterization, production and application of structures, devices and systems by controlling shape and size at nanometer scale [55]. When referring to nanoscale materials a combination of chemistry and physics occur mainly to develop novel properties of matter [56].

At this scale, materials often possess some novel size-dependent properties such as, high specific surface area, short intraparticle diffusion distance, more adsorption sites, compressible without significant surface area reduction, easy reuse, some are superparamagnetic [57]. Therefore its suggested that nanotechnology holds out the promise of immense improvements in manufacturing technologies, electronics, telecommunications, health and even environmental remediation [58] . Within the category of treatment and

remediation, nanotechnology has the potential to contribute to long-term water quality, availability, and viability of water resources, such as through the use of advanced filtration materials that enable greater water reuse, recycling and desalinization [10].

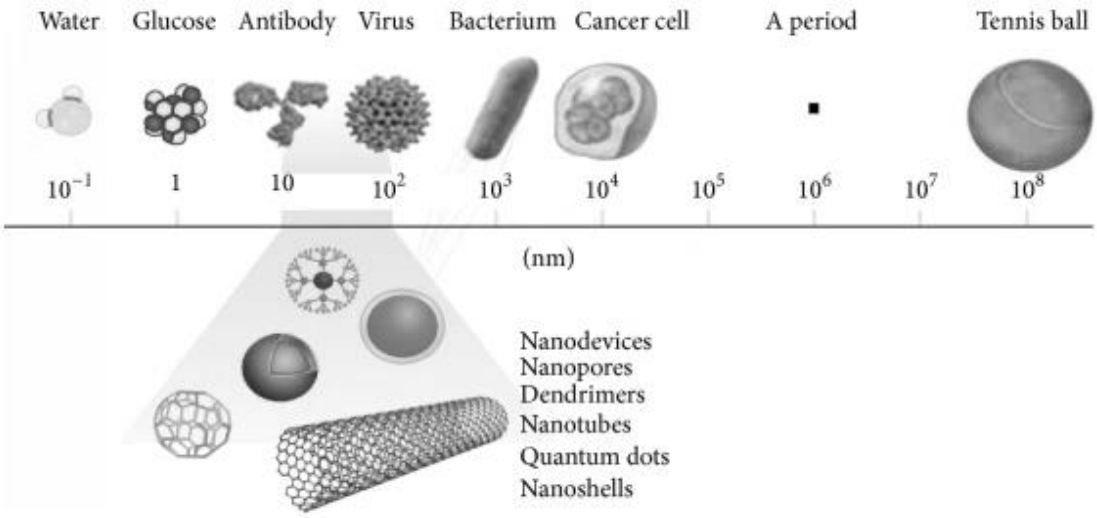

Figure 2.6. A size comparison of nanoparticle with other larger-sized materials [59].

Nanomaterial properties desirable for water and wastewater applications include high surface area for adsorption, high activity for (photo) catalysis, antimicrobial properties for disinfection and biofouling control, superparamagnetism for particle separation, and other unique optical and electronic properties that find use in novel treatment processes and sensors for water quality monitoring. Nanoparticles can infiltrate deeper in water and thus can treat water/wastewater which is generally not possible by conventional technologies [59,60].

Depending on practical applications, nanoscale particles regardless of engineered or natural ones, so far seen to fall into four basic categories: i) metal oxides, which is the group with the largest numbers of commercial nanomaterials, ii) nanoclys, naturally occurring plate like clay particles that strengthen or harden the materials or make them flame-retardant iii) nanotubes, which are tubular derivatives of fullerenes and used in coatings to dissipate or minimize static electricity and iv) quantum dots used in exploratory medicine or in the self-assembly of nanoelectronic structures. [55,61].

2.6.1. Production and application of nanoparticles

In general, manufactured NPs can be classified according to their chemical composition and properties. They can be produced by a huge range of procedures which can be grouped into top-down and bottom up strategies (Figure 2.7) [62].

Top-down approaches are defined as those by which NPs or well-organized assemblies are directly generated from bulk materials via the generation of isolated atoms by using various distribution techniques. The majority of the top-down strategies involve physical methods such as milling or attrition, repeated quenching and photolithography [55,62].

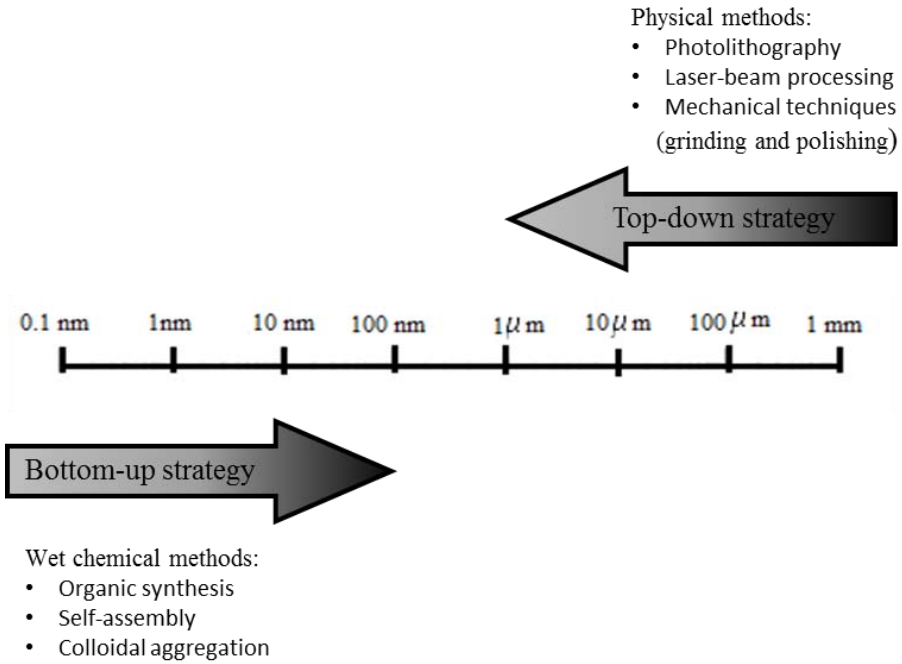

Figure 2.7. Top down and top bottom strategies [62].

The more convenient method for producing nanoparticles on a commercial scale is to use a bottom-up approach where a nanoparticle is ‘‘grown’’ from simple molecules. The regulation of size of nanoparticles varies with the media of their synthesis, in gas-phase concentration of precursors and temperature of the reaction, whereas in wet-phase, temperature and reaction time control the size of the nanoparticles [63]. The general

differences come from the medium in which the reaction is conducted, and this can play a key role in defining the final properties and surface chemistry of the particle [64].

Liquid-solid transformations are possibly the most broadly used to control morphological characteristics with certain "chemical" versatility and usually follow a "bottom-up" approach [65]. A variety of nanomaterials were used in this work, focused mainly in their application as adsorbents. Therefore, in each chapter we will discuss in more detail the methods employed in the preparation of each of the nanomaterials used.
Nanoparticles are characterized by X-ray diffraction (XRD), scanning electron microscopy (SEM), and transmission electron microscopy (TEM) techniques. The selection of the technique depends on the size, properties, starting materials, and the required applications of nanoparticles [66].

2.6.2. Present use of nanoparticles

A variety of nanomaterials are in various stages of research and development, each possessing unique functionalities that is potentially applicable to the remediation of industrial effluents, groundwater, surface water and drinking water (Table 2.3).

2.6.3. Toxicity

As a result of advances in methods of producing nanoparticles (NPs) with controlled morphology and composition, as well as the incipient development of protocols for large-scale synthesis, in recent years the use of engineered inorganic nanoparticles has increased exponentially [67]. These nanostructures are the base for manufacturing new materials with a variety of applications (e.g. skin creams and toothpastes), where these materials are in direct contact with the user's body or can enter the environment on a continual basis from the removal of such products [68].

Although the use of NPs for environmental remediation could help to reduce the cost of the process, the benefit obtained has to be balanced with the potential risks [69]. Nevertheless, little attention has so far been paid to the toxicity of nanoparticles made of heavy metals and their oxides. Any understanding of the toxicity of manufactured nanomaterials needs to look beyond the effects on cells and consider the systemic effects on higher organisms.

Several investigators have found that, at high doses of different nanoparticles, cytotoxic effects emerge in a dose- and time-dependent manner [70].

Table 2.3. Examples of nanoparticles and nanomaterials for use in water purification.

Nanoparticle/Nanomaterial	Pollutant	Reference
Nanocrystalline zeolites	Toluene, nitrogen dioxide	[71,72]
Carbonaceous nanomaterials		[73]
Activated carbon fibers (ACFs)	Benzene, toluene, xylene, ethylbenzene	[74,75]
CeO_2-carbon nanotubes (CNTs)	Heavy metal ions	[76]
CNT functionalized with Fe	Dimethylbenzene, Heavy metal ions	[77,78]
Zero-valent iron nanoparticles (nZVI)	Polychlorinated biphenyls (PCBs), inorganic ions, chlorinated organic compounds, heavy metal ions	[79–85]
TiO_2 photocatalysts Nanocrystalline TiO2	Heavy metal ions	[86]
Pt, Pd	Antimicrobial	[87–89]
Al_2O_3	Metal ions and biosorbent	[90]

The toxicities of nanoparticles are because of their shape, size, and greater surface area to volume ratio. These properties lead to high chemical reactivity and biological activity, which results into greater chemical reactivity and production of reactive oxygen species (ROS). The generation of ROS has been reported as the property of carbon fullerenes, carbon nanotubes, and metal oxide nanoparticles. The production of ROS and free radicals is one of the primary mechanisms of nanoparticle toxicity. The presence of ROS and free radicals may cause oxidative stress, inflammation, and consequent damage to proteins, membranes, and DNA [66,68,70].

One important issue considered in nanotoxicology is the assessment of biocompatibility of nanoparticles. Kirchner et al. [91] distinguish three main causes of nanoparticle toxicity following contact with live cells: i) due to chemical toxicity of materials from which they have been made (e.g. Cd^{2+} is released from nanoparticles of cadmium selenide), ii) due to their small size: nanoparticles may stick to cellular membranes and enter the cells and iii) due to their shape: e.g. carbon nanotubes can easily pierce cell membrane.).

Even there is not an exclusive standardized for NPs suspensions, several tests are commonly applied to waste and drinking water to determine the toxicity of NPs. Such as the bioluminescent test, applied to certain bacteria (*Vibrio fischeri*) [92] or cytotoxicity assays performed using human hepatoma cells (HepG2) [93]. The advantage of these tests is that they are easy to carry out in the laboratory; however the information obtained is not always straightforward mainly because the ultimate cause of toxicity us rarely known [69].

2.6.4. Metal oxide nanoparticles

Metal oxide nanoparticles (NMOs) have been used in a considerable number of applications from food, chemical to biological sciences [62]. Ferric oxides, manganese oxide, aluminum oxide, titanium oxides and cerium oxides are classified as promising ones for heavy metals removal from aqueous systems [94]. Oxide nanoparticles can exhibit unique physical and chemical properties owing to their limited size and a high density of corner or edge surface sites, turning them particularly attractive as sorbents [65]. The size and shape of NMOs are both important factors to affect their adsorption performance, therefore with the aim to obtain shape-controlled, highly stable and monodisperse MNOs, efficient synthetic methods has been extensively studied [94]. The sorption is mainly controlled by complexation between dissolved metals and the oxygen in metal oxides. It is a two-step process: fast adsorption of metal ions on the external surface, follow by the rate-limiting intraparticle diffusion along the micropore walls [57]. The structures of some commonly used nanoparticles for water treatment are given in Figure 2.8.

As for the characterization of NMOs, research efforts focused on their characteristics, such as morphology, size, crystal structure, specific surface area and the pH of zero point of charge (pHpzc) [94]. Through this work NMOs of the cerium oxide (CeO_2) nanoparticles

were mostly used, however the use of others suspension of nanoparticles, such as titanium (TiO_2) and iron oxide (Fe_3O_4) were also tested (Section 4.1 and 4.2).

The adsorptive properties of ceria vary significantly with morphologies, sizes, shapes and surface areas, hence the development of methodologies for the synthesis of monodispersed CeO_2 nanoparticles is the ultimate aim of this field [62,94].

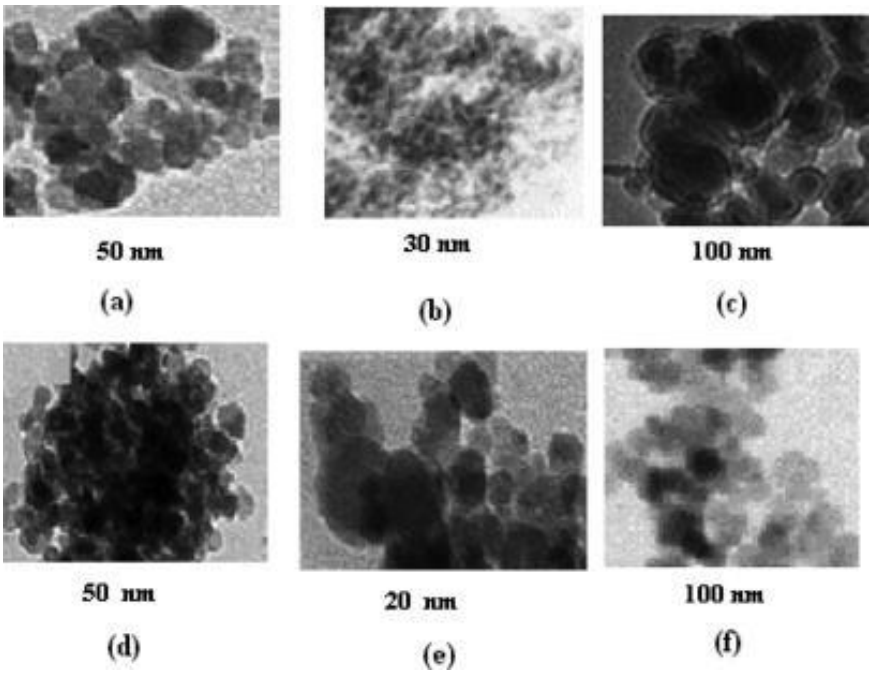

Figure 2.8. TEM images of some nanoparticles with their sizes. (a) maghemite, (b) akaganeite, (c) zerovalent iron, (d) γ-Fe_2O_3, (e) δ-FeOOH, and (f) chitosan bounded Fe_2O4 [66] .

CeO_2 adopts a fluorite-type crystal structure in which each metal cation is surrounded by eight oxygen atoms [65]. The nanoparticles in suspension used by Recillas et al. [95], present an average diameter obtained were 11.7±1.6nm of 6.5nm. These nanocrystals have more cerium atoms per unit of surface than oxygen atoms; these are related with the storage and releasing of oxygen, and the promotion of noble-metal activity and dispersion. Both phenomena are controlled by the type, size, and distribution of oxygen vacancies as the most relevant surface defects [95]. The results obtained for the removal of lead (189mg Pb^{2+}/g CeO_2) and chromium (121.95mg Cr^{6+}/g CeO_2) via adsorption process are promising [95,96].

TiO_2 exists in three main crystallographic structures e.g. anastate, rutile and brookite, each of these present different properties and therefore, different applications and environmental impacts [94,97]. It has been reported that bulk and nanoparticle TiO_2 anatase exhibit different chemical behavior, catalytic reactivity, and surface acidity based on their different surface planes [94]. TiO_2 is one of the most prominent oxide materials for performing various kinds of industrial applications from catalysis, to cosmetics even solar applications [39,65]. TiO_2 nanoparticles with an average size of 7.6 and amorphous shape were used in adsorption process. The adsorption capacity found for the removal of lead was 159 $mgPb^{2+/}gTiO_2$ [96].

Iron oxides exist in many forms in nature. Magnetite (Fe_3O_4), maghemite (γ-Fe_2O_3), and hematite (α-Fe_2O_3) are the most common forms [58]. With small particle sizes (>40 nm), they offer a large surface area and superparamagnetic properties; they are attracted to a magnetic field but do not retain magnetic properties when the field is removed, making them highly useful in novel separation processes [98]. However, the agglomeration and the interference of other compounds could interfere with the adsorption of the metals. Therefore surface modification, which can be achieved by the attachment of inorganic shells and/or organic molecules, not only stabilizes the nanoparticles and eventually prevents their oxidation, but also provides specific functionalities that can be selective for ion uptake and thus enhance the capacity for heavy metal uptake in water treatment procedures [58]. Fe_3O_4 nanoparticles stabilized with tetramethylammonium hydroxide (TMAOH) to avoid agglomeration were tested for the removal of lead. The results showed that the NPs completely removed Pb^{2+} up to 17 mg Pb^{2+}/L [96].

2.6.5. Graphene

As a newly developed member of carbon materials and a basic building block for graphitic materials of all other dimensionalities, graphene is a single atomic layer of graphite with hexagonally bonded and sp^2 hybridized carbons (Figure 2.9) [99]. Graphite can be exfoliated to generate single layers of graphene. This was initially demonstrated by micromechanical exfoliation [100]. Graphene has strong mechanical, thermal, and electrical properties, with a theoretical value of specific surface area at 2630 m^2/g [101].

The utilization of graphene-based materials as adsorbents may offer several advantages. First, single-layered graphene materials possess two basal planes available for pollutant adsorption. Second, graphene oxide (GO) and reduced graphene oxide (RGO) can be easily synthesized through chemical exfoliation of graphite, without using complex apparatus or metallic catalysts [100].

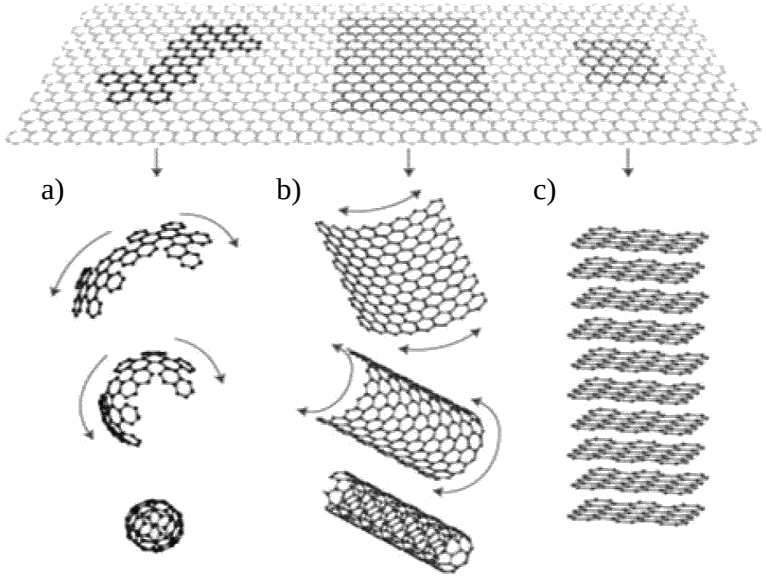

Figure 2.9. Schematic representation of different carbon nanomaterials. a) 0-dimensional buckyballs, b) 1-dimensional nanotubes and c) 3-dimensional graphite [102].

Sreeprasad et al. [103], reported a facile synthetic route for the preparation of reduced graphene oxide (RGO)-metal/metal oxide composites. The method was found to be versatile and applicable for the syntheses of a variety of RGO-composites; their application in water purification was examined. A redox-like reaction between RGO and metal precursor was the major cause for composite formation. As the metal precursors were being reduced, RGO was becoming progressively oxidized primarily to GO and the metal nanoparticles formed were closely anchored onto the carbon sheets [104].

As graphene has plate-like structure and extraordinary properties, there is great interest for using it as an attractive substrate for the deposition of inorganic nanoparticles. On the one hand, the disadvantage of aggregation of graphene sheets can be partly prevented by

intercalating particles within the graphene layers [105]. On the other hand, these composites can impart new functionality to graphene aiming at electronics, optics, sensor and catalytic application through the synergistic effects of individual components [106]. At present several metal/metal compound nanostructures has been composited with graphene or its derivatives, which involve metals (e.g Zn [107], Ag [108], etc.) metal oxides (e.g. TiO_2 [109] or MnO_2[110]). In this work, the CeO_2 nanoparticles were anchored to the surface of the GO and tested for the removal of heavy metal ions (Section 4.4).

2.6.6. Catechol

In the last years, nature has inspired the design and development of novel functional nanoparticles with removal and separation capacities for heavy metals. One example of this fruitful approach has been the fabrication of polydopamine (PDA) materials [111]. Mussels can strongly attach to diverse substrates with high binding strength, even on wet surfaces. Scientists have long investigated the wet adhesion property of mussels and found that it's due 3,4-dihydroxyphenylalanine (DOPA) and lysine-enriched proteins are responsible for the adhesion property [112]. On the basis of these findings, PDA (with a similar structure to DOPA) moves to the spotlight as a novel material. One of the advantages of PDA is that, as seen with mussels, it can be easily deposited on virtually all types of inorganic and organic substrates, including superhydrophobic surfaces, with controllable film thickness and durable stability [113]. The abundant functional groups especially catechol groups of PDA is expected to be the active sites for heavy metals ions, synthetic dyes and other organic pollutants through electrostatic, bidentate chelating, or hydrogen bonding interactions [114].

Although polydopamine can be produced in a facile and simple polymerization process, the molecular mechanism behind the formation of polydopamine has long been the topic of scientific debate, which continues to this day, due to the complex redox process as well as the generation of a series of intermediates during the polymerization and reaction processes [113]. Saiz-Poseu et al. [115], reported alternative and simple polymerization method based on the reaction of a catechol moiety substituted with appropriate functional chains and ammonia. The material showed to spontaneously structure in the form of nanoparticles a few hundred nanometers in diameter in water. Therefore the combination of advantages,

such as ease of preparation, solubility in appropriate solvents and improved surface functionalization, suggest it as a suitable adsorbent for adsorption process (Section 4.3)

2.7. Limitations in the application of nanotechnology to water/wastewater treatment

Although nanotechnology emerges as a promise technology to treat water and wastewater, there are still challenges to overcome. In full-scale applications, the research of the performance of various nanotechnologies in treating real natural waters and wastewaters needs to be tested. Another important issue is the long-term performance of these nanotechnologies is largely unknown, as most lab studies were conducted for relatively short period of time [57].

Broad acceptance of novel water and wastewater treatment nanotechnologies depends on both their affordability and performance. A considerable fraction of the nanomaterial production cost is related to separation and purification. One approach proposed is the production of lower purity nanomaterials without significantly compromising efficiency [60].

Overall it is difficult, to assess the effect of nanomaterials on health and the environment because the methods and tools for such a task have not been well developed yet. In addition, common frameworks for risk research, risk assessment, and risk management are lacking at present. It is vital that these processes be developed and investigated to ensure that nanomaterials are as safe as possible, while reaching their full potential [10].

3. *Analytical methods*

3.1. Synthetic wastewater preparation

Cadmium (II) chloride (99.99% of purity, Sigma Aldrich, Spain), lead (II) nitrate (99.99% of purity, Sigma Aldrich, Spain) and potassium dichromate (VI) (99.5% of purity, Panreac, Spain) were used as metal sources, respectively and diluted in ultra-pure water to be used as stock solutions. The synthetic water is used in the experiments reported in Chapter 4 of this study.

3.2. Heavy metal determination

In this section the determination of metals through colorimetric is described, due to it is applied in several sections. However, the specific materials and methods for the determination of the heavy metals could be found in each section.

3.2.1. Spectrophotometry methodology

For heavy metals analysis the Cary 50 Bio-UV-Visible Spectrophotometer was used. The calibration curves are prepared from the stock solutions to contain 1, 3, 5, 7 and 10 mg of each heavy metal ion and measured at the corresponding wavelength.

3.2.2. Cadmium (II)

Cadmium ions under suitable conditions react with dithizone to form a pink to red color complex that can be extracted with chloroform ($CHCl_3$). Chloroform extracts are measured photometrically and cadmium concentration is obtained from calibration curve prepared from a standard solution treated in the same manner as the sample.

To form the complex of cadmium the reagents are added to the samples in the following order: 0.25l ml of $NH_2OH{\cdot}HCl$ (200 mg/ml) solution, 15 ml of dithizone (10mg/L) and 5 ml of NaOH-KCN (NaOH- 400mg/ml; KCN-0.5 mg/ml). The mixture is shacked for 1 minute and then allowed to phase separation. Finally, discharge the $CHCl_3$ layer making as close as the separation as possible. The absorbance is measured at 518 nm. Due to the non-interference of other metals in the analytical technique used, the determination of cadmium was performed in a single extraction [116].

3.2.3. Lead (II)

A sample containing lead (II) is mixed with ammoniacal citrate-cyanide reducing solution and extracted with dithizone in $CHCl_3$ to from a cherry-red lead dithizonate. The calibration curve is prepared to contain 1, 3, 5, 8 and 10 mg of Pb^{2+}. The reagents are added to the samples in the following order: 12.5 ml of a solution containing 50g of dibasic ammonium citrate, 2.5 g of anhydrous sodium sulfite, 1.25 g of hydroxylamine hydrochloride, 5 g of potassium cyanide in 125 ml of water and 250ml of NH_4OH follow by 2.5 ml of dithizone (40mg/L). Shake for 1 minute, then phase is allow to separate follow by the discharge. The color of the mixed colored solution is measured photometrically at 510 nm [116].

3.2.4. Chromium (VI)

This procedure measures only hexavalent chromium. Therefore, is determined colorimetrically by the reaction with diphenylcarbazide in acid solution. A red-violet color of unknown composition is produced. To determine total chromium, 1 ml of sample is acidified with 60 µL of H_3PO_4 and the pH is adjusted to 1.00 (± 0.03) in 25 ml of water. Finally 0.5 ml of 1,5-diphenylcarbazide (5mg/ml) is added and let stand 10 min to the color develop .The absorbance is measured at 540 nm. [116].

4. Results and discussion

4.1 Potential use of CeO_2, TiO_2 and Fe_3O_4 nanoparticles for the removal of cadmium from water

---

The result presented in this chapter has been published in the Desalination and water treatment.

Potential use of CeO_2 , TiO_2 and Fe_3O_4 nanoparticles for the removal of cadmium from water. A.R. Contreras, A. García, E. González, E. Casals, V. Puntes, A. Sánchez, et al., Desalin. Water Treat. 41 (2012) 296–300. doi:10.1080/19443994.2012.664743.

4.1.1. General overview

Cadmium is a heavy metal with important adverse and toxic effects, when released to the environment [117]. As a result of the changes in the guidelines on cadmium, only small quantities of this metal are now released to wastewater from municipal and industrial sources. Nevertheless, this is often in excess of the extremely low recommended limits of cadmium in drinking water: a maximum of 0.003 mg/L is recommended by the World Health Organization [118] and in other countries such as Spain, the permissible limit of cadmium is similar (0.005 mg/L) [119]. Several treatments exist to remove cadmium from water, such as chemical precipitation, electrolysis, ionic exchange and membrane technologies [120,121]. Heavy metal adsorption onto nanoparticles (NPs) is an emerging technique for the removal of these pollutants. The high specific surface of NPs, together with a suitable electric charge given by an adequate Z-potential, makes them excellent candidates for the adsorption of heavy metals [122].

The objective of this part of the study is to explore the possibilities of using cerium oxide (CeO_2), iron oxide (Fe_3O_4) and titanium oxide (TiO_2) NPs for the adsorption of dissolved cadmium. Adsorption isotherms and kinetic models typically used for NPs are also tested to give a base for further studies.

4.1.2. Materials and methods

4.1.2.1. CeO2, TiO2 and Fe3O4 NPs synthesis and characterization

Different types NPs of metal and metal oxide were synthesized in aqueous phase, using milli-Q water. All synthesis are based on methodologies already fully describe elsewhere and available in the literature, with some modifications to suit large-scale productions. The synthesis of the cerium oxide (CeO_2) nanoparticles (NPs) is based on the Zhang et al [123] method. In this specific synthesis the cerium of the cerium nitrate is in ionic form, soluble in water with a "3+" valence, however the reaction that take place is a oxidation of the cerium from a "3+" to "4+" valence state, in which becomes insoluble in water. In this reaction the molecule of hexamethylenetetramine (HMT) is used as oxidizing agent

because it hydrolyzes to form ammonium ions and hydroxyl. Thereby the hydroxyl ion oxidizes the cerium.

For synthesis of TiO_2 NPs, the procedure is based in the Pottier et al. [124] procedure. The synthesis process involves decomposition of titanium tetrachloride ($TiCl_4$) at acid pH (2 to 6). Then followed by a growth step of the nanocrystals, which was held in an oven at 70 °C, purification by centrifugation and re-suspension with tetramethylammonium hydroxide (TMAOH) was also performed to stabilize the NPs. Depending on the pH used in the growth, the size and the shape of the TiO_2 NPs can vary, ranging from small sizes and spherical forms (5 nm, not used in this work) to large particles (about 10 nm, pH = 5, used in this work).

For Fe_3O_4 NPs a modification in the synthesized based in the method of Maasart [125]: 1mmol of iron chloride (II) ($FeCl_2$) and 2 mmol of iron (III) chloride ($FeCl_3$) were dissolved in 50 mL of deoxygenated water and then dropwise 50 ml of a deoxygenated solution is added 1M TMAOH. After 30 minutes of vigorous stirring under a stream of N_2, the Fe_3O_4 is precipitated and washed by gentle magnetic decantation, and re dissolved in 1 mM colloidal TMAOH for the final and stable solution of Fe_3O_4 NPs. Physical properties of the NPs are summarized in Table 4.1.1. A detailed description of the methodology and the resulting NPs are described by Recillas et al [96].

4.1.2.2. Adsorption and kinetic experiments

To test the adsorption capacity and to determine the adsorption isotherm of the different NPs tested, eight dilutions of cadmium were prepared at 25, 50, 100, 150, 200, 250, 300 and 350 mg/L. Solutions of TiO_2, Fe_3O_4 and CeO_2 NPs were prepared at 0.64 mg/mL. pH was adjusted to 7.0 with sodium hydroxide (0.1 M) and citric acid (0.15 M) where necessary. The mixture was centrifuged to separate NPs from the liquid solution at 14,000 rpm for 20 min. The supernatant was analyzed for residual dissolved cadmium. Kinetics was measured by analysis of dissolved cadmium at several time points after mixing. Aliquots from a stock cadmium solution (initial concentration 200 mg/L) were mixed with an equal volume of NP solution and analyzed as described above at 0, 0.5, 1, 2, 3, 5, 10, 24 and 48 h after mixing.

Table 4.1.1 Physical property of synthetic NPs.

Nanoparticle Composition	Shape	Z-potential (mV)	Surface coating	Concentration (NPs/mL)	Concentration (mg/mL)	Solvent concentration (nM)
Fe_3O_4	Irregular	-58	Inorganic TMAOH[a]	~10^{15}	0.67	TMAOH 1
CeO_2	Irregular	+12	Inorganic HMT[b]	~10^{16}	0.64	HMT 8.33
TiO_2	Irregular	-42	Inorganic TMAOH	~10^{16}	1.2	TMAOH 10

[a]TMAOH: tetramethylammonium hydroxide; [b]HMT: hexamethylenetetramine.

4.1.2.3. Adsorption and kinetics isotherms models

The data obtained from the adsorption experiments was fitted to the linear forms of the Langmuir Freundlich and Temkin isotherm models (Equation 2, 3 and 4, respectively). The kinecs data were fitted to the pseudo-first and pseudo-second order model (Equation 5 and 6, respectively).

4.1.2.4. Cadmium determination

The determination of the final concentration of cadmium ions was carried out according to the Section 3.2.1. in Chapter 3.

4.1.3. Results and discussion

4.1.3.1. Adsorption isotherms

The adsorption of dissolved cadmium by different NPs is presented in Fig. 4.4.1. The equilibrium capacity can be calculated according to Eq. (3.4) [52]:

$$q=(C_0-C_e)V/m \quad (6)$$

where C_0 and C_e are the initial and equilibrium concentrations of Cd^{2+} (mg/L) respectively, V is the solution volume (L) and m is the mass of the NPs (g).

Adsorption was modelled using the Langmuir, Freundlich and Temkin isotherms [54,126]. From the results presented in Table 4.1.2 the Freundlich isotherm gave the best fit to the experimental data, which suggest a chemical interaction on a heterogeneous surface [52]. It

has been shown that '*n*' values between 1 and 10 represent beneficial adsorption of the heavy metal [127,128]. On the other hand, isotherms with $n > 1$ are classified as L-type isotherms reflecting a high affinity between adsorbate and adsorbent and is indicative of chemisorption [52]. It can be observed that the correlation coefficients (Table 4.1.2) for the Temkin isotherm are also relatively good, which also supports the presence of a chemical interaction between cadmium and NPs. In contrast, the Langmuir isotherm could not be applied because the concentrations tested were far from adsorbent saturation.

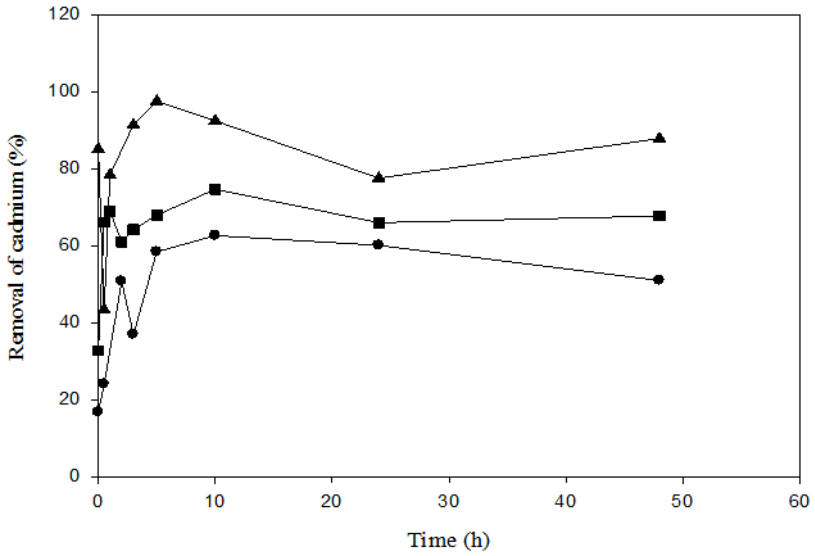

Figure 4.1.1. Cd^{2+} adsorption on Fe_3O_4 (squares), CeO_2 (circles) and TiO_2 (triangles) NPs. Conditions were pH= 7, temperature = 25 °C and initial concentrations of cadmium that produces the highest removal of Cd^{2+} for each nanoparticle (150mg Cd^{2+}/mL for Fe_3O_4 NPs, 100mg Cd^{2+}/mL for CeO_2 NPs and 25mg Cd^{2+}/mL for TiO_2 NPs) and for a concentration of NPs fixed at 0.64 mg/mL.

The three types of NPs clearly demonstrated sequestration of dissolved cadmium. The highest adsorption (101.1mg Cd^{2+}/g NP after 72 h) was observed for Fe_3O_4 NPs, more than twice that of the CeO_2 NPs (49.1mg Cd^{2+}/g NP) and almost 10 times that of TiO_2 NPs (12.2mg Cd^{2+}/g NP).

Despite the high capacity of the Fe_3O_4 NPs, the lowest equilibrium concentration of dissolved cadmium was achieved by treatment with the TiO_2 NPs. Figure 4.1.1 shows the evolution of the adsorption of cadmium using a solution of 0.64mg/mL of the different NPs tested at initial concentrations of Cd^{2+} that resulted in maximum percentage removal: 150mg Cd^{2+}/mL for Fe_3O_4 NPs, 100mg Cd^{2+}/mL for CeO_2 NPs and 25mg Cd^{2+}/mL for TiO_2 NPs. Maximum removal of ~ 90% of dissolved cadmium was obtained for TiO_2 NPs.

Table 4.1.2. Parameters for the Freundlich, Langmuir and Temkin isotherms using CeO_2, TiO_2 and Fe_3O_4 NPs

Isotherm	NPs	Parameter		
		k_F	n	R^2
Freundlich	CeO_2	2.727	0.95	0.968
	Fe_3O_4	2.231	1.087	0.969
	TiO_2	1.845	0.997	0.994
		q_m *(mg/g)*	$K_L\ 10^{-3}$ *(L/mg)*	R^2
Langmuir	CeO_2	111.111	4.87	0.313
	Fe_3O_4	2000	8.35	0.142
	TiO_2	-5000	-0.36	0.071
		k_T (L/g)	*b (J/mol)*	R^2
Temkin	CeO_2	0.777	5.379	0.801
	Fe_3O_4	0.865	7.733	0.966
	TiO_2	0.897	8.491	0.862

4.1.3.2. Kinetics of adsorption

The kinetics of the adsorption process was evaluated by the pseudo first-order and the second-order model. In this case, correlation coefficients for the pseudo first-order model were very poor (<0.4) and this model was discarded.

Although, both models assume that the driving force for adsorption is essentially the difference of concentration of cadmium between the bulk liquid and the surface of the NP,

the results obtained with the second-order model were in good agreement with the data (R^2=0.981 for CeO_2, R^2=0.995 for Fe_3O_4 and R^2=0.918 for TiO_2, respectively), as observed in Table 4.1.3. As expected, the theoretical equilibrium adsorption capacity is similar to that predicted by the model, a fact that has been also observed in the case of the adsorption of lead on NPs [126].

Fe_3O_4 NPs exhibit significantly higher equilibrium adsorption values than other widely used adsorbents, for example activated carbon (3.37 mg/g) [129], orange peel wastes (43.3 mg/g) [130] or chitin (14.7 mg/g) [117]. Cerium and titanium oxide NPs exhibit lower equilibrium adsorption values, similar to those of orange peel wastes and chitin, respectively.

Increased regulatory stringency has stimulated the investigation of a large number of new adsorbents for the removal of cadmium at low concentrations. In many of these studies, biowastes that are otherwise costly to dispose of have been proposed for cadmium sequestration. For instance, Fard et al. [131] tested the direct application of biosolids for the adsorption of cadmium, with a maximum adsorption capacity (q_e) of 46.0 mgCd^{2+}/g dry biosolid and an adsorption process that could be represented by the Langmuir isotherm. Similarly, Hamdaoui et al. [132] tested an agricultural waste material (melon peels) to remove cadmium with considerable success and a maximum adsorption capacity of 81.97 mgCd^{2+}/g using the Langmuir isotherm.

Table 4.1.3. Maximum adsorption capacity (q_e) at equilibrium (steady state, infinite time) and pseudo second-order rate constants (k_2) obtained using the pseudo second-order kinetic model. Concentration of NPs of CeO_2, Fe_3O_4 and TiO_2 was 0.64mg/L and initial Cd^{2+} concentration was 100 mg/L.

NPs	q_e (mg Cd^{2+}/g NPs)	k_2 (g NPs/(mg Cd^{2+}h)	R^2
CeO_2	48.30	0.016	0.981
Fe_3O_4	99.57	0.20	0.995
TiO_2	15.83	0.019	0.918

Other the adsorbent and the pollutant, as has been demonstrated with other toxic dissolved metals such as lead or chromium [95,96]. Further research is clearly needed to explore the reuse of NPs in the adsorption of heavy metals to make adsorption a competitive technology applicable to full-scale processes. Studies have also tested vegetal residues for the removal of dissolved cadmium [133]. However, the problem with these processes is that the toxic metal is transferred from a liquid medium to solid wastes, which themselves then present novel disposal challenges. In contrast, the use of NPs facilitates the recovery of both.

4.1.4. Summary

In this part of the study CeO_2, Fe_3O_4 and TiO_2 NPs were used as effective adsorbent for the removal of a wide range of cadmium ions concentration. The adsorption data fitted best the Freundlich isotherm model (R^2=0.968 for CeO_2; R^2= 0.969 for Fe_3O_4; R^2=0.994 for TiO_2). The kinetics adsorption follow the pseudo-second order (R^2=0.981 for CeO_2, R^2=0.995 for Fe_3O_4 and R^2=0.918 for TiO_2). The results show that Fe_3O_4 NPs offer the highest specific absorption capacity (99.57 mg Cd^{2+}/g NPs), while TiO_2 NPs offer the strongest adsorption (15.83 mg Cd^{2+}/g NPs). The magnetic properties of Fe_3O_4 NPs, which facilitate separation from the liquid medium, make them attractive candidates for the removal of dissolved cadmium at acceptable costs, in comparison with other complex and expensive adsorbents.

4.2 Use of cerium oxide (CeO_2) nanoparticles for the adsorption of dissolved cadmium (II), lead (II) and chromium (VI) at two different pH in single and multi-component systems

---

The results of this chapter are in press in the Global NEST Journal.
Use of cerium oxide (CeO_2) nanoparticles for the adsorption of dissolved cadmium (II), lead (II) and chromium (VI) at two different pH in single and multi-component systems,
A.R. Contreras, E. Casals, V. Puntes, D. Komilis, A. Sánchez and X. Font,
Global NEST. 17 (2015).

4.2.1. General overview

Nowadays, the world is facing a water crisis due to the lack of clean drinking water [134]. One of the main concerns is the presence of heavy metals such as cadmium, lead and hexavalent chromium, which have been extensively used as target pollutants in research studies due to their high toxicity and also because of the well-documented human health problems associated to these compounds [51,96,135]. Due to the contamination and shortage of fresh water the contaminant levels permitted are getting more stringent. This generates new challenges to meet the quality standards for drinking water [134], especially when there is a shortage. Therefore, it is necessary to develop more efficient remediation strategies that are able to remove heavy metals from contaminated water at very low concentrations [96].

Heavy metal adsorption onto nanoparticles (NPs) is an emerging technique for the removal of those pollutants. The use of NPs in adsorption processes presents some problems related to the comparison of CeO_2 NPs with other types of organic and inorganic adsorbents. This is because of the experimental conditions among the different types of adsorbents. In addition, the NPs synthesis can produce NPs with different physico-chemical properties on the surface, and, as a result, different values of adsorption capacities can be found in the literature [95]. Even though data on the removal of heavy metals ions from binary and ternary mixtures with different adsorbents such as peat [136], fly ash [43] or activated carbons [137,138] have been reported, experimental data on multi-component sorption systems involving NPs are still very limited in the literature. Multi-component systems are characterized by additional features such as the possible interaction effects among different species in solution and the potential interactions on the surface or the competition among the different metal ion species, which depend on the ionic characteristics. Accordingly, no single mechanism can explain the adsorption of complex mixtures of metal ions from aqueous solution onto NPs [137].

The aim of this section was to study the differences of the sorption capacity of CeO_2 NPs with regard to cadmium (II), lead (II) and chromium (VI), dissolved in water, both in single systems (one metal in the solution) as well as in multi-component (all 3 metals mixed

together in the solution) systems. This was done so that to study if there is a competitive sorption among metals on the NPs. The study was performed at two different pH (5 and 7), which correspond to typical pH found in environmental systems. A factorial experimental design was used to obtain an empirical equation that allowed describing the sorption capacities as a function of initial metal concentration, NP concentration and pH.

4.2.2. Materials and methods

4.2.2.1 Synthesis of nanoparticles

The synthesis of the cerium oxide nanoparticles is previously described in the section 3.2 of the previous chapter. The cerium oxide nanoparticles were synthesized in aqueous phase using milli-Q grade water. All reagents were purchased from Sigma-Aldrich® and used as received. The CeO_2 nanoparticles synthesis was based on Zhang (2004). Briefly, the Ce^{3+} ions from $Ce(NO_3)_3$ salt are oxidized at basic pH conditions to Ce^{4+} using hexamethylenetetramine (HMT). Then, the CeO_2 nanocrystals precipitate and are further stabilized in aqueous solution with the same reagent (HMT), which forms the double electrical layer to prevent NP agglomeration [95,96].

4.2.2.2 Adsorption experiments

For the adsorption studies, cadmium (II) chloride (99.99%), lead (II) nitrate (99.99%) and potassium dichromate (VI) (99.5%, Panreac) were used as metal sources, respectively. They were dissolved in deionized water and the corresponding dilutions were carried out. While lead and cadmium are dissolved cations, chromium is present as dichromate anion ($Cr_2O_7^{2-}$). However, along the text we will refer to it as Cr (VI). Each of these solutions was mixed with the corresponding suspensions of CeO_2 nanoparticles for single and multi-component systems, with a resultant pH of 7±0.1, and then the mixture was stirred at 130 rpm at room temperature for 24 hours. All the adsorption experiments were performed at equilibrium pH of 5±0.2 and 7±0.1. Solutions were adjusted to pH 5±0.2 by using 10 g/L citric acid solution. Final pH measurements were done at the end of the 24 h period; then samples were centrifuged (10,000 rpm) to separate the nanoparticles (solid phase) from the liquid phase. The supernatant was analyzed for residual dissolved heavy metals (non-

adsorbed metal). The equilibrium capacity was calculated with the following Equation 6, previously described in Chapter 3.

4.2.2.3 Experimental design

In this factorial experimental design, the primary goal was to investigate the simultaneous effects of the initial metal concentration and the initial NP concentration on sorption capacity. Therefore, a three-level central composite full factorial design containing all the possible combinations between the factors (*f*) and their levels (*L*) was used, leading to $N=L^{*}f$ experiments, including one four-replicated central point [139]. The two variables were the initial concentration of metals and the initial NPs concentration. Data is shown in Table 4.2.1. The initial metal concentrations selected were: 1 mg/L, 5.5 mg/L and 10 mg/L, in both the single and the multi-component systems. The initial NP concentrations were: 0.064 g/L, 0.352 g/L and 0.64 g/L, which corresponds to the range of metal and NPs concentrations typically found in literature in similar experiments [96].

Table 4.2.1. Initial conditions in the adsorption experiments.

	Coded concentration values		Actual initial concentrations	
Exp	NPs (g/L)	Metal (mg/L)	NPs (g/L)	Metal (mg/L)
1	-1	-1	0.064	1.0
2	-1	0	0.064	5.5
3	-1	1	0.064	10.0
4	0	-1	0.352	1.0
5	0	0	0.352	5.5
6	0	0	0.352	5.5
7	0	0	0.352	5.5
8	0	0	0.352	5.5
9	0	1	0.352	10.0
10	1	-1	0.64	1.0
11	1	0	0.64	5.5
12	1	1	0.64	10.0

4.2.2.4 Empirical modeling

Empirical modeling was performed in order to assess the effect of 4 parameters, initial sorbent concentration, initial metal concentration, pH and type of sorption system, on the sorption capacity. The generic equation 7 was fitted to the data:

$$q_t=b_1X_1+b_2X_2+b_3X_3+b_4X_4 \quad (7)$$

where: b_1, b_2, b_3, b_4 are the model coefficients, X_1 is the initial NP concentration (g/L), X_2 is the initial metal concentration (mg/L), X_3 is the pH, X_4 is a categorical variable that indicates type of system (1 for single system and 2 for multi-component system) and q_t as earlier defined. A constant was avoided to be included since it has no physical meaning. Interaction terms were not investigated.

According to the methodology presented in Berthouex and Brown (2002), only the significant terms (at $p<0.05$) should be used in the regression model equation to obtain the best reduced model (BRM). This is done by sequentially removing terms that are not statistically significant and by continuously re-fitting new models until all coefficients are statistically significant. The results obtained from the experimental design were processed with Minitab® v.17 and SigmaPlot® v.11.

4.2.2.5 Determination of metals

The determination of the ions of camdium lead and chromium were carried out in accordance with the Section 3.2.11, 3.2.1.2 and 3.2.1.3 respectively, previously described in Chapter 3.

4.2.3. Results and discussion

4.2.3.1 Adsorption results and isotherms

Figure 4.2.1 presents the isotherms for the 3 metals in both systems (single, multi-component) and at both pH (5 and 7).

According to Figure 4.2.1, a highest adsorption capacity (q_t) was obtained for Cd (II) (62.0 mg Cd^{2+}/g CeO_2) when compared with that previously obtained with cerium oxide nanoparticles (48.3 mg Cd^{2+}/g CeO_2) at the same pH [140]. This may suggest that for low initial concentrations of NPs, better adsorption capacities can be obtained. Although this seems unexpected, a possible explanation could be the fact that when the concentration of nanoparticles in the solution increases, the effective surface area for adsorption becomes lower, due to interaction among ions. Therefore, a relatively low initial concentration of nanoparticles could promote higher adsorption capacities. It is evident that this hypothesis should be confirmed with further specific experiments. For Cd (II), when the pH became more acidic, the adsorption capacities reduced; this could be due to the high concentration of H^+ that also occupy available adsorption sites [141]. In the case of Pb (II), there is no clear effect of the pH on the adsorption capacity. On the other hand, the Cr (VI) presented a similar behavior to Cd (II). It is well known that Cr (VI) can form several complexes (CrO_4^{2-}, $HCrO_4^-$) with different affinities for the adsorbent that may result in variable adsorption capacities [142]. Lead (II) and chromium (VI) exhibited maximum q_t values of 43.8 mg/g CeO_2 and 21.3 mg/g CeO_2, respectively, at the single system.

According to Figure 4.2.1, higher q_t values were obtained in the multi-component experiments for Cd (II) and Pb (II). Actually, the q_t for lead (128.1 mg Pb^{2+}/g CeO_2), obtained in the multi-component system at pH 5, was significantly higher than that obtained in the single component experiments (43.8 mg Pb^{2+}/g CeO_2). The adsorption capacities for lead were actually higher when compared with other adsorbents such as coconut (4.38 mg/g) [143]. In the case of Cr (VI), the adsorption capacity in the multi-component system was slightly higher than that obtained in the single component system. The maximum adsorption capacity was 34.4 mg Cr^{6+}/g NP, similar to that obtained with maghemite [144], and approximately three times higher than that of the EA-200 activated carbon sorption capacity [95]. From the results, we can observe that the sorption capacity for cadmium (93.4 mg Cd^{2+}/g) was higher in the neutral pH and at the multi-component system. Since Figure 4.2.1 does not clearly reveal the effects of the various parameters (initial concentration of metal and NP, pH, type of system) on the sorption capacities, empirical models were built to better investigate that.

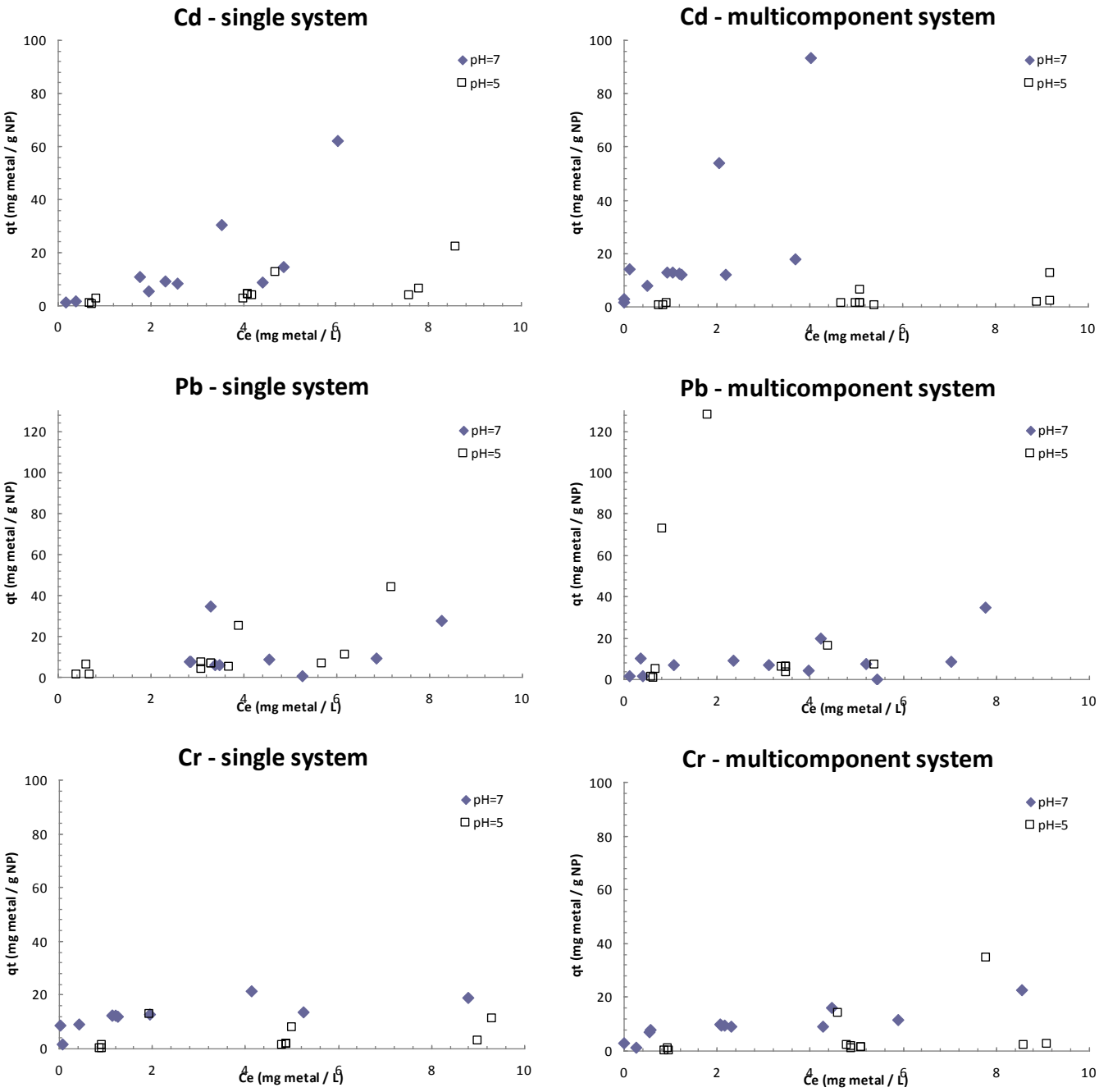

Figure 4.2.1. Isotherms for all 3 metals at the single and multi-components systems and at two different pH (5 and 7)

4.2.3.2 Empirical modeling

Empirical modeling was based on equation (7). The fitted equations (best reduced models) for each metal are included in Table 4.2.2.

Table 4.2.2. Best reduced models to predict sorption capacity as a function of several parameters.

Metal	Best reduced models	R^2
Cd (II)	-46.9 NP + 1.6 M + 3.3 pH	60.4%
Pb (II)	-31.5 NP + 3.9 M	45.6%
Cr (VI)	-17.8 NP + 1.0 M + 1.4 pH	78.5%

NP: initial CeO_2 NP concentration; M: initial metal concentration

All coefficients in the models are statistically significant at $p < 0.05$.According to the equations, the sorption capacity of all three metals was always affected significantly by the initial NP and initial metal concentration. That is, as the initial metal concentration in the solution increased, the sorption capacity increased as well, whilst the opposite was true with the initial NP concentration. Furthermore, it is interesting to note that the system (single, multi-component) did not statistically affect the sorption process with regard to any of the metals (the p-value of that coefficient was always much higher than 0.05). That is, the sorption capacity of all 3 metals was statistically similar in the single and multi-component systems. Apparently, the sorption sites of the NPs were enough so that not to allow competitive sorption phenomena to occur.

On the other hand, the equations of Table 4.2.2 reveal that pH significantly affected the sorption capacities of Cd (II) and Cr (VI), but not of Pb (II). It is reminded that these equations were based on experiments on two pH values only (5 and 7); thus, the effect of pH can be explained only within that range. Therefore, in the case of Cd (II) and Cr (VI), as pH increased from 5 to 7, the sorption capacity increased as well. This can be explained by the speciation of those metals in those pH and the fact that the abundance of H^+ (at low pH) competed with sorption sites. Actually, pH affected more the sorption capacity of Cd (II)

than that of Cr (VI). In the case of Pb (II), as was also evident in Figure 4.2.1, pH was not a predictor of the sorption capacity.

Figure 4.2.2 graphically depicts the original sorption capacities, as a function of initial NP and metal concentrations, as well as the response surfaces that were drawn based on the empirical modeling performed

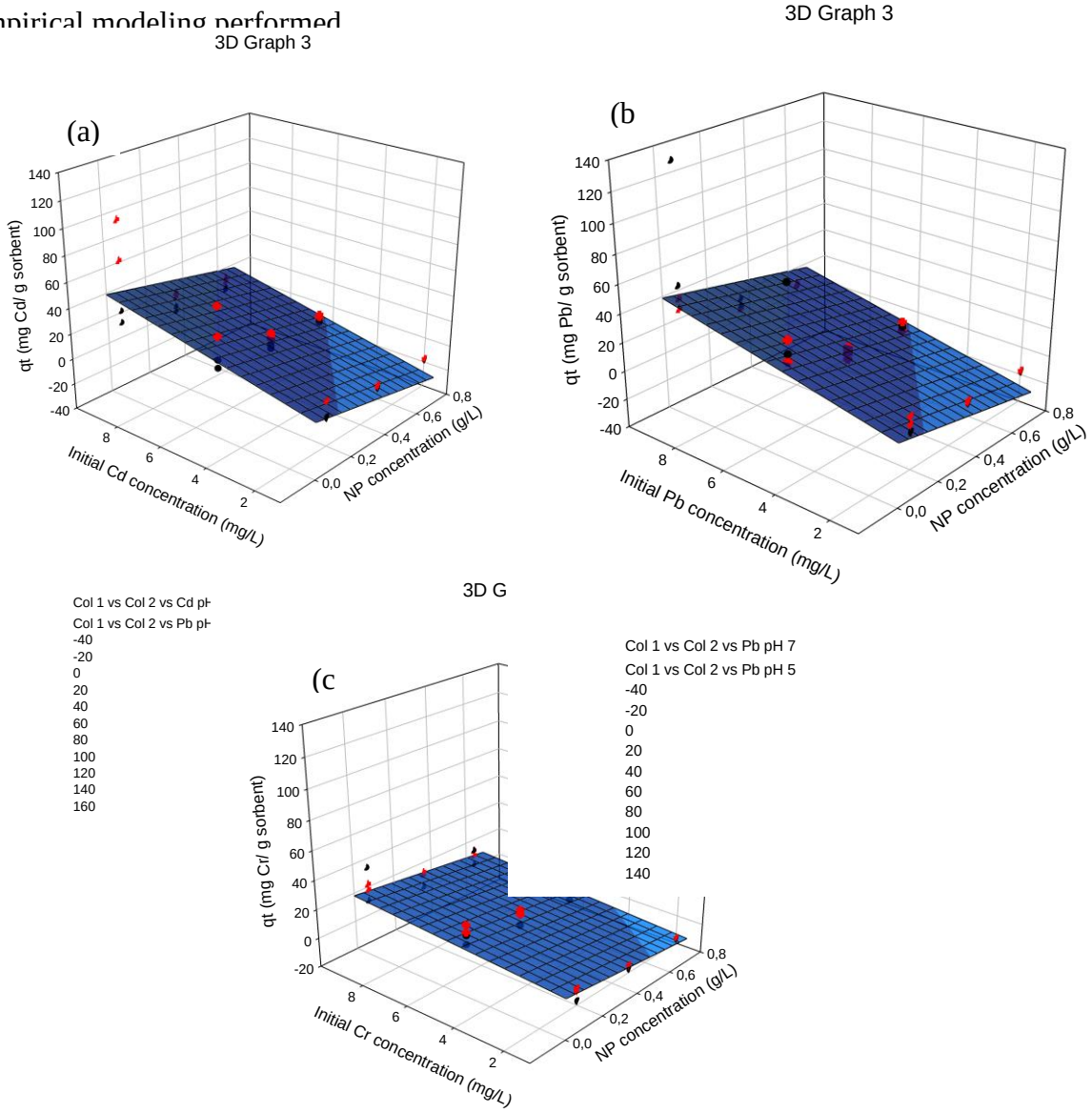

Figure 4.2.2. (a): C 1*M , (b): Pb (II) response surface equation -3 equation: 6.43 – 15.43 NP + 1.17 M; Red do NP: initial nanoparticle concentration (g/L),

4.2.4. Summary

In this part of the study the use of CeO_2 NPs were once again tested for the removal of cadmium lead and chromium ions in single and multicomponent systems. The coefficients for the best reduced model were obtained. From the statistical analysis it can be observed that the sorption capacity was statistically similar between the two systems (single and multi-component), i.e., the adsorption capacity is not affected by the presence of other metals. Both, the initial metal and the initial NP concentrations were statistically significant predictors of the sorption capacities of all the three metals. However, pH was found to affect the sorption capacity of cadmium and chromium, but not that of lead. The maximum sorption capacities recorded in this part of the study were 93.4 mg Cd^{2+}/g CeO_2 (multi-component system, pH 7), 128.1 mg Pb^{2+}/ g CeO_2 (multi-component system, pH 5), and 34.4 mg Cr^{6+}/g CeO_2 (multi-component system, pH 5).

4.3 Biocompatible mussel-inspired nanoparticles for the removal of heavy metals at extremely low concentrations

---

This chapter was performed in collaboration with: Institut Catala de Nanociencia i Nanotecnologia (ICN2), Institut de Biotecnologia i de Biomedicina and Departament de Bioquímica i de Biologia Molecular (UAB), Fundació Privada Ascamm and the Department of Chemistry (UAB).

4.3.1. General overview

Adsorption is considered effective and is widely applied for the removal and separation of heavy metals from drinking water, due to its simplicity and ease of operation [145]. A significant number of new low-cost adsorbents have been used for the removal of metals with variable adsorption capacities. For example, activated carbon derived from bagasse (27.49-49.07 mg/g) [146] and chitin (14.7 mg/g) [117] have been used for the removal of Cd(II); coconut fibers (4.38 mg/g) [146] and iron nanoparticles (82.64 mg/g) [96] have been used for the removal of Pb (II), and maghemite (19.2 mg/g) [144] and EA-200 activated carbon (10 mg/g) [95] have been used for the removal of Cr(VI). Recent advances also suggest that the adsorption of heavy metals using nanotechnology devices could improve or greatly ameliorate the challenge of improving drinking water quality [9,95,96]. Nanoparticles (NPs) have two key properties that make them particularly attractive as adsorbents: I) they have much larger surface areas than bulk particles on a mass basis, and II) they can be also functionalized to increase their affinity to specific compounds, such as metal ions [9]. Therefore, this approach turns out to be especially efficient for the removal of low concentration pollutants. In this regard, the fabrication of novel nanostructures, with simple and environmentally friendly compositions, that can effectively remove pollutants is highly desirable.

In recent years, polydopamine (PDA), which is a catecholic compound, has been used in the fabrication, design and development of novel materials [111] . PDA (a catecholic compound) is a novel bio-inspired material based on the catechol moiety, the presence of which on mussel byssus proteins is essential to their critical adhesive function in wet environments [147]. For metal adsorption applications, the catechol groups and nitrogen heteroatoms in PDA structures have also had a strong tendency to interact with positively charged metal ion species [148]. Despite its versatility and simplicity, PDA fabrication cannot be accurately controlled and exhibits a remarkable insolubility, being restricted by in-situ polymerization methodologies. Recently, we have reported a new experimental approach for the preparation of PDA-related nanoparticles derived from the polymerization of the amphiphile 4-heptadecylcatechol with ammonia[115]. Overall, the strategy reported combines advantages, such as ease of preparation, solubility in appropriate solvents and

improved surface functionalization. Likewise, the as-synthesized material was shown to spontaneously form nanoparticles (catechol-based) with a diameter of a few hundred nanometers in water.

The aim of this study is to explore the capacity of this new family of catechol-based NPs to adsorb Cd(II), Pb(II) and Cr(VI) dissolved in water at very low concentrations. Activated carbon was also used, under the same experimental conditions, as a reference adsorbent. In both cases, a factorial experimental design was adopted to mathematically describe adsorption capacity as a function of the heavy metal concentration and the adsorbent concentration. A bioluminescent bacteria test and a cytotoxicity assay were also carried out to assess the toxicity of the reported nanoparticles.

4.3.2. Materials and methods

4.3.2.1. Catechol-based synthesis of nanoparticles

The synthesis of catechol based NPs has been reported elsewhere [147]. A brief description is provided: A large excess of aqueous ammonia (100:1) was slowly added under vigorous stirring and under the presence of air to a solution of 4-heptadecylcatechol (0.2%, w/v) in methanol at 40 °C. The reaction was complete in 24 hours. Interestingly, the morphological characterization by SEM and TEM obtained from the (polar) reaction medium upon evaporation of the ammonia excess revealed the formation of solid nanoparticles (NPs) with diameters ranging from 100 to 350 nm (observed directly from SEM images) or an average diameter of 301 nm (PDI: 0.145) as obtained by DLS measurements.

4.3.2.2. Scanning Electron Microscopy (SEM)

SEM measurements were carried out with a HITACHI S-570 and a QUANTA FEI 200 FEG-ESEM, both operating at 15 kV. Samples for the observation of nanoparticles were prepared by casting a drop of the corresponding dispersion on aluminum tape and by further evaporation of the solvent at room temperature. Prior to observation with SEM, all samples were metalized with a thin layer of gold using a sputter coater K550 (Emitech).

4.3.2.3. Adsorption experiments

The heavy metals solutions were prepared from cadmium nitrate tetrahydrate (99.9%), lead

(II) nitrate (99.9%) and potassium dichromate (99.5, Panreac). The activated carbon (Merck, ref.no: 1021860250) that was used had a particle diameter of <100μm. All the experiments were carried out at room temperature and at pH 7. The adsorption equilibrium was considered to be reached at 24 h for all cases [95,96,140]. The mixture was then centrifuged (10,000 rpm for 10 min) and filtered (0.22 μm) to separate the catechol-based NPs from the solution. The supernatant was analyzed for the residual dissolved cadmium (II), lead (II) and chromium (VI).

4.3.2.4. Experimental design

In a factorial experimental design, all possible combinations between factors at all levels are investigated [149] in order to estimate the effects of the main factors (concentrations of metal and catechol) and of the (likely) interactions. This procedure can provide valid conclusions for a range of experimental conditions and permits a statistical validation of the results obtained [150]. In this work, a three-level and two-factor full factorial design was employed that contained all the possible combinations between the two factors ($f=2$) and their three levels ($L=3$), resulting in $N=L^f=9$ experiments with one central point replicated three times [139]. As a result, twelve experiments were performed as shown in Table 4.3.1 and Table 4.3.2, where the coded values represent the levels of each factor (i.e. lowest level (-1), center point (0), highest level (1)).

4.3.2.5. Regression modeling

The regression started with a full polynomial model and terms were sequentially removed in order to obtain the best reduced model (BRM), with the fewest possible statistically significant terms (at $p<0.05$), that can still adequately describe the data [151]. The initial quadratic equation (Equation 8) that was used to fit the experimental data was:

$$Y=b_0+b_1X_1+b_2X_2+b_3X_1^2+b_4X_2^2+b_5X_1X_2 \quad (8)$$

where: b_0, $b_1 \ldots b_5$ are the model coefficients, X_1 represents the concentration of the adsorbent (g/L), X_2 represents the initial concentration of the heavy metal (mg/L) and Y is the dependent variable, namely the adsorption capacity of each adsorbent (mg metal/g adsorbent). The statistical analysis was performed with MatLab (version 2011b, Mathworks).

4.3.2.6. Determination of the metal ions

Prior to metal analysis, all samples were acidified with concentrated HNO_3, to a final 1% concentration, so that to obtain a pH < 3. The determination of cadmium, lead and chromium was performed by a mass spectrometer (ICP-MS) Agilent, model 7500ce. Analysis was performed by the Servei d'Anàlisi Química (SAQ) in the UAB.

4.3.2.7. Bioluminescent test

Measurements based on microorganisms are fast, cost effective, reproducible and are becoming increasingly common to study toxicity [152]. The method used in this study is based on the determination of the inhibition of the luminescence produced by marine bacteria (*Vibrio fisheri*). The assay consists of serial dilutions that mix the pollutant and a suspension of luminescent bacteria in a cuvette; the reduction of the light emitted is directly related to the relative toxicity of the sample [153]. Toxicity values can be expressed as EC_{50} (half maximal effective concentration), which is a measure of the effectiveness of a compound in inhibiting biological or biochemical functions. It is obtained after plotting the percentage of luminescence reduction against the concentration after 5 and 15 min incubation times. Depending on EC_{50} values samples are classified as highly toxic ($EC_{50} \leq$ 25), moderately toxic (25-50%), toxic (51-74%), slightly toxic (76-100 %) or non-toxic ($\geq$100%) [68,96]. A commercial Microtox® model 500 analyzer (Azur Environmental, Berkshire, UK) was used. The 81.9% basic test protocol was used to determine the toxicity for the initial solutions of cadmium and lead (0.5 mg/L), for the initial suspensions of catechol (0.1 g/L) and also for the final suspension obtained from the adsorption process (heavy metal plus catechol). No visible precipitate or agglomeration was observed during the tests. Toxicity tests were all performed in triplicate.

4.3.2.8. Stability assays

The solubility and stability of catechol nanoparticles were investigated in several buffers in order to mimic different biological conditions. Dilutions of catechol nanoparticles were prepared at a concentration of 1 mg/ml in: Milli-Q purified water, phosphate saline buffer (PBS) (Invitrogen, Inc.) and Modified Eagle's Medium (MEM) (Invitrogen, Inc.) with and without the addition of 50 µg/ml Bovine Serum Albumin (BSA) or 10% (v/v) fetal Bovine

Serum (FBS) respectively. Samples were incubated for 72 h at 37ºC.

4.3.2.9. Protein binding assays

The binding of catechol nanoparticles to proteins was investigated by the tryptophan fluorescence of bovine serum albumin (BSA). Tryptophan fluorescence emission spectrum was measured in a Jasco FP-8200 spectrofluorimeter using and excitation wavelength of 275 nm and collecting the emission spectra between 290 and 450 nm. Slit widths were typically 5 nm for the excitation and 5 nm for emission and the spectra were acquired at 0.5 nm intervals, 500 nm min^{-1}. The spectrum of BSA at 50 µg/ml in 50 mM sodium phosphate buffer (pH 7.4) was acquired in absence and in the presence of catechol nanoparticles at 25 µg/ml, 50 µg/ml and 100 µg/ml. The spectrum of the buffer with 100 µg/ml catechol nanoparticles alone was used as control.

4.3.2.10. Cytotoxicity assays

The cytotoxicity assays were performed using human hepatoma cells (HepG2) (ATCC HB-8065). The cells were grown in Modified Eagle's Medium (MEM) alpha supplemented with 10% (v/v) heat inactivated fetal bovine serum (FBS) in a highly humidified atmosphere of 95% air with 5% CO_2 at 37ºC. The cytotoxicity of catechol-based NPs on HepG2 cells was measured using the XTT assay based on the determination of the ability of living cells to reduce 2,3-bis-(2-methoxy-4-nitro-5-sulfophenyl)-2H-tetrazolium-5-carboxanilide (XTT) to formazan [154,155]. To perform the experiments, cells were seeded into 96-well plates at a cell density of $4.0x10^3$ cells/well and growth for 24 h for complete cell adhesion. Then, catechol nanoparticles were added at different concentrations (from 1 µg/ml to 1000 µg/ml) and incubated for 24 h. After incubation, 20 µl of the XTT solution was added to each well. The color formed after 3h incubation at 37ºC was quantified by a spectophotometric plate reader (Perkin Elmer Victor3 V) at a 490 nm wavelength. Cell cytotoxicity was evaluated in terms of cell-growth inhibition in treated cultures and expressed as a % of the control conditions.

4.3.3. Results and Discussion

4.3.3.1. NPs fabrication and adsorption results

The morphological characterization by SEM of the material directly obtained from the reaction medium showed that the formed solid NPs had diameters between 200 and 350 nm (Figure 4.3.1a, b). The surface charge of the NP solution (measured as Zeta potential) was around -45 mV at pH ≈ 7, which is in agreement with the presence of a certain amount of polyphenol groups in the outermost layer that achieves a stable colloidal suspension for many days. Figure 4.3.1c shows the morphology of the same NPs after exposure to the heavy metal ions solution (*vide infra*). As can be seen, the NPs undergoing this treatment retain their overall dimensions.

The achieved adsorption capacities of the three metals in a single component system onto the catechol-based NPs and onto the activated carbon are included in Tables 4.3.1 and 4.3.2, respectively. In the adsorption experiments with catechol-based NPs, it was observed that only the solutions of cadmium (II) and lead (II) showed changes in concentration, whereas the chromium (VI) solution remained constant under all conditions. The maximum adsorption capacities (q_t) obtained for lead (9.60 mg Pb^{2+}/g NPs) and cadmium (9.08 mg Cd^{2+}/g NPs) were similar. Table 4.3.1 also shows that the adsorption capacity increased with an increase of the initial concentration of the metal and with a reduction of the concentration of NPs.

The maximum adsorption capacities obtained with activated carbon (Table 4.3.2) for cadmium (2.06 mg Cd^{2+}/g carbon activated) and lead (2.46 mg Cd^{2+}/g carbon activated) were lower than those obtained with NPs. In the case of activated carbon, only chromium (VI) observed a higher adsorption capacity (3.96 mg Cr^{6+}/g activated carbon) compared to that in NPs. The differences existing in the adsorption capacities of the different metals may be attributed to the specific properties of activated carbon, such as porosity (micropore volume, micropore size and distribution, etc.), chemical nature of the activated surface or the activation process (chemical, physical) [156].

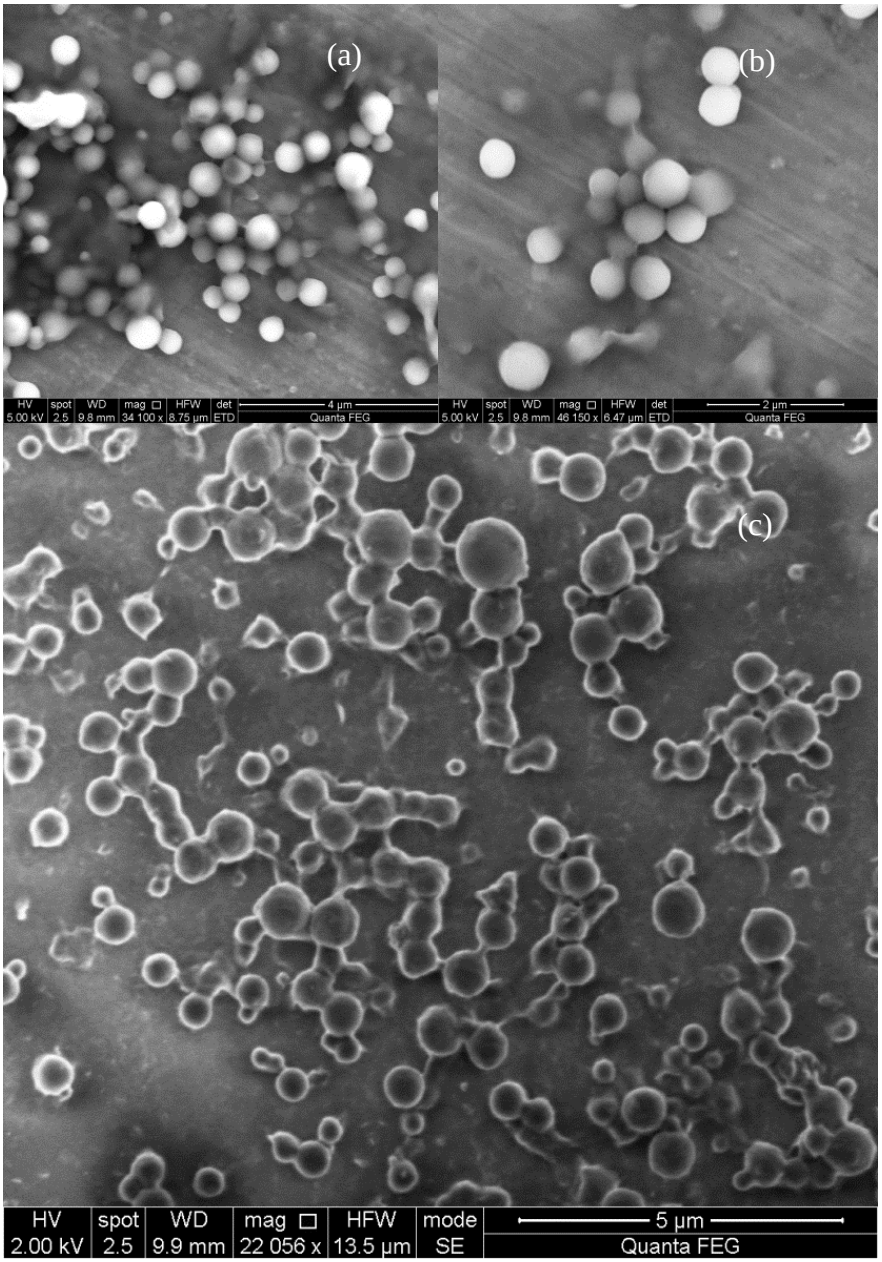

Figure 4.3.1. SEM images of the synthetized catechol nanoparticles: (a), (b) NPs ranging from 200 to 350 nm, (c) NPs morphology after exposure to the heavy metal ions solution

Table 4.3.1. Experimental design matrix used for the single metal adsorption experiments of Cd(II) and Pb(II) with catechol-based NPs.

	Coded values		Initial concentrations		Adsorption capacities and final metal concentrations			
					Cd(II)		Pb(II)	
Exp	Catechol NP concentration (g/L)	Metal concentration (mg/L)	Catechol NP concentration (g/L)	Metal concentration (mg/L)	q_t	Final concentration mg/L	q_t	Final concentration mg/L
1	-1	-1	0.05	0.05	0.934	0.0033	0.902	0.0049
2	-1	0	0.05	0.10	1.852	0.0074	N/A	*
3	-1	1	0.05	0.50	9.080	0.0460	9.600	0.0200
4	0	-1	0.10	0.05	0.445	0.0055	0.443	0.0057
5	0	0	0.10	0.10	0.963	0.0037	0.840	0.0160
6	0	0	0.10	0.10	0.963	0.0037	0.900	0.0100
7	0	0	0.10	0.10	0.973	0.0027	0.730	0.0270
8	0	0	0.10	0.10	0.850	0.0150	0.918	0.0082
9	0	1	0.10	0.50	4.690	0.0310	4.600	0.0400
10	1	-1	0.50	0.05	0.093	0.0036	0.097	0.0013
11	1	0	0.50	0.10	0.195	0.0027	0.193	0.0036
12	1	1	0.50	0.50	N/A	*	0.922	0.0390

* Below detection limit; q_t: adsorption capacity measured after 24 h and expressed in mg metal / g catechol-based NP; NP: catechol based nanoparticles, N/A: not available

Based on Tables 4.3.1 and 4.3.2, the highest adsorption capacities were obtained at the lowest concentrations of both adsorbents and at the highest metal concentrations. Other studies have found similar adsorption capacities with bituminous coal (8.89 mg Pb^{2+}/g) [157] or with furnace sludge (7.39 mg Cd^{2+}/g) [158] or even lower (3.27 mg Cd^{2+}/g) with peach stone carbon [159] and higher (93.2 mg Cd^{2+}/g) using coconut coirpith [160].

According to Tables 4.3.1 and 4.3.2, the metal removal percentages when catechol-based NPs were used as adsorbents were on average 94% for Cd^{2+} and 91% for Pb^{2+}. These removal percentages were up to around two times higher than those recorded for activated carbon (i.e. on average 40% for Cd^{2+}, 80% for Pb^{2+} and 73% for Cr^{6+}), which also indicates the higher affinity between catechol-based NPs and metals compared to activated carbon.

Table 4.3.2. Experimental design matrix used for the single metal adsorption experiments of Cd(II), Pb(II) and Cr(VI) with activated carbon

	Coded values		Initial concentrations		Adsorption capacities and final metal concentrations					
					Cd(II)		Pb(II)		Cr(VI)	
Exp	AC concentration (g/L)	Metal concentration (mg/L)	AC concentration (g/L)	Metal concentration (mg/L)	q_t	Final concentration mg/L	q_t	Final concentration mg/L	q_t	Final concentration mg/L
1	-1	-1	0.05	0.05	0.340	0.0330	0.939	0.0031	0.750	0.0125
2	-1	0	0.05	0.10	0.740	0.0630	1.468	0.0266	0.893	0.0553
3	-1	1	0.05	0.50	2.060	0.3970	2.451	0.3774	3.968	0.3016
4	0	-1	0.10	0.05	0.250	0.0250	N/A	*	0.419	0.0081
5	0	0	0.10	0.10	0.780	0.0220	0.986	0.0014	0.767	0.0233
6	0	0	0.10	0.10	0.360	0.0640	0.920	0.0080	0.816	0.0184
7	0	0	0.10	0.10	0.310	0.0690	0.979	0.0021	0.654	0.0346
8	0	0	0.10	0.10	0.410	0.0590	0.808	0.0192	0.636	0.0364
9	0	1	0.10	0.50	1.140	0.3860	1.107	0.3893	3.024	0.1976
10	1	-1	0.50	0.05	0.050	0.0250	N/A	*	N/A	*
11	1	0	0.50	0.10	0.096	0.0520	0.197	0.0015	0.196	0.0019
12	1	1	0.50	0.50	0.352	0.3240	0.825	0.0876	0.942	0.0291

* Below detection limit; q_t: adsorption capacity measured after 24 h and expressed in mg metal / g AC; AC: Activated carbon; N/A: not available

The speciation of heavy metals also plays an important role in the adsorption process. One parameter that has been pointed out by several authors is the pH [161–164], which affects metal speciation, and, depending on its variability, can favor or not the sorption of metal complexes. The adsorption capacities of activated carbon were in the same order of magnitude to those obtained with activated carbon derived from coconut shells (1.4 mg Cr(VI)/g) [165] and almond-shell carbon (1103 m^2/g; 2.7 mg Cd^{2+}/g) [159]. On the other hand, activated carbon prepared from apricot stone (566 m^2/g) presented much higher adsorption capacities for these 3 metals (33.57 mg Cd^{2+}/g, 22.85 mg Pb^{2+}/g, 29.47 mg Cr^{6+}/g) [14]. This variability is attributed to the variable surface properties of the sorbents as well as the ionic strength and solubility of the heavy metals, among other properties already mentioned [165].

4.3.3.2. Empirical modeling to describe adsorption capacity

Based on the model building methodology described in section 4.3.2.5, the initial heavy metal concentration (X_2) was found to be the only statistically significant (at $p<0.05$) variable to describe adsorption capacity. The BRM calculated is shown by Equation 9.

$$Y=b_2X_2 \quad (9)$$

The coefficient associated to X_2 and the *P-values* for each system are presented in Table 4.3.3. This finding indicates that the maximum adsorptive capacity of both sorbents has not been reached due to the low metal concentration range used in this study. The intercept was not included in the model since it did not have a physical meaning.

4.3.3.3. Stability assay

The stability of catechol-NPs was evaluated in phosphate saline buffer (PBS), in PBS plus Bovine Serum Albumin (BSA) 50 μg/ml and in Modified Eagle's Medium (MEM) cell culture medium (with or without Fetal Bovine Serum) buffers after 72h incubation to mimic a physiological environment. The objective was to study possible aggregation phenomena in biological environments, such as blood or tissues, which could affect their persistence of catechol-NPs once entering the human body.

Figure 4.3.2a shows NPs aggregates in PBS or in MEM without FBS after 72h incubation at 37 ºC. The addition of FBS to the cell culture media (MEM+FBS) and BSA in the PBS (PBS+BSA) buffer improved the solubility and protected nanoparticles from aggregation. Therefore, this increased the stability of the unmodified particles due to nonspecific protein adsorption.

One of the major biological functions of albumins is their ability to carry drugs as well as endogenous and exogenous substances. Serum albumins are the most abundant proteins in plasma. As the major soluble protein constituents of the circulatory system, they have many physiological functions [166]. BSA contains 582 amino acid residues with a molecular weight of 69,000, and two tryptophan moieties at positions 134 and 212 as well as tyrosine and phenylalanine [167].

Table 4.3.3. Empirical modeling results to describe the adsorption capacity of the NPs and of the activated carbon.

	Catechol-based NPs		Activated carbon		
	Cadmium	Lead	Cadmium	Lead	Chromium
Model					
Coefficient b_2 for term X_2 *	9.22	9.76	2.54	3.39	5.41
p value	0.0014	0.0007	0.0003	0.0008	<0.0001

*: X_2 corresponds to initial metal concentration in mg/L.

Conformational changes in BSA may disturb the microenvironment around the Trp residues and thus influence the fluorescence. As shown in Figure 4.3.2b, the value of Trp fluorescence decreased as the concentration of NPs increased this suggests that the polarity of the microenvironment around the Trp residues increased because of the conformational changes of BSA at the tertiary structure level [168]. Herein, we suggest that the adsorption of BSA on the catechol NPs forces the BSA molecules to transform into a less compact structure, which allows the solvent to penetrate into the hydrophobic cavity of BSA, which increases the polarity of the microenvironment around Trp-212.

4.3.3.4. Bioluminescent tests

For catechol-based NPs, the initial sample, the sample after 24 hours of adsorption and the catechol NPs without sorbed metals were tested. The results show that the catechol-based NPs do not present a toxic effect before or after mixing them with heavy metals, and remained without showing toxicity effects throughout the adsorption process. This is important, as sometimes nanoparticles are very effective adsorbents, but present toxicity on aquatic environments. Some metal-oxide NPs have been studied in this way. For example, TiO_2 absorbs considerable UV radiation, yielding in aqueous media, hydroxyl species that may cause substantial damage to DNA [69]. Other studies found that Al_2O_3, Zn and ZnO NPs could reduce root growth due to perturbation of the soil microbial flora [68].

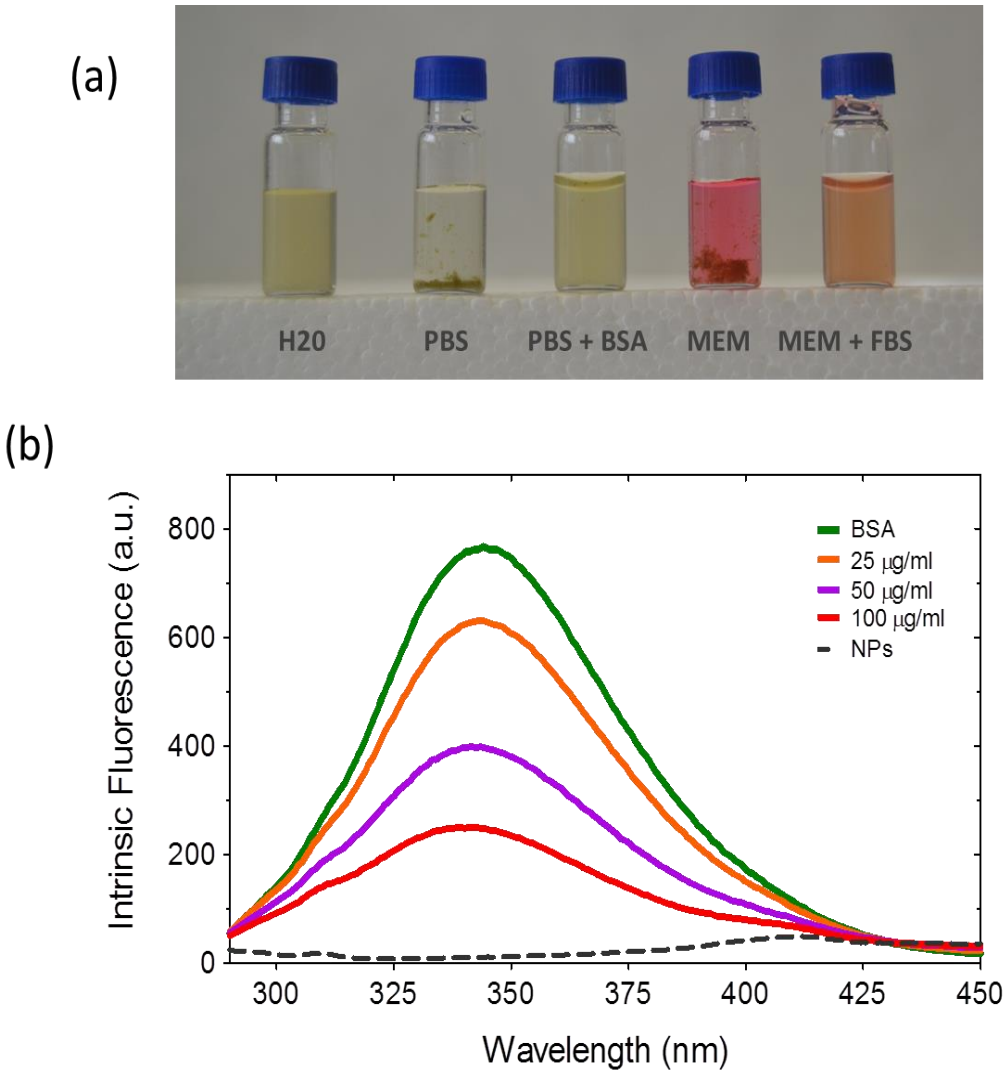

Figure 4.3.2. (a) Images of catechol nanoparticles re-suspended at 1 mg/ml in water, phosphate buffered saline (PBS) and Modified Eagle's Medium (MEM) alpha and incubated for 72 h at 37 ºC. (b) Tryptophan fluorescence spectra of BSA in absence (solid green line) and presence of 25 µg/ml (solid orange line), 50 µg/ml (solid purple line) and 100 µg/ml (solid red line) catechol nanoparticles. Nanoparticles bind to BSA triggering a concentration-dependent decrease of the intrinsic BSA tryptophan fluorescence.

4.3.3.5. Cytotoxicity of catechol NPs in cells

Finally, to clarify if catechol-based NPs display any kind of cytotoxicity towards human cells, they were tested against the hepatic cell line HepG2. The XTT assay was used to assess cell viability and is based on the reduction potential of metabolically active cells. After 24 h, no significant signs of toxicity were observed for a broad range from 25 to 1000 µg/ml of catechol NPs in HepG2 cells. Figure 4.3.3 shows no significant differences between viability of liver hepatocellular carcinoma cell line (HepG2) by the XTT assay at increasing concentrations of catechol-based NPs. Also optic microscope images of HepG2 cells after incubation in absence and presence of 1 mg/ml catechol-based NPs are shown to corroborate the absence of cytotoxic effects

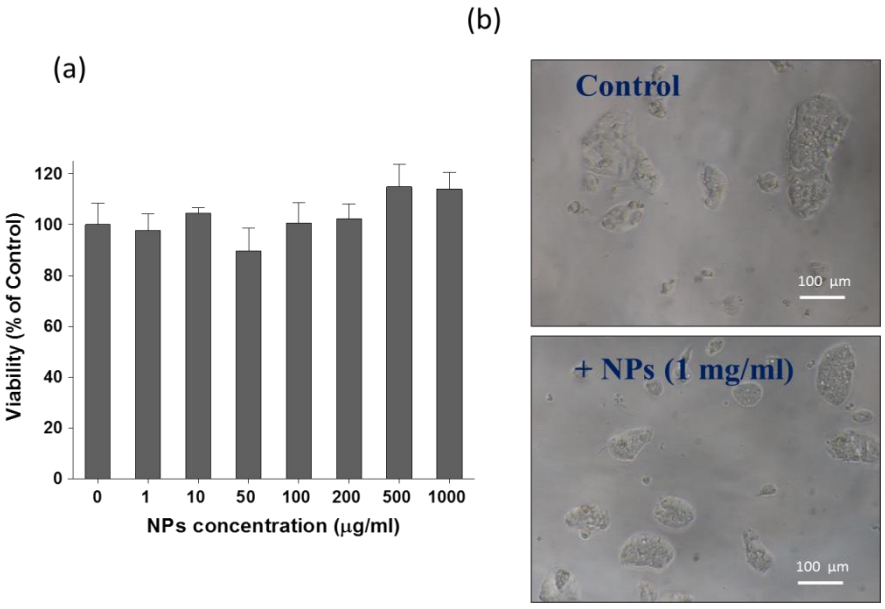

.

Figure 4.3.3. Cytotoxicity of catechol nanoparticles. (a) Cytotoxicity of catechol nanoparticles was evaluated against a liver hepatocellular carcinoma cell line (HepG2) by the XTT assay. Cells were incubated for 24 in absence and in presence of five increasing concentrations of catechol nanoparticles (up to 1000 µg/ml). (b) Optic microscope images of HepG2 cells after incubation in absence (Control) and presence (+NPs) of 1 mg/ml catechol nanoparticles.

4.3.4. Summary

The results obtained in this part of the study demonstrate that catechol-based nanoparticles can be effectively used as adsorbent for the removal of low concentrations of dissolved cadmium and lead ions, although they did not present affinity for chromium (VI). The catechol-based NPs had diameters between 200 and 350 nm. The maximum adsorption capacities obtained with the catechol-based NPs were 9.60 mg Pb^{2+}/g NPs and 9.08 mg Cd^{2+}/g NPs). Whereas the maximum adsorption capacity obtained with activated carbon were: 2.06 mg Cd^{2+}/g AC, 2.46 mg Pb^{2+}/g AC 2.46 mg Pb^{2+}/g AC and 3.96 mg Cr^{6+}/g AC, almost four times greater than catechol-based NPs. The regression equation coefficients for the simplest model were obtained, confirming that the initial heavy metal concentration variable in the model is significant. Toxicity tests using catechol-based NPs indicated no measurable toxicity neither in the case of Microtox assays nor in the case of human cells. Protein binding to catechol-based NPs confers stability to the particles in physiological environments and makes them cytocompatible thus amenable to applications in biological systems.

4.4 Cerium oxide (CeO_2) nanoparticles (NPs) anchored onto graphene oxide (GO) for the removal of heavy metal ions dissolved in water

---

The results presented in this part of the study were obtained during a stay at the Chemistry Department of Trinity College in Dublin.

4.4.1. General overview

Cerium oxide (CeO_2) is a rare earth oxide with a wide range of applications in catalysis, UV-blocking and oxygen sensors [169]. In addition, some studies used CeO_2 nanoparticles (NPs) as suitable adsorbent for the elimination of heavy metal ions [95,96,140]. Graphene and graphene oxide (GO) have been the hotspot in multidisciplinary areas due to its excellent mechanical, thermal, and electrical properties. In addition, both graphene and GO can be doped with metal oxides resulting in nanomaterials that usually have features that make them suitable materials for the effective sequestration of heavy metal ions due to their excellent adsorption performance [170,171]. Therefore they can be used to reduce the pollutant concentration by adsorption. Moreover, in the case of organic pollutants or persistent organic pollutants, those nanomaterials decompose the pollutants to less toxic molecules [172].

In this part of the study, we approach two different strategies, *in-situ* growth and *self-assembly* approach, to obtain a hybrid material composed of CeO_2 NPs anchored to the surface of GO, followed by a chemical reduction of the graphene oxide (RGO), becoming CeO_2/RGO. The *self-assembly* approach is based in a two-step synthesis, in which the first step is the synthesis of the nanoparticles with specific dimensions and morphologies using different stabilizers, such as 6-aminohexanoic acid (AHA) [169] or hexamethylenetetramine (HMT) [123], followed by the attachment of them to the surface of, in this case, the graphene oxide in a second step. On the other hand the *in-situ* growth, suggests the growth of the nanoparticles directly in the basal planes of the graphene oxide [169]. In most of hybrid materials, the metal NPs deposited on graphene often exhibit easily agglomeration under the high temperature used in the synthesis. Many studies suggest the addition of organic additives such as acrylamide (AM) [173] or poly(vinylpyrrolidone) (PVP) [169] to control the NPs dispersion and size.

The *in-situ* strategy (section 4.4.2.1.5) is based on the electrostatic adsorption of positively charged Ce^{3+} ions on the basal planes of GO sheets, that are highly negatively charged when dispersed in water [174], followed by in situ growth of CeO_2 on GO sheets, and finally, the conversion of GO into RGO. On the other hand, the *self-assembly* strategies

suggest (sections 4.4.2.1.3 and 4.4.2.1.4), go through the direct deposition of CeO_2 nanoparticles on the surface of the GO sheets followed by the reduction of GO to RGO [169].

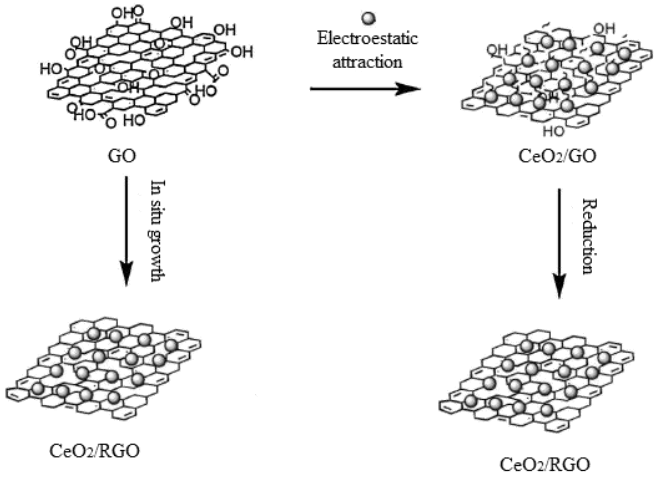

Figure 4.4.1 Synthesis of CeO_2/RGO nanomaterials by in situ growth (left) and self-assembly method (right). Adapted from Ling et al [173].

During the self-assembly process of the CeO_2/RGO-AHA nanomaterial, the AHA-stabilized CeO_2 were prepared as a first step, in which the carboxylic acid of the AHA would bind to the surface of the CeO_2 NPs and release a proton to form a carboxylate group. The proton would then protonate the amino group of AHA, generating a positively charged surface for the CeO_2 NPs [175]. As mentioned before the assembly of the CeO_2 NPs (stabilized with AHA) on the graphene oxide sheets is provide by the electrostatic interactions between the surface of the NPs and the surface of the GO, creating a well combined nanocomposite [169].

Ling et al. [173] proposed a similar approach for the formation of CeO_2/RGO-AM nanomaterial. Briefly, the acrylamide (AM) is hydrolyzed to produce a polymer which reacts to the metal ions and forms a polymer metal complex (PMC), where the cerium ions and the amino groups are bonded. The PMC with a positive charge is attracted by the GO negatively charged and the self-assembly befall once again by electrostatic attraction; therefore the metal ions are anchored to the surface of the GO maintaining the layered structure and finally reduced with ascorbic acid.

In the case of the in-situ synthesis, the AM is added in the first step (hydrolysis of the cerium salt) of the synthesis of CeO_2 NPs using HMT to form the PMC which generate a positive charge in the surface as well as favor the dispersion of the NPs on the surface of the GO, as shown in the above synthesis. The GO is directly mixed with the HMT and then added to the cerium solution in order that the hydroxyl ions oxidase the cerium and therefore obtain the NPs anchored on the surface of the GO.

The objective of this study was to investigate the influence of these two strategies in the distribution and the size of the NPs. Furthermore, the adsorption capacity of cadmium (II), lead (II) and chromium (VI) ions onto the new materials was tested and fitted to Langmuir and Freundlich isotherm adsorption models.

4.4.2. Materials and methods

4.4.2.1. Synthesis of CeO2 NPs in GO sheets

4.4.2.1.1. Synthesis of graphene oxide (GO) sheets

The synthesis of GO is based in the Hummers method starting from graphite flakes [176]. In this study, 1g of the graphite powder is mixed with 0.5 g of sodium nitrate ($NaNO_3$) in 23 ml of H_2SO_4 on an ice bath, then, the mixture is stirred for 15 minutes. Afterwards, 3 g of $KMnO_4$ were added gradually under stirring, the resulting mixture was continually stirred for 30 min at 35 °C and then diluted with 46 ml of deionized water and stirred for 15 more minutes. The mixture was maintained below 10 °C and kept stirred for 4 h at the same conditions. The reaction was terminated adding 140 ml of deionized water and 3.5 ml of H_2O_2. The solid product was separated by centrifugation and washed repeatedly with 10% HCl solution and water. Finally, the product was dried at 60 °C for 48 h.

4.4.2.1.2. Assembly of CeO_2 NPs onto GO sheets

Once the graphene oxide is successfully synthesized the strategies of *self-assembly* and *in-situ* growth are used as routes to obtain a hybrid nanomaterial constituted of cerium oxide nanoparticles on reduced graphene oxide.

4.4.2.1.3. Synthesis of 6-aminohexanoic acid CeO_2 nanoparticles and their deposit onto GO by self-assembly approach

The method to prepare 6-aminohexanoic acid (AHA)-stabilized CeO_2 NPs can be found in the literature, however some modifications were made [169]. Firstly, a solution containing 0.87 g of $Ce(NO_3)_3 \cdot 6H_2O$ and 80 ml of deionized water was heated to 95 °C under magnetic stirring. Then, 8 ml of 6-aminohexanoic acid (AHA) aqueous solution (131.25g/L) and 40 µl of 37% HCl solution were added in sequence to the previous solution. The final solution was kept at 95 °C for 6 h. The resultant solution is a homogeneous suspension containing positively charged CeO_2 nanocrystals.

The assembly process was conducted by mixing CeO_2 nanoparticles and graphene oxide nanosheets, followed by a reduction process of the GO to RGO. To obtain the negatively charged GO nanosheets colloidal dispersion 130 mg of graphite oxide and 433.33 mg of PVP (polyvinylpyrrolidone) were dispersed in 345 ml of deionized water by sonication for about 30 min. Afterwards, 43.33 ml of positively charged CeO_2 suspension was slowly added under magnetic stirring. After 4 h of stirring, 2 ml (2nM) of ascorbic acid was added to the above solution. The resulting mixture was refluxed at 95 °C for 1 h. The solid product was separated by centrifugation and well washed with water and ethanol to remove any impurities and then dried at 50 °C for 24 h. Finally the obtained product was designated as CeO_2/RGO-AHA.

4.4.2.1.4. Synthesis of acrylamide CeO_2 nanoparticles and their deposit onto GO by self-assembly approach

The method followed to synthetize the CeO_2/RGO-AM was previously describe by Ling et al. [173]. A solution of 1 mM $Ce(NO_3)_3 \cdot 6H_2O$ and 5 mM AM (acrylamide) were dissolved in 26 ml N,N-dimethylformamide (DMF) with ultrasonic treatment. At par 130 mg of GO was dispersed into 260 ml distilled water also with ultrasonic treatment for 2 h to form a brown solution.

For the assembly, the above two solutions were mixed and heated to 90 °C with continuous stirring for 1 h. Then, 2 ml of ascorbic acid (2mM) were added to reduce the graphene

oxide (RGO) and the solutions were refluxed at 90 °C for 6 h. The solid was separated by centrifugation and washed several times with ethanol and distilled water before drying at 60 °C for 24 h. The final product is designated as CeO_2/RGO-AM.

4.4.2.1.5. Synthesis of CeO_2 nanoparticles with hexamethylenetetramine and their deposit onto GO by in-situ growth

While in the two approaches previously describe the self-assembly strategy was followed, for the synthesis of CeO_2 NPs using hexamethylenetetramine (HMT) based on Zhang et al [123] an *in-situ* growth was used. Although some modifications were made in the synthesis in order to achieve the assembly, the initial conditions to precipitate the CeO_2 NPs remain the same.

A solution of 0.5 mM of acrylamide (AM) dissolved in 20 ml N,N-dimethylformamide (DMF) with ultrasonic treatment is mixed with 0.04M of $Ce(NO_3)_3 \cdot 6H_2O$ under stirring for 30 min. Then a solution of 0.5M of HMT and 130 mg of GO, also with ultrasonic treatment, was added to the previous solution. After 1 h stirring 2 ml of 2 mM of ascorbic acid was added. The final solution was maintained under mild stirring and room temperature for 24 h. The product was washed several times with ethanol and water and dried at 60 °C for 24 h. The nanocomposite material is designed as CeO_2/RGO-HMT.

4.4.2.2. Characterization methods

4.4.2.2.1. Raman spectrometry

Raman spectra were recorded using Renishaw 1000 micro-Raman system fitted with a Leica microscope and Grams Research™ analysis software. The excitation wavelength was 633 nm from a Renishaw RL633 HeNe laser. The 50x magnifying objective of the Leica microscope was capable of focusing the beam onto a spot of approximately 2–3 μm in diameter. Analyses were performed in the Trinity College.

4.4.2.2.2. Electron transmission microscopy

The physical and chemical properties of nanophase materials rely on their crystal and surface structures. Transmission electron microscopy (TEM) is a powerful and unique

technique for structure characterization. The most important application of TEM is the atomic-resolution real-space imaging of nanoparticles [177]. TEM images were obtained on a Jeol JEM-2100. Samples were prepared by deposition of each of the CeO_2/RGO nanomaterials dispersed in water onto a carbon coated 300 mesh copper grid. Diameters were measured with the Image J software program and the average values were calculated by counting a minimum of 100 particles. Analyses were performed in the Trinity College.

4.4.2.2.3. Inductively coupled plasma-optical emission spectrometry

Inductively coupled plasma-optical emission spectrometry (ICP-OES) is widely recognized as a suitable technique for the determination of metals. The samples of the heavy metal ions were acidified with concentrated HNO_3 (pH < 3). The determination of cadmium (II), lead (II) and chromium (VI) was performed by an ICP-OES Perkin-Elmer Optima 4300DV model. The experimental analyses were performed by the Servei d'Anàlisi Química in the UAB.

4.4.2.3. Metal adsorption experiments and isotherm models

The adsorption experiments were performed using cadmium (II) chloride (99.9%), lead (II) nitrate (99.9%) and potassium dichromate (VI) (99.5%) as metal sources. To test the adsorption capacity and determine the adsorption isotherms of the different nanomaterials synthetized, eight dilutions of cadmium, lead and chromium (5, 30 50, 100, 150, 200, and 250 mg/L) were carried out. Each of these solutions were mixed with 0.05 mg of CeO_2/RGO (HMT, AM and AHA) nanomaterial. GO was used as control at the same conditions, all the experiments were stirred at 200 rpm at room temperature for 24 hours. No adjustment in the pH was performed (pH= 5.5-6). The samples were filtrated (40 µm) to separate the nanomaterial (solid phase) from the liquid phase. The supernatant was analyzed for residual dissolved heavy metals (non-adsorbed metal). The adsorption capacity at the equilibrium was calculated with the Equation 7 (Section 4.1).

Normally, the adsorption of metal ions from aqueous solutions is largely based on ion exchanges or chemical/physical adsorptions on specific sites of the adsorbents, and therefore the pore structures and surface areas of the adsorbents would play the vital roles

[99]. Equilibrium adsorption isotherms are usually used to determine the capacities of adsorbents. The most common models used are the Langmuir and the Freundlich models (previously mentioned and described in Chapter 2). The linear form of the previous models was used to fit the experimental data (Equation 1 and 2).

4.4.3. Results and discussion

4.4.3.1. Structural characterization of the nanomaterials

We have described two different strategies for the fabrication of CeO_2/RGO nanomaterials: *in situ* growth and the *self-assembly* approach. Through these approaches different materials were obtained: CeO_2/RGO-AHA, CeO_2/RGO-AM and CeO_2/RGO-HMT. Each obtained product was characterized by Raman spectroscopy and Transmission electron microscopy.

4.4.3.1.1. Raman spectroscopy

Raman scattering is a powerful tool to characterize carbon based materials in a non-destructive way. The most prominent features in the Raman spectra of monolayer graphene are the so-called G band appearing at 1582 cm^{-1} (graphite) and the G′ band at about 2700 cm^{-1} using laser excitation at 2.41 eV. Figure 4.4.2 shows the Raman spectra of the CeO_2/RGO-AHA, CeO_2/RGO-HMT and the GO yet due to technical problems the CeO_2/RGO-AM could be analyzed. Two distinct pics corresponding to the well-known G and D bands are displayed. The G band is usually assigned to the vibration of sp^2 carbon atoms in a graphitic 2D hexagonal lattice, while the D band is associated with the vibrations of sp^3 carbon atoms of defects and disorder [169,170]. In a typical synthesis, GO showed D-band at 1345cm^{-1} and G-band at 1598cm^{-1}. After the reduction, the D-band remained the same but G-band shifted to lower frequency region (1580cm^{-1}), confirming the reduction [103]. The peak of the CeO_2 NPs at 455cm^{-1} also appears, this suggests that cerium oxide nanoparticles are successfully attached on the reduced graphene oxide.

4.4.3.1.2. Transmission electron microscopy

Using TEM it is possible to elucidate the size, morphology and microstructure of the GO, by dropping a small quantity of the dispersion onto holey carbon grids [178]. Figure 4.4.3 shows the TEM images of the CeO_2/RGO nanomaterials prepared by both strategies: *self-assembly* and *in situ* growth as well as their size distribution.

Figure 4.4.2. Ramman spectra of (a) graphene oxide (GO) and (b) CeO_2/RGO by *self-assembly* by suing AHA and (c) CeO_2/RGO by *in situ* using HMT.

As shown in Figure 4.4.3A, cerium oxide nanoparticles (CeO_2/RGO-AM) are deposited uniformly dispersed on the graphene oxide. The size of the nanoparticles falls mainly in the range of 2nm (Figure 4.4.3A'). From Figure 4.4.3B, it can be seen some agglomeration of the nanoparticles (AHA-stabilized) deposited on the surface of the RGO; however all the cerium nanoparticles are found exclusively attached to the graphene oxide. The size of the nanoparticles is 16 nm (Figure 4.4.3B'). The TEM image of the CeO_2/RGO-HMT, Figure

4.4.3C, present high density of nanoparticles attached to the RGO with nanoparticles of the size in the range between 2-4nm (Figure 4.4.3C').

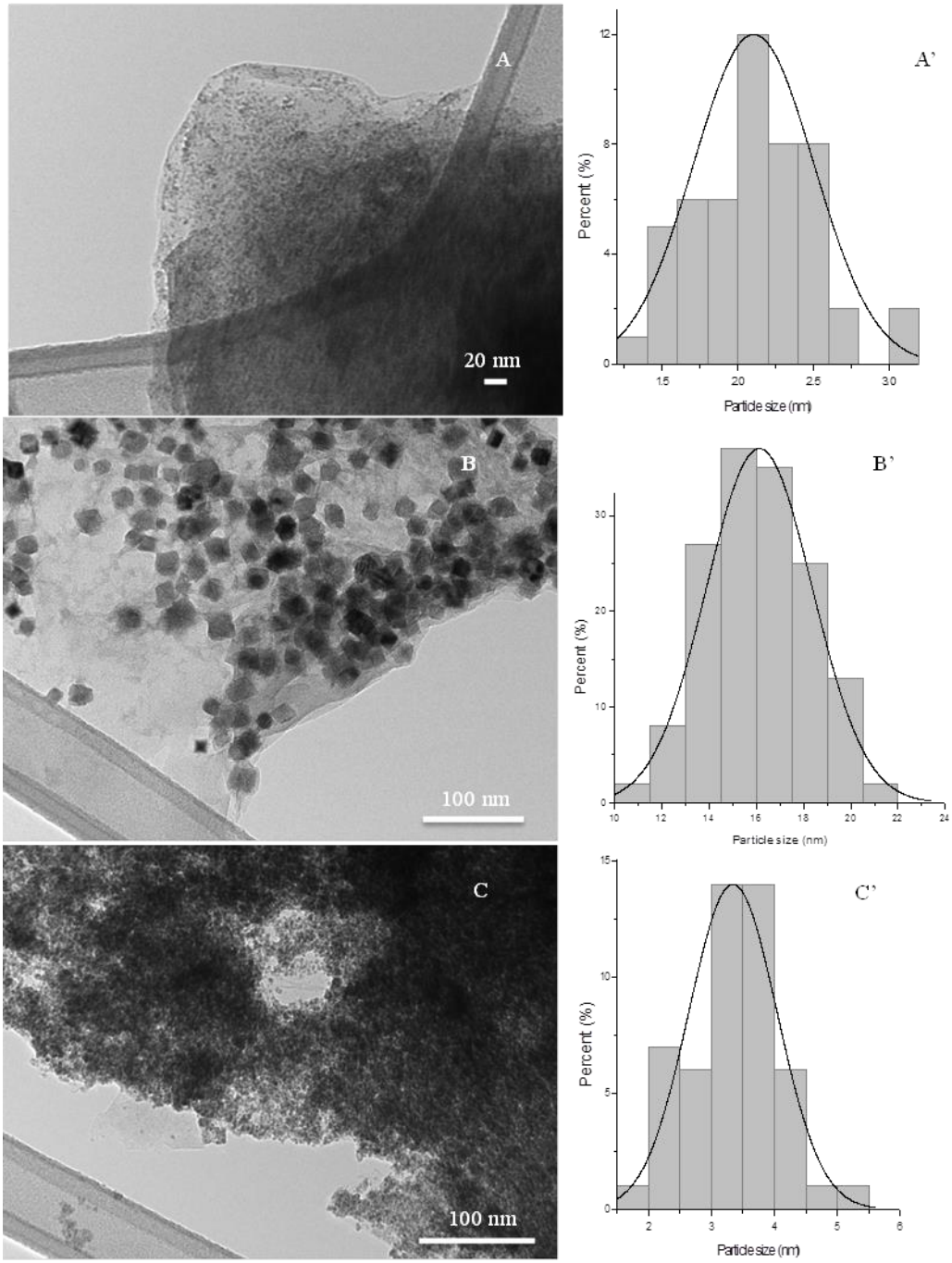

Figure 4.4.3. TEM images of (A) CeO_2/RGO-AM, (B) CeO_2/RGO-AHA and (C) CeO_2/RGO-HMT nanocomposites as well as the size distribution (A')-(C').

4.4.3.2. Adsorption Isotherms

The adsorption of lead (II), cadmium (II) and chromium (VI) from aqueous solutions onto graphene oxide nanosheets impregnated with cerium oxide nanoparticles were tested. The Tables 4.4.1 to 4.4.3 shows the adsorption capacity of each metal with each adsorbent, as well as the final metal concentration. It was observed that mainly lead (II) showed changes in the concentration and cadmium (II) was adsorbed at lower concentrations. Moreover the adsorption of chromium (VI) in solution does not follow a clear tendency and therefore, no adsorption model was applied. As previously mentioned chromium is present in its anionic form thus, the repulsion with the negative charge of the GO appear to be stronger than the interaction with the NPs showing very little affinity for the nanomaterial in general.

Table 4.4.1 Adsorption experiments for the removal of Pb (II) dissolved in water with different CeO_2/RGO nanomaterials.

Initial Pb (II) concentration	Adsorption capacities and final metal concentrations							
	GO		CeO_2/RGO-AHA		CeO_2/RGO-AM		CeO_2/RGO-HMT	
Ci (mg/L)	C_e (mg/L)	q_t (mg/g)	C_e (mg/L)	q_t (mg/g)	C_e (mg/L)	q_t (mg/g)	C_e (mg/L)	q_t (mg/g)
5	0.500	18.000	0.726	17.098	0.595	17.620	0.500	18.000
10	2.037	31.851	2.948	28.207	3.994	24.025	2.367	30.530
30	22.558	29.770	19.837	40.654	22.504	29.983	16.288	54.847
50	40.854	36.584	38.037	47.854	42.779	28.886	30.953	76.189
100	87.518	49.927	85.550	57.799	91.430	34.281	77.539	89.845
150	*	N/A	137.920	48.322	141.553	33.789	132.558	69.769
200	196.025	15.900	187.076	51.697	186.365	54.539	182.859	68.564
250	*	N/A	238.305	46.782	234.301	62.798	226.061	95.756

*Higher than the initial concentration; q_t: adsorption capacity measured after 24 h and expressed in mg metal / g nanomaterial; N/A: not available

Table 4.4.2 Adsorption experiments for the removal of Cd (II) dissolved in water with different CeO_2/RGO nanomaterials.

Initial Cd (II) concentration	Adsorption capacities and final metal concentrations							
	GO		CeO_2/RGO-AHA		CeO_2/RGO-AM		CeO_2/RGO-HMT	
C_i (mg/L)	C_e (mg/L)	q_t (mg/g)	C_e (mg/L)	q_t (mg/g)	C_e (mg/L)	q_t (mg/g)	C_e (mg/L)	q_t (mg/g)
5	2.472	10.113	4.493	2.026	2.821	8.715	3.320	6.720
10	6.143	15.429	9.202	3.192	7.770	8.919	7.081	11.675
30	27.242	11.032	30.580	N/A	28.855	4.581	27.107	11.572
50	49.000	4.001	45.821	16.715	49.078	3.688	50.014	N/A
100	*	N/A	*	N/A	99.470	2.120	*	N/A
150	*	N/A	*	N/A	*	N/A	*	N/A
200	*	N/A	*	N/A	196.730	13.081	*	N/A
250	*	N/A	*	N/A	242.184	31.262	*	N/A

*Higher than the initial concentration; q_t: adsorption capacity measured after 24 h and expressed in mg metal / g nanomaterial; N/A: not available

Table 4.4.3 Adsorption experiments for the removal of Cr (VI) dissolved in water with different CeO_2/RGO nanomaterials.

Initial Cr (VI) concentration	Adsorption capacities and final metal concentrations							
	GO		CeO_2/RGO-AHA		CeO_2/RGO-AM		CeO_2/RGO-HMT	
Ci (mg/L)	C_e (mg/L)	q_t (mg/g)	C_e (mg/L)	q_t (mg/g)	C_e (mg/L)	q_t (mg/g)	C_e (mg/L)	q_t (mg/g)
5	*	N/A	3.993	4.026	*	N/A	*	N/A
10	*	N/A	8.591	5.637	9.969	0.123	*	N/A
30	*	N/A	29.005	3.979	*	N/A	*	N/A
50	*	N/A	49.174	3.302	*	N/A	*	N/A
100	94.703	21.190	87.549	49.804	*	N/A	*	N/A
150	*	N/A	*	N/A	148.896	4.418	*	N/A
200	*	N/A	*	N/A	*	N/A	*	N/A
250	*	N/A	*	N/A	245.110	19.560	*	N/A

*Higher than the initial concentration; q_t: adsorption capacity measured after 24 h and expressed in mg metal / g nanomaterial; N/A: not available

The adsorption capacities obtained for lead (II) are presented in Table 4.4.1. The highest adsorption capacity obtained was for the adsorption of lead ions onto the CeO_2/RGO-HMT material (95.75 mgPb^{2+}/g CeO_2/RGO-HMT), almost the double than the obtained with the GO (49.927 mgPb^{2+}/g GO), this may be attributed to the fact that the concentration of CeO_2

NPs is higher in the in-situ synthesis. However in all the cases that the nanosheets of GO are impregnated with CeO_2 an increase in the adsorption was shown. Nevertheless, the values for the removal of lead (II) obtained are higher compared with other adsorbents such as, *Ficus religiosa* leaves (37.45 mgPb^{2+}/g) [179], plant maize (2.3 mgPb^{2+}/g) [180] or bagasse fly ash, (2.50 mgPb^{2+}/g) [181], but no as higher as the previous adsorption capacities obtained with the just the metal oxide nanoparticles (181.2 mg Pb^{2+}/g CeO_2, 153.24 mg Pb^{2+}/g TiO_2 and 81.6 mg Pb^{2+}/g NPs Fe_3O_4) [96].

From the adsorption capacity values for the removal of cadmium (Table 4.4.2), it can be observed that the maximum value was obtained with GO. It has been reported that in many cases, the adsorption capacity of GO is much higher than other carbonaceous materials, such as carbon nanotubes [182]. This results can be attributed not only to the high surface area, but also to the high oxygen content of GO [174]. In addition, the abundant oxygen-containing functional groups on the surfaces of graphene oxide nanosheets make the adjacent oxygen atoms available to bind metal ions [183]. It can be seen that the values obtained with GO (15.42 mg Cd^{2+}/g GO) and CeO_2/RGO-HMT (11.67 mg Cd^{2+}/g CeO_2/RGO-HMT) can be compared with those obtained with Filtrasorb 400 (9.5 mg Cd^{2+}/g) [184], carbon aerogel (15.5 Cd^{2+}/g) [185] or Indonesian peat (14 mg Cd^{2+}/g) [186] or TiO_2 (15.83mg Cd^{2+}/g TiO_2) previously describe in this work, while Fe_3O_4 (99.57 mg Cd^{2+}/g Fe_3O_4) and CeO_2 (48.30 mg Cd^{2+}/g CeO_2) presented higher adsorption capacities.

The adsorption isotherms have been quite useful in expressing the feasibility of an adsorbent for an adsorbate. The data obtained for the removal of cadmium (II) and lead (II) in adsorption method were fitted to the Freundlich, Langmuir and Temkin isotherm models. The parameters were calculated using Equation 1, 2 and 3 (Chapter 2), and are listed in the Table 4.4.1. The regression coefficients show that the Langmuir model fitted better than the Freundlich and the Temkin models, suggesting that Pb(II) and Cd (II) ions adsorption on four different nanocomposites are all monolayer coverage. The Langmuir isotherm best describes chemisorption processes. Chemisorption involves a more specific binding of the adsorbate to the solid. It is a process that is more similar to a chemical reaction and hence, only monolayer adsorption is possible [187]. The Temkin isotherm contains a factor (*b*) that explicitly takes into account adsorbent–adsorbate interactions. By ignoring the extremely

low and large value of concentrations, the model assumes that heat of adsorption (function of temperature) of all molecules in the layer would decrease linearly rather than logarithmic with coverage [188,189]. On the other hand, the Freundlich coefficient (*n*), which should have values ranging from 1 to 10 and in this case is high (5.283 –6.76), supports the favorable adsorption of the metal ions onto the adsorbent [190].

Table 4.4.1. Parameters for Langmuir and Freundlich models of Pb(II) and Cd(II) ions adsorption on different CeO_2/RGO nanomaterials.

		Parameter		
Isotherm	Adsrobent	q_m (mg/g)	k_L (L/mg)	R^2
Langmuir	GO	50.251	0.150	0.9066
	CeO2/RGO-HMT	70.423	1.753	0.9888
	CeO2/RGO-AHA	48.780	0.519	0.9937
	CeO2/RGO-AM	63.694	0.036	0.9145
		k_F	n	R^2
Freundlich	GO	22.465	6.676	0.7673
	CeO2/RGO-HMT	23.862	4.047	0.9238
	CeO2/RGO-AHA	20.893	5.048	0.9119
	CeO2/RGO-AM	17.775	5.283	0.8538
		k_T (L/g)	b (J/mol)	R^2
Temkin	GO	126.974	4.560	0.7314
	CeO2/RGO-HMT	5.437	13.873	0.9674
	CeO2/RGO-AHA	31.504	6.114	0.9603
	CeO2/RGO-AM	664.543	3.000	0.6955

Overall, although the *self-assembly* approach produced nanomaterials with CeO_2 nanoparticles well dispersed on reduced graphene oxide sheets, a key step in the process is the preparation of well-defined nanoparticles to position itself as an advantageous synthetic procedure against the *in-situ* growth [169]. However, the adsorption results suggest that the material synthetized by *in-situ* growth not only presented higher adsorption capacities but also simplify the process avoiding a prior step of prepared the CeO_2 NPs separately.

4.4.4. Summary

Graphene oxide was successfully synthetized. The Raman spectroscopy showed the peak associated to the G and D band of the GO and the peak of the CeO_2 NPs at 455cm^{-1} , which confirm that cerium oxide nanoparticles were anchored to the surface. The size of the CeO_2 NPs attached to GO, was from 2nm to 16 nm. The highest % removal (90%) was obtained with CeO_2/RGO-HMT and GO, for the removal of Pb (II). The correlation coefficient (R^2) for Langmuir (0.9066-0.9937) isotherm model suggests chemisorption and monolayer coverage. Although Pb (II) and Cd (II) showed the main adsorption capacities, Cr (VI) was removed at lower concentrations; the higher adsorption capacity obtained was 49.804mg Cr^{6+}/g CeO_2/RGO-AHA. Future studies will explore the reuse of the nanomaterial to give a better understanding of the reusability of the adsorbent. Another important parameter is to test the nanomaterial in multicomponent systems as a first step towards their utilization with real wastewaters. GO owns an excellent hydrophilicity property, which has been used to remove organic compounds. Therefore, the use of this nanomaterial to remove organic compounds such as pesticides or dyes should be tested.

4.5 Summary of adsorption capacities

A fair comparison of adsorption capacity between the nanomaterials used throughout this work and other adsorbents could be obtained. This comparison is shown in Table 4.5.1.

According to literature each material used present different sorption mechanisms. The sorption process on NMOs is mainly controlled by complexation between dissolved metals and oxygen in the metal oxides nanoparticle. The NMOs are also know for exhibit high adsorption capacity, fast kinetics and preferable sorption for heavy metals in water and wastewater [94]. The abundant functional groups especially catechol groups of PDA are expected to be the active sites for heavy metals ions through electrostatic, bidentate chelating, or hydrogen bonding interactions, which has stimulated extensive research on the polydopamine-based adsorbent materials anticipating a high adsorption capacities [114]. Finally, GO possess not only a great surface area, but also abundant oxygen containing groups capable of binding with metal ions. Yet, the reduction and the anchor of the CeO_2 NPs to the surface may reduce the oxygen content, and therefore decreasing available sites for metal ions to bind. Although the CeO_2/GO nanomaterials can be used effectively as adsorbent, the metal oxide NPs can be replaced by magnetic nanomaterials in order not only to remove the metal ions but, to remove other kinds of contaminants such as, organics pollutants presents in more complex matrix.

In comparison with the other adsorbents, the adsorptive capacity of metal oxide nanoparticles for the removal of cadmium (94.44 mg $Cd^{2+/}$g CeO_2) was found to be higher than activated carbon (2.06 mg $Cd^{2+/}$ g AC), the catechol-based nanoparticles (9.08 mg $Cd^{2+/}$g catechol-based NPs), graphene oxide and graphene oxide-based nanomaterial (15.42 mg $Cd^{2+/}$g GO, 11.67 mg $Cd^{2+/}$g CeO_2/RGO-HMT). Although the graphene oxide-based nanoparticles showed high values of adsorption capacity for the removal of lead (49.92 mg $Pb^{2+/}$g GO, 95.75 mg $Pb^{2+/}$g CeO_2/RGO-HMT), the values are lower than the values obtained with NMOs (128.13 mg $Pb^{2+/}$g CeO_2, 153.24 mg $Pb^{2+/}$g TiO_2, 81.6 1 mg $Pb^{2+/}$g Fe_3O_4). On the other hand the best adsorption capacity for chromium was obtained with CeO_2/RGO-AHA (48.80 mg Cr^{6+}/g CeO_2/RGO-AHA), follow by GO (21.19 mg Cr^{6+}/g) which present a similar adsorption capacity than the CeO_2 NPs in single systems (21.3 mg Cr^{6+}/g CeO_2).

Through this comparison it is important also to consider the aqueous chemistry of the metal ions, for example the anionic species of chromium do no present affinity with the mussel inspired nanoparticles. In addition, it was found that the pH was a statistically significant parameter in the adsorption process, i.e., changing this parameter affects the adsorption capacities, in this case cadmium and chromium. Overall, the results obtained suggest that CeO_2 NPs can be used for water treatment process at neutral pH in a wide range of metal concentration aiming for drinking water purification. On the other hand the feasibility of the catechol-based NPs and the CeO_2/RGO nanomaterials to adsorb the metal ions at a slightly acidic pH (pH corresponding to the solutions of metals) is an advantage when the adsorption process is considered to remove metals ions from industrial wastewater, since it is not necessary to adjust the pH to maintain the nanomaterials intact.

The statistical analysis for the adsorption process in uni/multicomponent systems also show that the adsorption was significantly affected by the initial metal and NPs concentration regardless the type of system. These results suggest that all the surface area of the NMOs were available to adsorption process with enough sites avoiding competitive sorption phenomena.

Although different nanomaterials were tested for the removal of heavy metals, the reaction conditions of the adsorption process, such as temperature and reaction time tried to remain as close as possible between the experiments (only pH were modified) to make a suitable comparison. However, it should be noted that it is not easy comparing adsorption results because each nanomaterial possess different physico-chemical properties on the surface. Nevertheless, from the results presented in Table 4.5.1 it can be seen that the adsorption process is a suitable option for the removal of heavy metals in water and wastewater.

Table 4.5.1. Summary of Cd(II), Pb(II) and Cr(VI) adsorption capacity of various adsorbents

Type of adsorbent	qt (mg metal/g NPs)	pH	Reference
CeO_2	48.30 mg Cd^{2+}/g	7	Present study
	181.2 mg Pb^{2+}/g		Recillas et al.[96]
	121.81 mg Cr^{6+}/g		Recillas et al.[95]
Single system	62.03mg Cd^{2+}/g	7	Present study
	43.75 mg Pb^{2+}/g	5	
	21.3 mg Cr^{6+}/g		
Multicomponent system	94.44 mg Cd^{2+}/g	7	Present study
	128. 13 mg Pb^{2+}/g	5	
	34.4 mg Cr^{6+}/g		
TiO_2	15.83 mg Cd^{2+}/g	7	Present study
	153.24 mg Pb^{2+}/g		Recillas et al. [96]
Fe_3O_4	99.57 mg $Cd^{2+/}$g	7	Present study
	81.6 mg Pb^{2+}/g		Recillas et al.[96]
Slag	20.96 mg Cd^{2+}/g		
	5.59 mg Pb^{2+}/g	5.5	Pesent study
	16.16 mg Cr^{6+}/g		
Catechol-based	9.08 mg Cd^{2+}/g	5.5	Present study
	9.60 mg Pb^{2+}/g		
Activated carbon	2.06 mg Cd^{2+}/g		
	2.45 mg Pb^{2+}/g	5.5	Present study
	3.96 mg Cr^{6+}/g		
	178.5 mg Cd^{2+}/g	2	Karnib M. et al. [3]
	294.11mg Pb^{2+}/g	2	Karnib M. et al. [3]
GO	15.42 mg Cd^{2+}/g		
	49.92 mg Pb^{2+}/g	~5.5	Present study
	21.19 mg Cr^{6+}/g		
	91.29 mg Cd^{2+}/g	6	Kyzas G.Z. et al. [104]
Chitosan/GO	76.94 mg Pb^{2+}/g	5	Fan L. et al. [191]
CeO_2/RGO-AHA	3. 19 mg Cd^{2+}/g		
	57.79 mg Pb^{2+}/g	~5.5	Present study
	48.80 mg Cr^{6+}/g		
CeO_2/RGO-AM	8.91 mg Cd^{2+}/g		
	32.79 mg Pb^{2+}/g	~5.5	Present study
	19.56 mg Cr^{6+}/g		
CeO_2/RGO-HMT	11.67 mg Cd^{2+}/g	~5.5	Present study
	95.75 mg Pb^{2+}/g		

5. Other preliminary works

5.1 Removal of heavy metals from real water/wastewater

The results presented in this part of the study were obtained in collaboration with the Agència de Residus de Catalunya and the local municipal wastewater treatment plant (LMWWTP) of Riu Sec

5.1.1. General overview

As mentioned before, the increased use of heavy metals in industry has resulted in increased availability of metallic substances in natural water sources. The presence of zinc, chromium, nickel and others metals in the aqueous environment has a potentially damaging effect on human physiology and other biological systems when the acceptable levels are exceeded [3,77]. In natural surface waters, the concentration of zinc is usually below 0.01 mg/L, and in ground waters, 0.01– 0.040 mg/L [192]. In Europe, reported nickel concentrations in drinking-water were generally below 0.01 mg/L [193].

Samples of real water were obtained from two different sources. The first one is the Agència de Residus de Catalunya (ARC), the public entity of Catalonia for the management of wastes. It has jurisdiction over the waste generated in Catalonia and those that are managed on its territory; excluding radioactive waste, waste resulting from prospecting, extraction, treatment and storage of mineral resources and quarrying, farm waste that are not dangerous and used exclusively within the farm, declassified explosives, wastewater and gaseous effluents emitted into the atmosphere [194]. The second one is the local municipal wastewater treatment located in Sabadell (LMWWT-Riu-Sec) (Catalonia, Spain). It is a plant which consists of a primary treatment option with physico-chemical treatment for a mean flow of 50 000 m^3/day and a second phase of biological treatment with anaerobic digestion sludge for a flow of 33 000 m^3/day. In 2007 expansion works were made to set-up a pioneer treatment in Spain based on a Membrane Bioreactor (MBR) which allow direct reuse of treated water [195].

It should be emphasized that, besides heavy metal ions, industrial-metal-bearing wastewater also contains other materials, examples being the following: i) other cations, such as: calcium, sodium or magnesium; ii) chelating agents, and iii) other organic materials. All these other materials can produce three possible types of behavior: synergism, antagonism and noninteraction. Also, the literature is still insufficient to cover the problem of adsorption from real wastewaters [196]. The aim of this part is to test CeO_2 NPs for the removal of heavy metals in more realistic conditions. Only punctual test were performed, however, this results could be considered as a first approach towards a real application of

the nanomaterials.

5.1.2. Materials and methods

5.1.2.1. Wastewater from Agència de Residus de Catalunya

The wastewaters from the ARC, were selected on the basis of metal content, although the objective was to select samples with the heavy metals previously described (cadmium, lead and chromium), these metals do not were found in the wastewater. Therefore, samples with other metals of interest such as zinc, nickel and chromium were used instead. The initial metal concentration are listed in the Table 5.1.1

Table 5.1.1 Initial metal concentrations

Metal	Metal concentration (mg/L)
Cr^{6+}	0.2
	2
Ni^{2+}	0.3
	4.4
Zn^{2+}	0.2
	1.1

5.1.2.2. Wastewater from the local municipal wastewater treatment plant-Riu-Sec (Sabadell, Spain)

In this case, wastewaters collected at the end of the process do not have any kind of metal present. Therefore, for the adsorption experiments, heavy metals were added. Table 5.1.2 shows the initial concentrations used. Adsorption in single component system (one metal only) and multicomponent system (cadmium, lead and chromium) were performed using the same initial concentration of metal for both systems.

Table 5.1.2. Initial metal concentrations

Metal	Metal concentration (mg/L)
Cd^{2+}	0.5
Pb^{2+}	0.5
Cr^{6+}	0.5

5.1.2.3. CeO_2 NPs

CeO_2 NPs were used in this part of the study. A brief description of the synthesis methodology of these NPs can be found in Chapter 4, Section 4.1. The concentration of CeO_2 NPs in all the experiments was 0.064 mg/L.

5.1.2.4. Determination of metal concertation

The determination of the final concentration of chromium, zinc and nickel ions was carried out by ICP-MS in the ARC. The determination of the final concentration of cadmium, lead and chromium ions was carried out by the Servei d'Anàlisi Química in the UAB.

5.1.3. Results and discussion

5.1.3.1. Adsorption of Zn (II), Ni (II) and Cr (VI)

CeO_2 NPs were assayed for adsorption of chromium (VI), zinc (II) and nickel (II) from ARC wastewater. From the Table 5.1.3, it is possible to observe that the CeO_2 NPs remove all the heavy metals. The adsorption of nickel ions presented the highest adsorption capacity (3.541 mg Ni^{2+}/g CeO_2), followed by zinc (7.234 mg Zn^{2+}/ g CeO_2) and finally chromium (5.179 mg Cr^{6+}/g CeO_2).

Table 5.1.3 Adsorption capacities and % removal for ARC wastewater.

Metal	Initial metal concentration (mg/L)	Final metal concentration (mg/L)	qt (mg/g)	% Removal
Cr^{6+}	0.1870	0.158	0.442	15.152
	2.0315	1.700	5.179	16.318
Ni^{2+}	0.3853	0.158	3.541	58.824
	4.0860	3.545	8.453	13.240
Zn^{2+}	0.1873	0.245	0.245	N/A
	1.1723	0.866	7.234	26.073

5.1.3.2. Adsorption of Cd (II), Pb (II) and Cr (VI)

The results of the adsorption of Cd (II), Pb (II) and Cr (VI) for the wastewater obtained from LMWWTP-Riu Sec with CeO_2 NPs are listed in Table 5.1.4 for single and multicomponent systems. The highest adsorption capacity in single systems was obtained for the removal of lead (7.687 mg Pb^{2+}/g CeO_2), followed by cadmium (6.859 mg Cd^{2+}/g CeO_2) and finally chromium (0.937 mg Cr^{6+}/g CeO_2). The adsorption capacities of the multicomponent systems presented similar adsorption capacities than the single system (6.796 mg Pb^{2+}/g CeO_2, 7.692 mg Cd^{2+}/g CeO_2, 1.046mg Cr^{6+}/g CeO_2).

Table 5.1.4 Adsorption capacities for the removal of Cd (II), Pb(II) and Cr (VI) in single and multicomponent systems

	Single system				Multicomponent system		
Metal	Initial metal concentration (mg/L)	Final metal concentration (mg/L)	qt (mg/g)	% Removal	Final metal concentration (mg/L)	qt (mg/g)	% Removal
Cd^{2+}	0.5	0.061	6.8594	87.800	0.065	6.7969	87.000
Pb^{2+}	0.5	0.008	7.6875	98.400	0.0077	7.6922	98.460
Cr^{6+}	0.5	0.44	0.9375	12.000	0.433	1.0469	13.400

5.1.4. Summary

In this study, CeO_2 NPs demonstrated to be effective adsorbents for the removal of heavy metal ions from real wastewater. CeO_2 NPs showed the greatest affinity in multicomponent systems firstly, towards lead (98.4 % removal), followed by nickel (58.9 % removal), then cadmium (87 % removal) and finally chromium (13-16 % removal). Nevertheless, experiments incrementing the adsorbent dose could be performed in order to increase the adsorption efficiency.

5.2 Removal of heavy metals with metallurgical slag

The results presented in this part of the study were obtained in collaboration with the Universidad Nacional Autónoma de México (UNAM), Department of Environmental Engineering, through a research stay in our laboratories of Bertha Mercado.

5.2.1. General overview

Due to the toxicity and the bio-accumulation of the heavy metals, the regulations for the discharge of contaminant effluents are getting strictest. Therefore non-conventional materials are being considered to remove heavy metals [197]. Slag as an alternative adsorbent has been used to remove heavy metals due to its unique properties. Steel-making slag is a major by-product in steel-making process and a waste material reused widely for their useful properties [198]. Slag consists of calcium oxide, magnesium oxide, and other metal oxides. Oxides contained in the slag are similar to those of Portland cement which slag has been used such as raw material in road construction [199]. For its sorptive characteristics, slag has been used in water and wastewater treatments as a low cost adsorbent replacing granular activated carbon. Adsorptions of dye, nickel, phosphorus, and lead are some of the examples [200].

5.2.2. Materials and methods

5.2.2.1. Synthetic water

The preparation of the solutions containing the heavy metals was made as described in Chapter 3.

5.2.2.2. Characterization of slag

The main constituents of the slag were determinate by X-ray Fluorescence (XRF). The crystalline and mineralogical phases of the main constituents were identified by X-ray Diffraction (XRD). The characterization analyses were performed at UNAM.

5.2.2.3. Determination of metals

The determination of the final concentration of cadmium, lead and chromium ions was carried out by the colorimetric methodology described in Chapter 3.

5.2.2.4. Adsorption experiments

A 3^k factorial experimental design with three levels and two factors plus three replications in the central point was applied; as a result twelve experiments were performed. Initial

concentrations used for the factorial design were 1 mg/L, 5.5 mg/L and 10 mg/L for each heavy metal, while concentrations of slag were 0.064 g/L, 0.352 g/L and 0.64 g/L. All experiments were performed under agitation at 130 rpm for 24h and pH 5.5.

5.2.3. Results and discussion

5.2.3.1. Slag characterization

Table 5.2.1 shows the main constituents identified by XRF in steel slag, which are iron, aluminum and silicon. In general, these values coincide with data previously reported in literature [201]. In the case of this study, steel slag could be a good candidate to remove heavy metals because its major components are aluminum and silicates.

Table 5.2.1. XRF chemical analysis of steel slag. All values in weight percent: μ=mean value, σ=standard variation for three samples, DL: Detection Limits for chemical composition

	$\%Fe_2O_3$	%CaO	%MgO	$\%Al_2O_3$	$\%SiO_2$	%MnO	$\%TiO_2$	$\%P_2O_5$	$\%Na_2O$	$\%K_2O$
μ	13.331	2.928	3.808	16.670	55.101	6.825	0.182	0.057	1.795	2.450
σ	0.453	0.392	0.563	0.325	1.910	0.078	0.003	0.023	0.473	0.438
DL	0.006	0.04	0.015	0.018	0.05	0.004	0.004	0.004	0.03	0.05

Table 5.2.2 shows the content of the main crystalline phases identified in slag, which were divided into two families: silicates and oxides/hydroxides. However, the crystalline phases and mineral constituents confirmed that aluminum and silicon were the main components of steel slag.

Table 5.2.2. Percentage of crystalline phases and minerals identified in iron and steel slags (n=3).

Silicate		Oxides and hydroxides	
Quartz SiO_2	10.7%	Brownmillerite $Ca_2(Al,Fe)_2O_5$	26.3%
Larnite Ca_2SiO_4	16.6%	Aluminum calcium oxide $Ca_3Al_2O_6$	46.3%

5.2.3.2. Adsorption of Cd (II), Pb (II) and Cr (VI)

The results of the adsorption of heavy metals with slag are listed in Table 5.3.1. The highest adsorption capacities were obtained for the removal of cadmium (20.96 mg Cd^{2+}/g slag) followed by chromium (16.16 mg Cr^{6+}/g slag), and finally lead (5.59 mg Pb^{2+}/g slag). The higher adsorption capacity for each metal was found with the lowest initial metal concentration and the highest initial concentration of slag.

Table 5.3.1 Adsorption capacities for the removal of Cd (II), Pb (II) and Cr (VI) with slag.

Metal	Initial slag concentration (mg/L)	Initial metal concentration (mg/L)	Final slag concentration (mg/L)	qt (mg/g)	% Removal
Cd^{2+}	0.064	10	0.36	20.96	64.12
Pb^{2+}	0.064	10	0.66	5.59	32.30
Cr^{6+}	0.064	5.5	0.024	16.16	75.96

The analysis of variance shows that, the independent variables (initial concentration of adsorbent and initial concentration of metal) were significant, the higher dose of slag and lower metal concentration greater the removal, this was for the three metals cadmium (II), chromium (II) and lead (II). Regression equations for Cd^{2+}, Cr^{6+} and Pb^{2+} adsorption (%) on steel slag are:

$$Cd^{2+}\text{ adsorption (\%)} = 50.79 + 14.77x - 8.79y_1 - 17.892x^2 - 0.82xy_1 + 1.78{y_1}^2 \quad (1)$$

$$Cr^{6+}\text{ adsorption (\%)} = 59.65 + 22.90x - 10.52y_2 - 18.90x^2 - 0.377xy_2 - 1.33{y_2}^2 \quad (2)$$

$$Pb^{2+}\text{ adsorption (\%)} = 18.16 + 9.01x - 6.30y_2 - 1.49x^2 - 1.73xy_3 - 0.07\,{y_3}^2 \quad (3)$$

where: x is the adsorbent dose in g/L and y_1, y_2 and y_3 are the concentrations of cadmium, chromium and lead in mg/L, respectively. All coefficients in the models were statistically significant at $p < 0.05$. From the above equations it can be seen that, the dose of slag have a positive effect, while heavy metal concentration has a negative effect on the Cd^{2+}, Cr^{6+} and Pb^{2+} removal by adsorption in the variation range of each variable selected for the present study.

5.2.4. Summary

The cadmium, lead and chromium metals were removed by the use of metallurgical slag. The maximum metal removal obtained using slag was Cr^{6+} 74% > Cd^{2+} 64% > Pb^{2+} 34%. The best conditions for the three metals removal were obtained with the highest dose of slag and lower of metal. The main adsorption mechanism of these pollutants is apparently achieved through the adsorption process by the aluminum and silicates compounds present in this industrial by-product.

6. *Conclusions and future work*

6.1. Conclusions

The main conclusions of this work are summarized in this Chapter.

The principal aim of this work was to test the feasibility of a series of nanomaterials for the removal of cadmium (II), lead (II) and chromium (VI) dissolved in water. In this frame, the main achievements of this thesis were:

Potential use of cerium oxide (CeO_2), titanium oxide (TiO_2) and iron oxide (Fe_3O_4) nanoparticles for the removal of cadmium from water

- The present study is the first critical assessment of the potential for inorganic NPs to sequester dissolved cadmium.
- The results show that Fe_2O_3 NPs offer the highest specific absorption capacity, while TiO_2 NPs offer the strongest adsorption.
- The adsorption follows the Freundlich isotherm model which suggests chemisorption.
- The kinetics adsorption data fit the pseudo-second order model.
- The magnetic properties of Fe_3O_4 NPs, which facilitate separation from the liquid medium, make Fe_2O_3 NPs attractive candidates for the removal of dissolved cadmium at acceptable costs.

Use of cerium oxide (CeO_2) nanoparticles for the adsorption of dissolved cadmium (II), lead (II) and chromium (VI) at two different pH in single and multi-component systems

- The results demonstrate that cerium oxide nanoparticles can be effectively used as adsorbents for the removal of dissolved Cd (II), Pb (II) and Cr (VI) in both single and multi-component aqueous systems.
- The initial concentrations of both, metal and NP were found statistically significant.
- pH was found to affect the sorption capacity of cadmium and chromium, but not that of lead.
- All The maximum sorption capacities obtained in this part of the study were in multicomponent systems.

Biocompatible mussel-inspired nanoparticles for the removal of heavy metals at extremely low concentrations

- The results obtained showed that the catechol-based NPs can be effectively used as adsorbents for the removal of low concentrations of cadmium (II) and lead (II) in water, although they did not present any affinity to chromium (VI).
- AC adsorbed all three heavy metals, but the catechol-based NPs resulted in adsorption capacities up to four times greater than those of AC with respect to cadmium and lead.
- The removal percentages of Cd and Pb were higher with NPs than with AC.
- The empirical modeling done in this work showed that the initial heavy metal concentration was the only statistically significant variable affecting adsorption capacity.
- Toxicity tests using catechol-based NPs indicated no measurable toxicity via Microtox assays.

Cerium oxide (CeO_2) nanoparticles anchored onto graphene oxide (GO) for the removal of heavy metal ions dissolved in water

- Graphene oxide was successfully synthetized and decored with cerium oxide nanoparticles by two different strategies.
- In situ growth as well as self-assembly approach show well distributed nanoparticles onto the RGO sheets.
- CeO_2/RGO could be used as effective adsorbent for the removal of divalent metal ions.
- The best affinity presented toward lead ions, obtaining the highest adsorption capacity.
- Removal of Cr (VI) occurs only at low initial metal concentrations.

Removal of heavy metals from real water/wastewaters

- Cerium oxide nanoparticles effectible remove chromium, nickel and zinc ions from a real wastewater system.

- The nickel ions presented the highest affinity towards cerium oxide nanoparticles.
- The removal of cadmium, lead and chromium in real treated water with cerium oxide nanoparticles were tested.
- In single systems the highest adsorption capacity was obtained with lead ions.
- In multicomponent systems the highest adsorption capacity was obtained with lead ions.

Removal of heavy metals with metallurgical slag

- Metallurgical slag was successfully used as adsorbent for the removal of cadmium, lead and chromium.
- The highest adsorption capacity was obtained in the removal of chromium.
- From the statistical analysis, the initial concentrations of adsorbent as well as the initial concentration of metal were found significant.

6.2. Future work

The present study shows that heavy metal adsorption can be achieved by using different type of nanomaterials and is just an initial study of their capacities. However, more work need to be made prior to implement the present findings as industrial applications:

- Laboratory assays with real multicomponent waters.
- Effect of temperature and pH on adsorption capacity.
- Nanoparticles recovery and reuse. Adsorption/desorption cycles.
- A life cycle assessment should be done; it would be a helpful technique to analyze the potential environmental and human health consequences of nanomaterials over their entire life cycle.
- An economic analysis.
- Scale-up system (pilot scale) needs to be designed and investigated to test how effective the adsorbent is in an industrial unit where conditions are not necessarily as ideal as in a laboratory.

7. References

[1] T. Pradeep, Noble metal nanoparticles for water purification: A critical review, Thin Solid Films. 517 (2009) 6441–6478.

[2] I. Sheet, A. Kabbani, H. Holail, Removal of Heavy Metals Using Nanostructured Graphite Oxide, Silica Nanoparticles and Silica/ Graphite Oxide Composite, Energy Procedia. 50 (2014) 130–138.

[3] M. Karnib, A. Kabbani, H. Holail, Z. Olama, Heavy metals removal using activated carbon, silica and silica activated carbon composite, Energy Procedia. 50 (2014) 113–120.

[4] K. Iwahori, J.I. Watanabe, Y. Tani, H. Seyama, N. Miyata, Removal of heavy metal cations by biogenic magnetite nanoparticles produced in Fe(III)-reducing microbial enrichment cultures, J. Biosci. Bioeng. 117 (2014) 333–335.

[5] I. Report, Global Risks 2015 10th Edition, World Econ. Forum. (2015).

[6] WHOandUnicef, Progress on Sanitation and Drinking Water 2013 Update, 2013.

[7] A. El Rahman, M. Gepreel, Nanotechnology Applications in Water Treatment: Future Avenues and Challenges: A review, in: 6th Int. Perspect. Water Resour. Environ. Conf., Izmir, Turkey., 2013.

[8] J. Brame, Q. Li, P.J.J. Alvarez, Nanotechnology-enabled water treatment and reuse: emerging opportunities and challenges for developing countries, Trends Food Sci. Technol. 22 (2011) 618–624.

[9] N. Savage, M.S. Diallo, Nanomaterials and Water Purification: Opportunities and Challenges, J. Nanoparticle Res. 7 (2005) 331–342.

[10] J. Theron, J. a Walker, T.E. Cloete, Nanotechnology and water treatment: applications and emerging opportunities., Crit. Rev. Microbiol. 34 (2008) 43–69.

[11] K. Kadirvelu, K. Thamaraiselvi, C. Namasivayam, Removal of heavy metals from industrial wastewaters by adsorption onto activated carbon prepared from an agricultural solid waste, Bioresour. Technol. 76 (2001) 63–65.

[12] F. Ge, M.-M. Li, H. Ye, B.-X. Zhao, Effective removal of heavy metal ions Cd2+, Zn2+, Pb2+, Cu2+ from aqueous solution by polymer-modified magnetic nanoparticles., J. Hazard. Mater. 211-212 (2012) 366–72.

[13] W.S. Wan Ngah, M.A.K.M. Hanafiah, Removal of heavy metal ions from wastewater by chemically modified plant wastes as adsorbents: a review., Bioresour. Technol. 99 (2008) 3935–48.

[14] M. Kobya, E. Demirbas, E. Senturk, M. Ince, Adsorption of heavy metal ions from aqueous solutions by activated carbon prepared from apricot stone., Bioresour. Technol. 96 (2005) 1518–21.

[15] P.C. Nagajyoti, K.D. Lee, T.V.M. Sreekanth, Heavy metals, occurrence and toxicity for plants: A review, Environ. Chem. Lett. 8 (2010) 199–216.

[16] EPA, Toxic and priority pollutants, (2015).

[17] M.A. Hashim, S. Mukhopadhyay, J.N. Sahu, B. Sengupta, Remediation technologies for heavy metal contaminated groundwater., J. Environ. Manage. 92 (2011) 2355–88.

[18] A.-M. Florea, D. Büsselberg, Occurrence, use and potential toxic effects of metals and metal compounds., Biometals. 19 (2006) 419–427.

[19] S. Tong, Y.E. Von Schirnding, T. Prapamontol, Environmental lead exposure: a public health problem with global dimensions, Servir. 49 (2000) 35–43.

[20] M. Fleischer, A.F. Sarofim, D.W. Fassett, P. Hammond, H.T. Shacklette, C.T. Nisbet, et al., Environmental Impact of Cadmium : A review by the Panel on Hazardous Trace Substances, Environ. Health Perspect. (1974) 253–323.

[21] L. Järup, Hazards of heavy metal contamination, Br. Med. Bull. 68 (2003) 167–182.

[22] J. Godt, F. Scheidig, C. Grosse-Siestrup, V. Esche, P. Brandenburg, A. Reich, et al., The toxicity of cadmium and resulting hazards for human health., J. Occup. Med. Toxicol. 1 (2006) 22.

[23] M. Owlad, M.K. Aroua, W.A.W. Daud, S. Baroutian, Removal of hexavalent chromium-contaminated water and wastewater: A review, Water. Air. Soil Pollut. 200 (2009) 59–77.

[24] J. Kotaś, Z. Stasicka, Chromium occurrence in the environment and methods of its speciation, Environ. Pollut. 107 (2000) 263–283.

[25] V. Gómez, M.P. Callao, Chromium determination and speciation since 2000, TrAC Trends Anal. Chem. 25 (2006) 1006–1015.

[26] A. Nakajima, Y. Baba, Mechanism of hexavalent chromium adsorption by persimmon tannin gel., Water Res. 38 (2004) 2859–64.

[27] G.-R.R. Bernardo, R.-M.J. Rene, A.-D.L.T. Ma Catalina, Chromium (III) uptake by agro-waste biosorbents: chemical characterization, sorption-desorption studies, and mechanism., J. Hazard. Mater. 170 (2009) 845–54.

[28] M. Karvelas, A. Katsoyiannis, C. Samara, Occurrence and fate of heavy metals in the wastewater treatment process, Chemosphere. 53 (2003) 1201–1210.

[29] M.A. Barakat, New trends in removing heavy metals from industrial wastewater, Arab. J. Chem. 4 (2011) 361–377.

[30] G. Aragay, J. Pons, A. Merkoçi, Recent trends in macro-, micro-, and nanomaterial-based tools and strategies for heavy-metal detection, Chem. Rev. 111 (2011) 3433–3458.

[31] T.H.E. Council, O.F. The, E. Union, COUNCIL DIRECTIVE 98/83/EC of 3 November 1998 on the quality of water intended for human consumption, Off. J. Eur. Communities. L 330 (1998) 32–54.

[32] T.A. Kurniawan, G.Y.S. Chan, W.-H. Lo, S. Babel, Physico–chemical treatment techniques for wastewater laden with heavy metals, Chem. Eng. J. 118 (2006) 83–98.

[33] EPA, Wastewater Technology Fact Sheet Chemical precipitation, Washington, D.C, 2000.

[34] D. Feng, C. Aldrich, H. Tan, Treatment of acid mine water by use of heavy metal precipitation and ion exchange, Miner. Eng. 13 (2000) 623–642.

[35] T.M. Zewail, N.S. Yousef, Kinetic study of heavy metal ions removal by ion exchange in batch conical air spouted bed, Alexandria Eng. J. 54 (2015) 83–90.

[36] F. Fu, Q. Wang, Removal of heavy metal ions from wastewaters: a review., J. Environ. Manage. 92 (2011) 407–18.

[37] A. Dabrowski, Z. Hubicki, P. Podkościelny, E. Robens, Selective removal of the heavy metal ions from waters and industrial wastewaters by ion-exchange method., Chemosphere. 56 (2004) 91–106.

[38] S.H. Lin, C.D. Kiang, Chromic acid recovery from waste acid solution by an ion exchange process: equilibrium and column ion exchange modeling, Chem. Eng. J. 92 (2003) 193–199.

[39] G. Zhao, X. Wu, X. Tan, X. Wang, Sorption of heavy metal ions from aqueous solutions : A review, Open Colloid Sci. J. 4 (2011) 19–31.

[40] S. Sen Gupta, K.G. Bhattacharyya, Kinetics of adsorption of metal ions on inorganic materials: A review., Adv. Colloid Interface Sci. 162 (2011) 39–58.

[41] S. Lyubchik, A. Lyubchik, O. Lygina, S. Lyubchik, I. Fonseca, Comparison of the Thermodynamic Parameters Estimation for the Adsorption Process of the Metals

from Liquid Phase on Activated Carbons, in: D.J.C. Moreno (Ed.), Thermodyn. - Interact. Stud. - Solids, Liq. Gases, InTech, 2011: pp. 95–122.

[42] K. Swayampakula, V.M. Boddu, S.K. Nadavala, K. Abburi, Competitive adsorption of Cu (II), Co (II) and Ni (II) from their binary and tertiary aqueous solutions using chitosan-coated perlite beads as biosorbent., J. Hazard. Mater. 170 (2009) 680–9.

[43] M. Visa, C. Bogatu, A. Duta, Simultaneous adsorption of dyes and heavy metals from multicomponent solutions using fly ash, Appl. Surf. Sci. 256 (2010) 5486–5491.

[44] G. Cornelissen, P.C.M. van Noort, J.R. Parsons, H. a J. Govers, Response to comment on "Temperature dependence of slow adsorption and desorption kinetics of organic compounds in sediments," Environ. Sci. Technol. 32 (1998) 1360.

[45] C.J. Werth, M. Reinhard, Effects of temperature on trichloroethylene desorption from silica gel and natural sediments. 1. Isotherms, Environ. Sci. Technol. 31 (1997) 689–696.

[46] C.H. Giles, D. Smith, A. Huitson, A general treatment and classification of the solute adsorption isotherm. I. Theoretical, J. Colloid Interface Sci. 47 (1974) 755–765.

[47] C. Hinz, Description of sorption data with isotherm equations, Geoderma. 99 (2001) 225–243.

[48] G. Limousin, J.-P. Gaudet, L. Charlet, S. Szenknect, V. Barthès, M. Krimissa, Sorption isotherms: A review on physical bases, modeling and measurement, Appl. Geochemistry. 22 (2007) 249–275.

[49] R. Calvet, Adsorption of organic chemicals in soils, Environ. Health Perspect. 83 (1989) 145–177.

[50] J. Tóth, Thermodynamical Correctness of Gas/Solid Adsorption Isotherm Equations, J. Colloid Interface Sci. 163 (1994) 299–302.

[51] G. Tan, D. Xiao, Adsorption of cadmium ion from aqueous solution by ground wheat stems., J. Hazard. Mater. 164 (2009) 1359–63.

[52] H.K. Boparai, M. Joseph, D.M. O'Carroll, Kinetics and thermodynamics of cadmium ion removal by adsorption onto nano zerovalent iron particles., J. Hazard. Mater. 186 (2011) 458–65.

[53] R.R. Bhatt, B.A. Shah, Sorption studies of heavy metal ions by salicylic acid–formaldehyde–catechol terpolymeric resin: Isotherm, kinetic and thermodynamics, Arab. J. Chem. (2013).

[54] V.S. Mane, P.V.V. Babu, Studies on the adsorption of Brilliant Green dye from aqueous solution onto low-cost NaOH treated saw dust, Desalination. 273 (2011) 321–329.

[55] A.P. Kumar, D. Depan, N. Singh Tomer, R.P. Singh, Nanoscale particles for polymer degradation and stabilization—Trends and future perspectives, Prog. Polym. Sci. 34 (2009) 479–515.

[56] G.M. Whitesides, Nanoscience, nanotechnology, and chemistry, Small. 1 (2005) 172–179.

[57] X. Qu, P.J.J. Alvarez, Q. Li, Applications of nanotechnology in water and wastewater treatment., Water Res. 47 (2013) 3931–46.

[58] P. Xu, G.M. Zeng, D.L. Huang, C.L. Feng, S. Hu, M.H. Zhao, et al., Use of iron oxide nanomaterials in wastewater treatment: a review., Sci. Total Environ. 424 (2012) 1–10.

[59] M.T. Amin, a a Alazba, U. Manzoor, A review on removal of pollutants from water / wastewater using different types of nanomaterials, 2014 (2014).

[60] X. Qu, J. Brame, Q. Li, P.J.J. Alvarez, Nanotechnology for a Safe and Sustainable Water Supply: Enabling Integrated Water Treatment and Reuse., Acc. Chem. Res. 46 (2012) 834–843.

[61] R.A. Vaia, H.D. Wagner, Framework for nanocomposites, Mater. Today. 7 (2004) 32–37.

[62] Y. Ju-Nam, J.R. Lead, Manufactured nanoparticles: an overview of their chemistry, interactions and potential environmental implications., Sci. Total Environ. 400 (2008) 396–414.

[63] I. Bhatt, B.N. Tripathi, Interaction of engineered nanoparticles with various components of the environment and possible strategies for their risk assessment., Chemosphere. 82 (2011) 308–17.

[64] P. Christian, F. Von Der Kammer, M. Baalousha, T. Hofmann, Nanoparticles: Structure, properties, preparation and behaviour in environmental media, Ecotoxicology. 17 (2008) 326–343.

[65] M. Fernández-García, J.A. Rodriguez, Metal Oxide Nanoparticles, Encycl. Inorg. Bioinorg. Chem. (2011) 1–11.

[66] I. Ali, New generation adsorbents for water treatment, Chem. Rev. 112 (2012) 5073–5091.

[67] A. García, R. Espinosa, L. Delgado, E. Casals, E. González, V. Puntes, et al., Acute toxicity of cerium oxide, titanium oxide and iron oxide nanoparticles using standardized tests, Desalination. 269 (2011) 136–141.

[68] R. Barrena, E. Casals, J. Colón, X. Font, A. Sánchez, V. Puntes, Evaluation of the ecotoxicity of model nanoparticles., Chemosphere. 75 (2009) 850–7.

[69] A. Sánchez, S. Recillas, X. Font, E. Casals, E. González, V. Puntes, Ecotoxicity of, and remediation with, engineered inorganic nanoparticles in the environment, TrAC Trends Anal. Chem. 30 (2011) 507–516.

[70] G. Bystrzejewska-Piotrowska, J. Golimowski, P.L. Urban, Nanoparticles: their potential toxicity, waste and environmental management., Waste Manag. 29 (2009) 2587–95.

[71] W. Song, V.H. Grassian, S.C. Larsen, High yield method for nanocrystalline zeolite synthesis., Chem. Commun. (Camb). 20 (2005) 2951–2953.

[72] W. Song, R.E. Justice, C.A. Jones, V.H. Grassian, S.C. Larsen, Synthesis , Characterization , and Adsorption Properties of Nanocrystalline ZSM-5, Langmuir. 20 (2004) 8301–8306.

[73] C.L. Mangun, Z. Yue, J. Economy, S. Maloney, P. Kemme, D. Cropek, Adsorption of Organic Contaminants from Water Using Tailored ACFs, 13 (2001) 2356–2360.

[74] X. Peng, Z. Luan, J. Ding, Z. Di, Y. Li, B. Tian, Ceria nanoparticles supported on carbon nanotubes for the removal of arsenate from water, Mater. Lett. 59 (2005) 399–403.

[75] Z.-C. Di, J. Ding, X.-J. Peng, Y.-H. Li, Z.-K. Luan, J. Liang, Chromium adsorption by aligned carbon nanotubes supported ceria nanoparticles., Chemosphere. 62 (2006) 861–5.

[76] K.L. Salipira, B.B. Mamba, R.W. Krause, T.J. Malefetse, S.H. Durbach, Carbon nanotubes and cyclodextrin polymers for removing organic pollutants from water, Environ. Chem. Lett. 5 (2007) 13–17.

[77] C. Lu, H. Chiu, Adsorption of zinc(II) from water with purified carbon nanotubes, Chem. Eng. Sci. 61 (2006) 1138–1145.

[78] C. Lu, Y.-L. Chung, K.-F. Chang, Adsorption of trihalomethanes from water with carbon nanotubes., Water Res. 39 (2005) 1183–9.

[79] F. He, D. Zhao, Preparation and characterization of a new class of starch-stabilized bimetallic nanoparticles for degradation of chlorinated hydrocarbons in water., Environ. Sci. Technol. 39 (2005) 3314–3320.

[80] S. Choe, Y.-Y. Chang, K.-Y. Hwang, J. Khim, Kinetics of reductive denitrification by nanoscale zero-valent iron, Chemosphere. 41 (2000) 1307–1311.

[81] J. Cao, D. Elliott, W.X. Zhang, Perchlorate reduction by nanoscale iron particles, J. Nanoparticle Res. 7 (2005) 499–506.

[82] G.C.C. Yang, H.-L. Lee, Chemical reduction of nitrate by nanosized iron: kinetics and pathways., Water Res. 39 (2005) 884–94.

[83] W.-X. Zhang, C.-B. Wang, Rapid and complete dechlorination of TCE and PCBs by nanoscale Fe and Pd/Fe particles, Environ. Sci. Technol. 37, No. 1 (1997) 78–79.

[84] W. Zhang, C.-B. Wang, H.-L. Lien, Treatment of chlorinated organic contaminants with nanoscale bimetallic particles, Catal. Today. 40 (1998) 387–395.

[85] R. Cheng, J.-L. Wang, W. Zhang, Comparison of reductive dechlorination of p-chlorophenol using Fe0 and nanosized Fe0., J. Hazard. Mater. 144 (2007) 334–9.

[86] M.E. Pena, G.P. Korfiatis, M. Patel, L. Lippincott, X. Meng, Adsorption of As(V) and As(III) by nanocrystalline titanium dioxide., Water Res. 39 (2005) 2327–37.

[87] S. Artelt, O. Creutzenberg, H. Kock, K. Levsen, D. Nachtigall, U. Heinrich, et al., Bioavailability of fine dispersed platinum as emitted from automotive catalytic converters: A model study, Sci. Total Environ. 228 (1999) 219–242.

[88] S.M. Lloyd, L.B. Lave, H.S. Matthews, Life Cycle Benefits of Using Nanotechnology To Stabilize Platinum-Group Metal Particles in Automotive Catalysts Life Cycle Benefits of Using Nanotechnology To Stabilize Platinum-Group Metal Particles in Automotive Catalysts, 39 (2005) 1384–1392.

[89] M. Ohde, H. Ohde, C.M. Wai, Recycling nanoparticles stabilized in water-in-CO_2 microemulsions for catalytic hydrogenations, Langmuir. 21 (2005) 1738–1744.

[90] K. Schmid, M. Riediker, Use of nanoparticles in swiss industry: A targeted survey, Environ. Sci. Technol. 42 (2008) 2253–2260.

[91] C. Kirchner, T. Liedl, S. Kudera, T. Pellegrino, H.E. Gaub, S. Sto, et al., Cytotoxicity of Colloidal CdSe and CdSe / ZnS Nanoparticles, Nano Lett. 5 (2005) 331–338.

[92] I. Teodorovic, I. Planojevic, P. Knezevic, S. Radak, I. Nemet, Sensitivity of bacterial vs. acute Daphnia magna toxicity tests to metals, Cent. Eur. J. Biol. 4 (2009) 482–492.

[93] K. Kawata, M. Osawa, S. Okabe, In vitro toxicity of silver nanoparticles at noncytotoxic doses to HepG2 human hepatoma cells, Environ. Sci. Technol. 43 (2009) 6046–6051.

[94] M. Hua, S. Zhang, B. Pan, W. Zhang, L. Lv, Q. Zhang, Heavy metal removal from water/wastewater by nanosized metal oxides: a review., J. Hazard. Mater. 211-212 (2012) 317–31.

[95] S. Recillas, J. Colón, E. Casals, E. González, V. Puntes, A. Sánchez, et al., Chromium VI adsorption on cerium oxide nanoparticles and morphology changes during the process., J. Hazard. Mater. 184 (2010) 425–31.

[96] S. Recillas, A. García, E. González, E. Casals, V. Puntes, A. Sánchez, et al., Use of CeO2, TiO2 and Fe3O4 nanoparticles for the removal of lead from water. Toxicity of nanoparticles and derived compounds, Desalination. 277 (2011) 213–220.

[97] Y. Li, N.-H. Lee, E.G. Lee, J.S. Song, S.-J. Kim, The characterization and photocatalytic properties of mesoporous rutile TiO2 powder synthesized through self-assembly of nano crystals, Chem. Phys. Lett. 389 (2004) 124–128.

[98] W. Yantasee, C.L. Warner, T. Sangvanich, R.S. Addleman, T.G. Carter, R.J. Wiacek, et al., Removal of heavy metals from aqueous systems with thiol functionalized superparamagnetic nanoparticles., Environ. Sci. Technol. 41 (2007) 5114–9.

[99] J.-G. Yu, L.-Y. Yu, H. Yang, Q. Liu, X.-H. Chen, X.-Y. Jiang, et al., Graphene nanosheets as novel adsorbents in adsorption, preconcentration and removal of gases, organic compounds and metal ions., Sci. Total Environ. 502 (2015) 70–9.

[100] F. Perreault, A.F. De Faria, M. Elimelech, Environmental applications of graphene-based nanomaterials, Chem. Soc. Rev. (2015).

[101] Y. Zhu, S. Murali, W. Cai, X. Li, J.W. Suk, J.R. Potts, et al., Graphene and graphene oxide: Synthesis, properties, and applications, Adv. Mater. 22 (2010) 3906–3924.

[102] a K. Geim, K.S. Novoselov, Geim A. K., Novoselov K. S., The rise of graphene., Nat. Mater. (2007) 183–191.

[103] T.S. Sreeprasad, S.M. Maliyekkal, K.P. Lisha, T. Pradeep, Reduced graphene oxide-metal/metal oxide composites: facile synthesis and application in water purification., J. Hazard. Mater. 186 (2011) 921–31.

[104] G.Z. Kyzas, E. a. Deliyanni, K. a. Matis, Graphene oxide and its application as an adsorbent for wastewater treatment, J. Chem. Technol. Biotechnol. 89 (2014) 196–205.

[105] B.F. Machado, P. Serp, Graphene-based materials for catalysis, Catal. Sci. Technol. 2 (2012) 54.

[106] H. Wang, X. Yuan, Y. Wu, H. Huang, X. Peng, G. Zeng, et al., Graphene-based materials: fabrication, characterization and application for the decontamination of wastewater and wastegas and hydrogen storage/generation., Adv. Colloid Interface Sci. 195-196 (2013) 19–40.

[107] B. Li, H. Cao, ZnO@graphene composite with enhanced performance for the removal of dye from water, J. Mater. Chem. 21 (2011) 3346.

[108] M. Giovanni, H.L. Poh, A. Ambrosi, G. Zhao, Z. Sofer, F. Šaněk, et al., Noble metal (Pd, Ru, Rh, Pt, Au, Ag) doped graphene hybrids for electrocatalysis, Nanoscale. 4 (2012) 5002.

[109] B. Neppolian, A. Bruno, C.L. Bianchi, M. Ashokkumar, Graphene oxide based Pt-TiO2 photocatalyst: ultrasound assisted synthesis, characterization and catalytic efficiency., Ultrason. Sonochem. 19 (2012) 9–15.

[110] J.G. Radich, P. V Kamat, Origin of reduced graphene oxide enhancements in electrochemical energy storage, ACS Catal. 2 (2012) 807–816.

[111] H. Lee, S.M. Dellatore, W.M. Miller, P.B. Messersmith, Mussel-inspired surface chemistry for multifunctional coatings., Science. 318 (2007) 426–30.

[112] M.J. Harrington, A. Masic, N. Holten-Andersen, J.H. Waite, P. Fratzl, Iron-Clad Fibers: A Metal-Based Biological Strategy for Hard Flexible Coatings, Science. 328 (2010) 216–220.

[113] Y. Liu, K. Ai, L. Lu, Polydopamine and its derivative materials: Synthesis and promising applications in energy, environmental, and biomedical fields, Chem. Rev. 114 (2014) 5057–5115.

[114] H. Gao, Y. Sun, J. Zhou, R. Xu, H. Duan, Mussel-inspired synthesis of polydopamine-functionalized graphene hydrogel as reusable adsorbents for water purification, ACS Appl. Mater. Interfaces. 5 (2013) 425–432.

[115] J. Saiz-Poseu, J. Sedó, B. García, C. Benaiges, T. Parella, R. Alibés, et al., Versatile nanostructured materials via direct reaction of functionalized catechols., Adv. Mater. 25 (2013) 2066–70.

[116] American Public Health Association, Standard methods for the examination of water and wastewater, American Public Health Association, Washington :, 1981.

[117] B. Benguella, H. Benaissa, Cadmium removal from aqueous solutions by chitin: kinetic and equilibrium studies., Water Res. 36 (2002) 2463–74.

[118] WHO, WHO guidelines for drinking-water quality., WHO Chron. 38 (2008) 104–8.

[119] Ministerio de la Presidencia, Ministerio de la presidencia Real decreto 140/2003, 2003.

[120] A.H. Sulaymon, A.O. Sharif, T.K. Al-Shalchi, Removal of cadmium from simulated wastewaters by electrodeposition on stainless steel tubes bundle electrode, J. Chem. Technol. Biotechnol. 86 (2011) 651–657.

[121] D. Zhang, X. Zeng, W. Li, H. He, P. Ma, J. Falandysz, Selection of optimum formulation for biosorbing lead and cadmium from aquatic solution by using PVA-SA's immobilizing Lentinus edodes residue, Desalin. Water Treat. 31 (2011) 107–114.

[122] A. Zach-Maor, R. Semiat, H. Shemer, Removal of heavy metals by immobilized magnetite nan-particles, Desalin. Water Treat. 31 (2011) 64–70.

[123] F. Zhang, Ceria nanoparticles: Size, size distribution, and shape, J. Appl. Phys. 95 (2004) 4319.

[124] A. Pottier, S. Cassaignon, C. Chanéac, F. Villain, E. Tronc, J.-P. Jolivet, Size tailoring of TiO2 anatase nanoparticles in aqueous medium and synthesis of nanocomposites. Characterization by Raman spectroscopy, J. Mater. Chem. 13 (2003) 877–882.

[125] R. Massart, Preparation of aqueous magnetic liquids in alkaline and acidic media, IEEE Trans. Son Magn. 17 (1981) 1247–1248.

[126] H.. K. An, B.. Y. Park, D.. S. Kim, Crab shell for the removal of heavy metals from aqueous solution., Water Res. 35 (2001) 3551–6.

[127] U. Kumar, M. Bandyopadhyay, Sorption of cadmium from aqueous solution using pretreated rice husk., Bioresour. Technol. 97 (2006) 104–9.

[128] M.M. Rao, A. Ramesh, G.P.C. Rao, K. Seshaiah, Removal of copper and cadmium from the aqueous solutions by activated carbon derived from Ceiba pentandra hulls., J. Hazard. Mater. 129 (2006) 123–9.

[129] L.R. Skubal, N.K. Meshkov, T. Rajh, M. Thurnauer, Cadmium removal from water using thiolactic acid-modified titanium dioxide nanoparticles, J. Photochem. Photobiol. A Chem. 148 (2002) 393–397.

[130] a B. Pérez-Marín, V.M. Zapata, J.F. Ortuño, M. Aguilar, J. Sáez, M. Lloréns, Removal of cadmium from aqueous solutions by adsorption onto orange waste., J. Hazard. Mater. 139 (2007) 122–31.

[131] R. Fouladi Fard, A.A. Azimi, G.R. Nabi Bidhedi, Batch kinetics and isotherms for biosorption of cadmium onto biosolids, Desalin. Water Treat. 28 (n.d.) 69–74.

[132] O. Hamdaoui, F. Saoudi, M. Chiha, Utilization of an agricultural waste material, melon (Cucumis melo L.) peel, as a sorbent for the removal of cadmium from aqueous phase, Desalin. Water Treat. 21 (2010) 228–237.

[133] M. Allawzi, S. Al-Asheh, H. Allaboun, O. Borini, Assessment of the natural jojoba residues as adsorbent for removal of cadmium from aqueous solutions, Desalin. Water Treat. 21 (2010) 60–65.

[134] S. Wang, Y. Peng, Natural zeolites as effective adsorbents in water and wastewater treatment, Chem. Eng. J. 156 (2010) 11–24.

[135] W. Förstner, Metal Pollution in the Aquatic Environment. Chapter B: toxic metals, Springer, Berlin (Germany), 1984.

[136] G. McKay, J.F.F. Porter, G.M. Fellow, J.F.F. Porter, A Comparison of Langmuir Based Models for Predicting Multicomponent Metal Ion Equilibrium Sorption Isotherms on Peat, Process Saf. Environ. Prot. 75 (1997) 171–180.

[137] D. Mohan, S. Chander, Single component and multi-component adsorption of metal ions by activated carbons, Colloids Surfaces A Physicochem. Eng. Asp. 177 (2001) 183–196.

[138] D. Mohan, K.P. Singh, Single- and multi-component adsorption of cadmium and zinc using activated carbon derived from bagasse--an agricultural waste., Water Res. 36 (2002) 2304–18.

[139] B. Dejaegher, Y. Vander Heyden, Experimental designs and their recent advances in set-up, data interpretation, and analytical applications., J. Pharm. Biomed. Anal. 56 (2011) 141–58.

[140] A.R. Contreras, A. García, E. González, E. Casals, V. Puntes, A. Sánchez, et al., Potential use of CeO2 , TiO2 and Fe3O4 nanoparticles for the removal of cadmium from water, Desalin. Water Treat. 41 (2012) 296–300.

[141] L. Dong, Z. Zhu, H. Ma, Y. Qiu, J. Zhao, Simultaneous adsorption of lead and cadmium on MnO2-loaded resin, J. Environ. Sci. 22 (2010) 225–229.

[142] A.E. Navarro, K.P. Ramos, K. Campos, H.J. Maldonado, Elucidación del efecto del pH en la adsroción de metales pesadsos mediante biolorímeros naturales: cationes divalentes y superficies activas, Rev. Iberoam. Polímeros. 7 (2006) 113–126.

[143] B. Nowack, T.D. Bucheli, Occurrence, behavior and effects of nanoparticles in the environment., Environ. Pollut. 150 (2007) 5–22.

[144] J. Hu, G. Chen, I.M.C. Lo, Removal and recovery of Cr(VI) from wastewater by maghemite nanoparticles., Water Res. 39 (2005) 4528–36.

[145] K.-Y. Shin, J.-Y. Hong, J. Jang, Heavy metal ion adsorption behavior in nitrogen-doped magnetic carbon nanoparticles: isotherms and kinetic study., J. Hazard. Mater. 190 (2011) 36–44.

[146] I. Mobasherpour, E. Salahi, M. Pazouki, Comparative of the removal of Pb2+, Cd2+ and Ni2+ by nano crystallite hydroxyapatite from aqueous solutions: Adsorption isotherm study, Arab. J. Chem. 5 (2012) 439–446.

[147] J. Sedó, J. Saiz-Poseu, F. Busqué, D. Ruiz-Molina, Catechol-based biomimetic functional materials., Adv. Mater. 25 (2013) 653–701.

[148] Y. Liu, K. Ai, L. Lu, Polydopamine and its derivative materials: synthesis and promising applications in energy, environmental, and biomedical fields., Chem. Rev. 114 (2014) 5057–115.

[149] D.C. Montgomery, Design and Analysis of Experiments, Eigth edit, John Wiley & Sons, Hoboken (USA), 2012.

[150] R. Leardi, Experimental design in chemistry: A tutorial., Anal. Chim. Acta. 652 (2009) 161–72.

[151] L. Mac Berthouex, Pau lBrown, Statistics for Environmental Engineers, Second Edition, Second edi, CRC Press, USA, 2002.

[152] S. Parvez, C. Venkataraman, S. Mukherji, A review on advantages of implementing luminescence inhibition test (Vibrio fischeri) for acute toxicity prediction of chemicals., Environ. Int. 32 (2006) 265–268.

[153] A. Garcia, S. Recillas, A. Sánchez, X. Font, The Luminescent Bacteria Test to Determine the Acute Toxicity of Nanoparticle Suspensions, Nanotoxicity Methods Protoc. 926 (2012) 255–259.

[154] C. You, C. Han, X. Wang, Y. Zheng, Q. Li, X. Hu, et al., The progress of silver nanoparticles in the antibacterial mechanism, clinical application and cytotoxicity, Mol. Biol. Rep. 39 (2012) 9193–9201.

[155] A.H. Cory, T.C. Owen, J.G. Barltrop, Use of an aqueous soluble tetrazolium/formazan assay for cell growth assays in culture, Cancer Commun. 3 (1991) 207–212.

[156] C.P. Huang, The removal of chromium (VI) from diluted aqueous solution by activated carbon, Water Res. 11 (1977) 673–679.

[157] D. Singh, N.S. Rawat, Sorption of Pb(II) by bituminous coal, Indian J. Chem. Technol. 2 (n.d.) 49–50.

[158] A. López-Delgado, C. Pérez, F.A. López, Sorption of heavy metals on blast furnace sludge, Water Res. 32 (1998) 989–996.

[159] M.. Ferrero-García, J. Rivera-Ultrilla, J. Rodríguez-Gordillo, I. Bautista-Toledo, Adsorption of zinc, cadmium, and copper on activated carbons obtained from agricultural by-products, Carbon N. Y. 26 (1988) 363–373.

[160] K. Kadirvelu, C. Namasivayam, Activated carbon from coconut coirpith as metal adsorbent: adsorption of Cd(II) from aqueous solution, Adv. Environ. Res. 7 (2003) 471–478.

[161] R. Leyva-Ramos, J. Rangel-Mendez, J. Mendoza-Barron, L. Fuentes-Rubio, R. Guerrero-Coronado, Adsorption of Cadmium(II) from aqueous solution onto activated carbon, Water Sci. Technol. 35 (1997) 205–211.

[162] A.K. Bhattacharya, C. Venkobachar, Removal of Cadmium (II) by Low Cost Adsorbents, J. Environ. Eng. 110 (1984) 110–122.

[163] A. Netzer, Adsorption of copper, lead and cobalt by activated carbon, Water Res. 18 (1984) 927–933.

[164] M. Pérez-Candela, J. Martín-Martínez, R. Torregrosa-Maciá, Chromium(VI) removal with activated carbons, Water Res. 29 (1995) 2174–2180.

[165] D. Mohan, C.U. Pittman, Activated carbons and low cost adsorbents for remediation of tri- and hexavalent chromium from water., J. Hazard. Mater. 137 (2006) 762–811.

[166] R.E. Olson, D.D. Christ, Chapter 33. Plasma Protein Binding of Drugs, Annu. Rep. Med. Chem. 31 (1996) 327–336.

[167] L.A. Sklar, B.S. Hudson, R.D. Simonir, Conjugated Polyene Fatty Acids as Fluorescent Probes : Binding to Bovine Serum Albumin, Biochemistry. 16 (1977) 5100–5108.

[168] C. a Royer, Probing protein folding and conformational transitions with fluorescence., Chem. Rev. 106 (2006) 1769–84.

[169] Z. Ji, X. Shen, M. Li, H. Zhou, G. Zhu, K. Chen, Synthesis of reduced graphene oxide/CeO2 nanocomposites and their photocatalytic properties., Nanotechnology. 24 (2013) 115603.

[170] S. Wu, K. Zhang, X. Wang, Y. Jia, B. Sun, T. Luo, et al., Enhanced adsorption of cadmium ions by 3D sulfonated reduced graphene oxide, Chem. Eng. J. 262 (2015) 1292–1302.

[171] S. Wang, H. Sun, H.M. Ang, M.O. Tadé, Adsorptive remediation of environmental pollutants using novel graphene-based nanomaterials, Chem. Eng. J. 226 (2013) 336–347.

[172] K. Lü, G.X. Zhao, X.K. Wang, A brief review of graphene-based material synthesis and its application in environmental pollution management, Chinese Sci. Bull. 57 (2012) 1223–1234.

[173] Q. Ling, M. Yang, R. Rao, H. Yang, Q. Zhang, H. Liu, et al., Simple synthesis of layered CeO2–graphene hybrid and their superior catalytic performance in dehydrogenation of ethylbenzene, Appl. Surf. Sci. 274 (2013) 131–137.

[174] R. Sitko, B. Zawisza, E. Malicka, Graphene as a new sorbent in analytical chemistry, TrAC Trends Anal. Chem. 51 (2013) 33–43.

[175] T. Yu, J. Zeng, B. Lim, Y. Xia, Aqueous-phase synthesis of Pt/CeO2 hybrid nanostructures and their catalytic properties, Adv. Mater. 22 (2010) 5188–5192.

[176] J.W.S. Hummers, R.E. Offeman, Preparation of Graphitic Oxide, J. Am. Chem. Soc. 80 (1958) 1339.

[177] Z. Wang, Transmission electron microscopy of shape-controlled nanocrystals and their assemblies, J. Phys. Chem. B. 104 (2000) 1153–1175.

[178] Y. Hernandez, V. Nicolosi, M. Lotya, F.M. Blighe, Z. Sun, S. De, et al., High-yield production of graphene by liquid-phase exfoliation of graphite., Nat. Nanotechnol. 3 (2008) 563–568.

[179] S. Qaiser, A.R. Saleemi, M. Umar, Biosorption of lead from aqueous solution by Ficus religiosa leaves: batch and column study., J. Hazard. Mater. 166 (2009) 998–1005.

[180] Y. Zhang, C. Banks, A comparison of the properties of polyurethane immobilised Sphagnum moss, seaweed, sunflower waste and maize for the biosorption of Cu, Pb, Zn and Ni in continuous flow packed columns., Water Res. 40 (2006) 788–98.

[181] V.K. Gupta, I. Ali, Removal of lead and chromium from wastewater using bagasse fly ash--a sugar industry waste., J. Colloid Interface Sci. 271 (2004) 321–8.

[182] R. Sitko, B. Zawisza, E. Malicka, Modification of carbon nanotubes for preconcentration, separation and determination of trace-metal ions, TrAC Trends Anal. Chem. 37 (2012) 22–31.

[183] G. Zhao, J. Li, X. Ren, C. Chen, X. Wang, Few-layered graphene oxide nanosheets for heavy metal ion pollution management, Environ. Sci. Technol. 45 (2011) 1–4.

[184] M. Sánchez-Polo, J. Rivera-Utrilla, Adsorbent-adsorbate interactions in the adsorption of Cd(II) and Hg(II) on ozonized activated carbons, Environ. Sci. Technol. 36 (2002) 3850–3854.

[185] J. Goel, K. Kadirvelu, C. Rajagopal, V.K. Garg, Cadmium (II) Uptake from Aqueous Solution by Adsorption on Carbon Aerogel Using a Response Surface Methodological Approach, Ind. Eng. Chem. Res. 45 (2006) 6531–6537.

[186] R. Balasubramanian, S. V. Perumal, K. Vijayaraghavan, Equilibrium isotherm studies for the multicomponent adsorption of lead, zinc and cadmium onto Indonesian peat, Ind. Eng. Chem. Res. 48 (2009) 2093–2099.

[187] R.J. Sime, The Langmuir Adsorption Isotherm, 2000.

[188] K.Y. Foo, B.H. Hameed, Insights into the modeling of adsorption isotherm systems, Chem. Eng. J. 156 (2010) 2–10.

[189] B.H. Hameed, I.A.W. Tan, A.L. Ahmad, Adsorption isotherm, kinetic modeling and mechanism of 2,4,6-trichlorophenol on coconut husk-based activated carbon, Chem. Eng. J. 144 (2008) 235–244.

[190] G. Alagumuthu, V. Veeraputhiran, R. Venkataraman, Adsorption Isotherms on Fluoride Removal : Batch Techniques, Arch. Appl. Sci. Res. 2 (2010) 170–185.

[191] L. Fan, C. Luo, M. Sun, X. Li, H. Qiu, Highly selective adsorption of lead ions by water-dispersible magnetic chitosan/graphene oxide composites, Colloids Surfaces B Biointerfaces. 103 (2013) 523–529.

[192] World Health Organization, Zinc in Drinking-water, Guid. Drink. Qual. 2 (2003) 1–6.

[193] W.H. Organization, Nickel in Drinking-water, 2005.

[194] Generalitat de catalunya, Agencia de Residus de Catalunya, (2015).

[195] Ajuntament de Sabadell, EDAR-Sabadell, (2015).

[196] M. Šćiban, B. Radetić, Ž. Kevrešan, M. Klašnja, Adsorption of heavy metals from electroplating wastewater by wood sawdust, Bioresour. Technol. 98 (2007) 402–409.

[197] N. Ortiz, M. a F. Pires, J.C. Bressiani, Use of steel converter slag as nickel adsorber to wastewater treatment, Waste Manag. 21 (2001) 631–635.

[198] V.K. Jha, Y. Kameshima, a. Nakajima, K. Okada, Hazardous ions uptake behavior of thermally activated steel-making slag, J. Hazard. Mater. 114 (2004) 139–144.

[199] D.H. Kim, M.C. Shin, H.D. Choi, C. Il Seo, K. Baek, Removal mechanisms of copper using steel-making slag: adsorption and precipitation, Desalination. 223 (2008) 283–289.

[200] S.Y. Liu, J. Gao, Y.J. Yang, Y.C. Yang, Z.X. Ye, Adsorption intrinsic kinetics and isotherms of lead ions on steel slag, J. Hazard. Mater. 173 (2010) 558–562.

[201] A. Drizo, C. Forget, R.P. Chapuis, Y. Comeau, Phosphorus removal by electric arc furnace steel slag and serpentinite, Water Res. 40 (2006) 1547–1554.